Impacts of retrogressive permafrost thaw slumps on aquatic systems in the Peel Plateau, Northwest Territories, Canada

By

Stephanie Delaney
B.A. Physical Geography, Carleton University, 2011

A thesis submitted to the Faculty of Graduate and Postdoctoral Affairs in partial fulfillment of the requirements for the degree of

Master of Science

in

Physical Geography

Carleton University
Ottawa, Ontario

© 2015

Stephanie Delaney

ABSTRACT

Along the slopes of the Richardson Mountains, west of the Mackenzie Delta in the Northwest Territories of Canada, the stratigraphies of two lakes with large retrogressive thaw slumps within their catchments are examined using paleolimnological techniques. The lacustrine geomorphological impacts of current thaw activity are examined, as well as the past occurrence of large-scale thermokarst disturbances. Sediment stratigraphies from the larger lake suggest repeated erosion through time. The sediment stratigraphy from the smaller lake records ~55 cm of deposition due to thaw slump activity in the past 20 – 40 years. Aside from the recent thaw slump activity recorded in the smaller lake basin, neither system provided discernable evidence of long-term, ancient slump activity. The difference in the magnitude of impacts of the two systems is primarily attributed to catchment area to lake area and disturbance area to lake area ratios.

ACKNOWLEDGEMENTS

I would like to thank my supervisor Dr. Michael Pisaric for all of the wonderful opportunities he has brought into my life. I first discovered my passion for Physical Geography after taking Mike's intro course during my first year at Carleton, which swayed me into transferring into the program. During my fourth year, Mike was the supervisor of my undergraduate thesis, which sparked my interest for paleolimnology and led to a summer position working at CUPL and this Masters project. I have him to thank for all of this, but most especially for introducing me to my one true love: the Canadian north. THANK YOU MIKE!

I would also like to thank Dr. Steven Kokelj- for teaching me absolutely everything I know about fieldwork and being a wonderful mentor during four amazing field sessions in the Tundra. From the moment I met Steve after being told to "look for the tallest man you see with a ponytail in the Yellowknife airport", he has done nothing but enrich my mind with knowledge.

This project could not have been completed without the help of Dr. Scott Lamoureux who was always willing to lend a hand. Scott was present for the best of all field sessions with his vibracorer to core Husky Lake; the memories from that trip remain in the top 5 of my life. Thanks Scott for everything- from driving down to Ottawa to help split the cores, to spending hours in Kingston going over my data and mostly, for inventing the roulette of shame ☺.

I would also like to thank Dr. Murray Richardson, who provided great insight towards pulling the project together at the end and was always quick and efficient with all of his contributions. Thank you so much Murray!

I am also indebted to Colin Mustaphi & Ray Caron, who were always available for help every step of the way, no matter what time of day/night. Thank you for all of the endless laughs!

Thanks also to Kathy- for always supporting me and encouraging me to work on my thesis after long days at work. Thanks to Bruin and Hugo for being by my side during the long nights of writing alone.

Most of all THANK YOU to my mom and dad- whose unconditional love and encouragement drove me to finish this project when I never thought I could (Love you the most xo).

TABLE OF CONTENTS

LIST OF FIGURES

LIST OF TABLES

LIST OF APPENDICES

CHAPTER ONE

BACKGROUND INFORMATION AND RESEARCH CONTEXT

1.1 INTRODUCTION

The 20th century has been a period of exceptional change in the Arctic in response to warming trends that commenced in the late 19th century and continued throughout the 20th and 21st centuries (ACIA, 2005; Serreze *et al.* 2000). As temperature has increased, a number of landscape responses to this warming have been noted. Chief amongst these responses have been changes in permafrost conditions, including active-layer thickness and permafrost temperature (Romanovsky *et al.* 2013). For example, on the North Slope of Alaska and in the Brooks Range, permafrost temperature at 20 m depth in 2012 was the warmest since measurements began in the late 1970s and early 1980s (Romanovsky *et al.* 2013). Across northern Russia, permafrost temperature has increased 1-2° C during the past 30-35 years (Romanovsky *et al.* 2010). Similar trends in permafrost temperature have been noted across northern Canada (Smith *et al.* 2010), especially at Alert, NU, where temperature at >15 m depth has increased at the rate of >1.0° C per decade since 2000 (Smith *et al.* 2012).

1.2 NATURE AND ORIGIN OF RETROGRESSIVE THAW SLUMPS

As air and ground temperatures have increased, the frequency and magnitude of terrain disturbances due to permafrost degradation have also increased (Lantz & Kokelj, 2008). Retrogressive thaw slumps represent one of

the most rapid erosive features in present-day periglacial environments (French, 2007). Some of the largest slumps observed to date have developed along the slopes of the Richardson Mountains on the Peel Plateau in northwest Canada (Figure 1.1). Active slumps may be recognized on the landscape as horseshoe-shaped features (Mackay, 1966), which contain a retreating headwall, a slump floor, and an evacuation channel (Figure 1.2). In the western Arctic of Canada, thaw slumps affect up to 10% of lake catchments (Lantz & Kokelj, 2008; Kokelj *et al.* 2009; Thienpont *et al.* 2013). These retrogressive "mega slumps" are large-scale detachment scars (Figure 1.3), and the magnitude of these disturbances is such that the thawed material is changing the physical and chemical parameters of both small and large-scale aquatic systems (Kokelj *et al.* 2013; Malone *et al.* 2013). While the impact of retrogressive mega slumps has been remarkable in the past few decades, less is understood about the occurrence and frequency of these events across longer timescales. Using paleolimnological techniques it may be possible to discern past slumping events in the sedimentological record of lacustrine sediment. By examining the sedimentological record from lake basins, the magnitude of effects of current thaw activity may be determined, while also gaining insight into the frequency of these disturbance events during past warming episodes. This knowledge may provide insights as to what may be expected in this landscape under continued warming trends in the future.

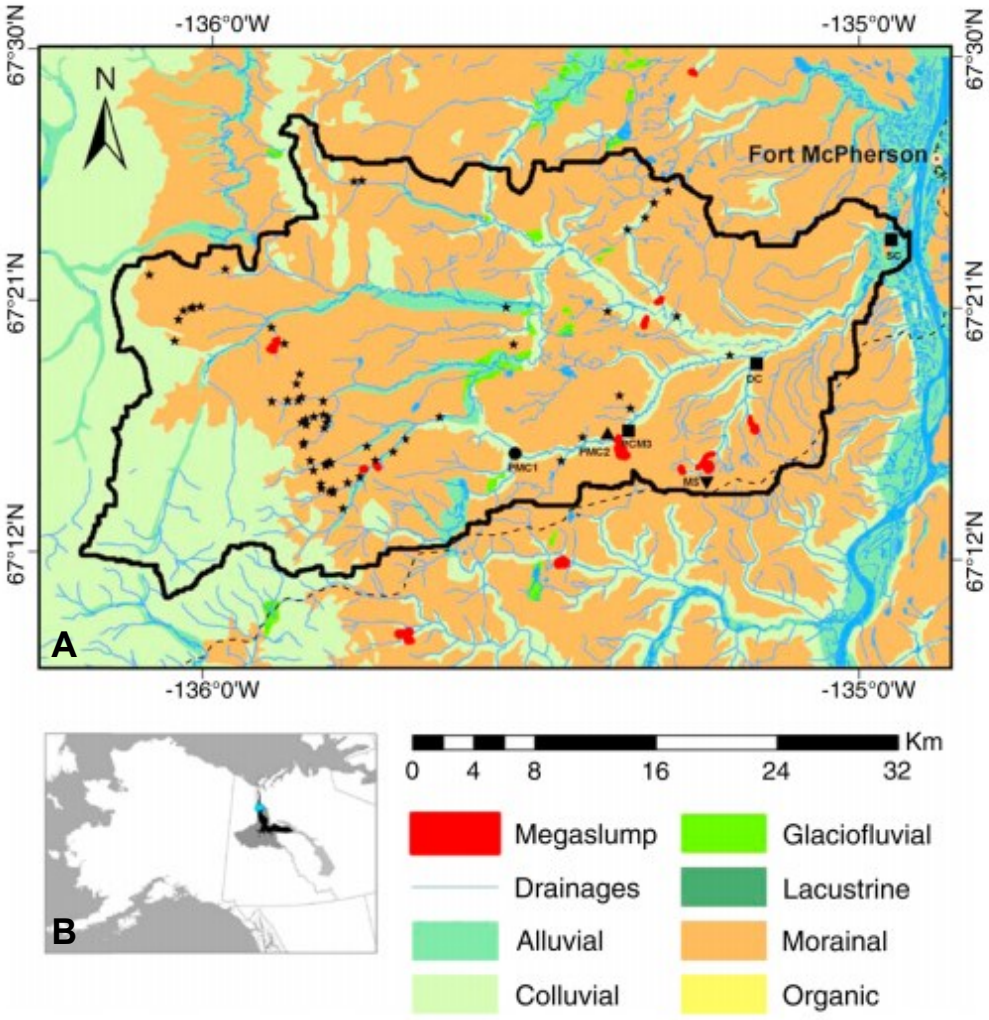

Figure 1.1: Map of the Peel Plateau.
A)This map outlines the location of the Stony Creek watershed (one of the primary watersheds of the Peel Plateau) in black. Mega slumps within the region are indicated in red, while smaller, stable slumps are identified by the star symbols and the Dempster Highway by the dashed line. All other symbols on the map identify streams and study sites examined by Kokelj *et al.* 2013. B) The location of the Peel Plateau (black) and the Peel River watershed (grey) in the Northwest Territories of Canada, east of the Yukon border. The blue dot identifies the Stony Creek watershed investigated by Kokelj *et al.* 2013.

Figure 1.2: Diagram of a retrogressive thaw slump.
The headwall is characterized by a steep incline. As the slump erodes into the headwall, material accumulates in the slump floor and flows downslope in the evacuation channel, further eroding the landscape (Lacelle *et al.* 2010).

Retrogressive thaw slumps typically occur in fine-grained, ice rich permafrost-laden soils and within the Peel Plateau are commonly initiated by mechanical erosion through fluvial processes, or mass wasting by conditions of extreme precipitation or temperature (Lacelle *et al.* 2010). When such soils are exposed to a warmer atmosphere, ablation of the ground ice occurs and the thawed materials behave as a "slurry", being discharged to the slump floor, or carried as a debris flow downslope (Kokelj *et al.* 2013). Active slump growth may be attributed to ice content of the terrain, morphology and slump aspect (Lewkowicz, 1986) and can persist for several years impacting large expanses of terrain prior to stabilizing (Kokelj *et al.* 2009). Thaw slumps stabilize when the supply of exposed ground ice has become exhausted or covered by debris. The average slump remains active for 30-50 years before vegetation re-colonizes the disturbed slump floor (Lacelle, 2010).

Figure 1.3: Photograph of a mega slump in the Peel Plateau.
This photo demonstrates the size of mega slumps occurring within the Peel Plateau. This slump is located 1 km from the Dempster Hwy and was part of the research conducted by Kokelj *et al.* (2013). The red arrow is pointing to Dr. Steven Kokelj standing beside a debris flow from the slump floor. Dr. Kokelj is about 2 m in height, which gives scale to the image and an idea of the size of this thermokarst disturbance. (Photo taken by Stephanie Delaney, 2012).

1.3 EXAMINING DISTURBANCE IN LACUSTRINE SEDIMENTS

Paleolimnology is the study of past processes and conditions within lake and river basins and the interpretation of the histories of these systems (Smol & Last, 2001). Lake sediments provide stratigraphic records with information on depositional changes at various spatial and temporal scales. The physical, chemical and biological properties of a lake may constantly be altered as climate and environmental conditions change (Anderson *et al.* 2007). Subsequently, changes in sedimentation may occur, leaving behind a record in lake sediments. Through the analysis of sediment samples, insight into the rate and mode of sedimentation and landscape denudation in past environments may be obtained (Anderson *et al.* 2007).

The sediments of a lake comprise allochthonous and autochthonous components (Smol & Last, 2001). Allochthonous material is derived from outside of the lake basin and is typically carried in by inflowing streams or blown in by the wind. Autochthonous material is produced within the lake and normally consists of biological materials such as algae, macrophytic vegetation or precipitates. The delivery of terrestrial matter to lacustrine environments is highly responsive to the hydrograph, as water flow is the primary method of transport (Bloesch, 2004). A surface disturbance such as a retrogressive thaw slump will destabilize the system, affecting not only the catchment, but its receiving waters as well. Acute, localized perturbation can increase sediment erosion at exceptional rates, leading to significant increases in suspended sediment and solute loads (Burn &

Lewkowicz, 1990). Sediment pulses become disturbances to lakes when the present assemblages of organisms can no longer tolerate or are not able to adapt to the destabilization of the system by the imposed variability (O'Sullivan, 2004). Thermokarst disturbances have been widely documented in geomorphic studies, however the impacts of these major disturbances on downstream aquatic systems have only become a topic of interest in recent years (Lamoureux & Lafreniere, 2009; Kokelj *et al.* 2013; Malone *et al.* 2013).

1.4 RESEARCH SIGNIFICANCE AND OBJECTIVES

With air temperatures generally increasing over the last century in the western Canadian Arctic and future increases predicted, the knowledge of the response of past permafrost and thermokarst conditions is of upmost importance in predicting how periglacial landscapes may respond to future warming. Should disturbance regimes continue to change as predicted, it is uncertain what changes may occur to nearby aquatic systems.

Using paleolimological techniques, the stratigraphies of two lakes with large retrogressive thaw slumps within their catchments are examined. The study was conducted along the slopes of the Richardson Mountains, west of the Mackenzie Delta in the Northwest Territories of Canada (Figure 1.4). The lakes and their respective catchments vary greatly in size. Lake FM1 (unofficial name) covers an area of ~6 ha with a maximum depth of ~1.2 m and a catchment of ~803 ha. Husky Lake is much larger with a surface area of ~895 ha, a maximum depth of ~16 m and a catchment area of ~6973 ha (Figure 1.4).

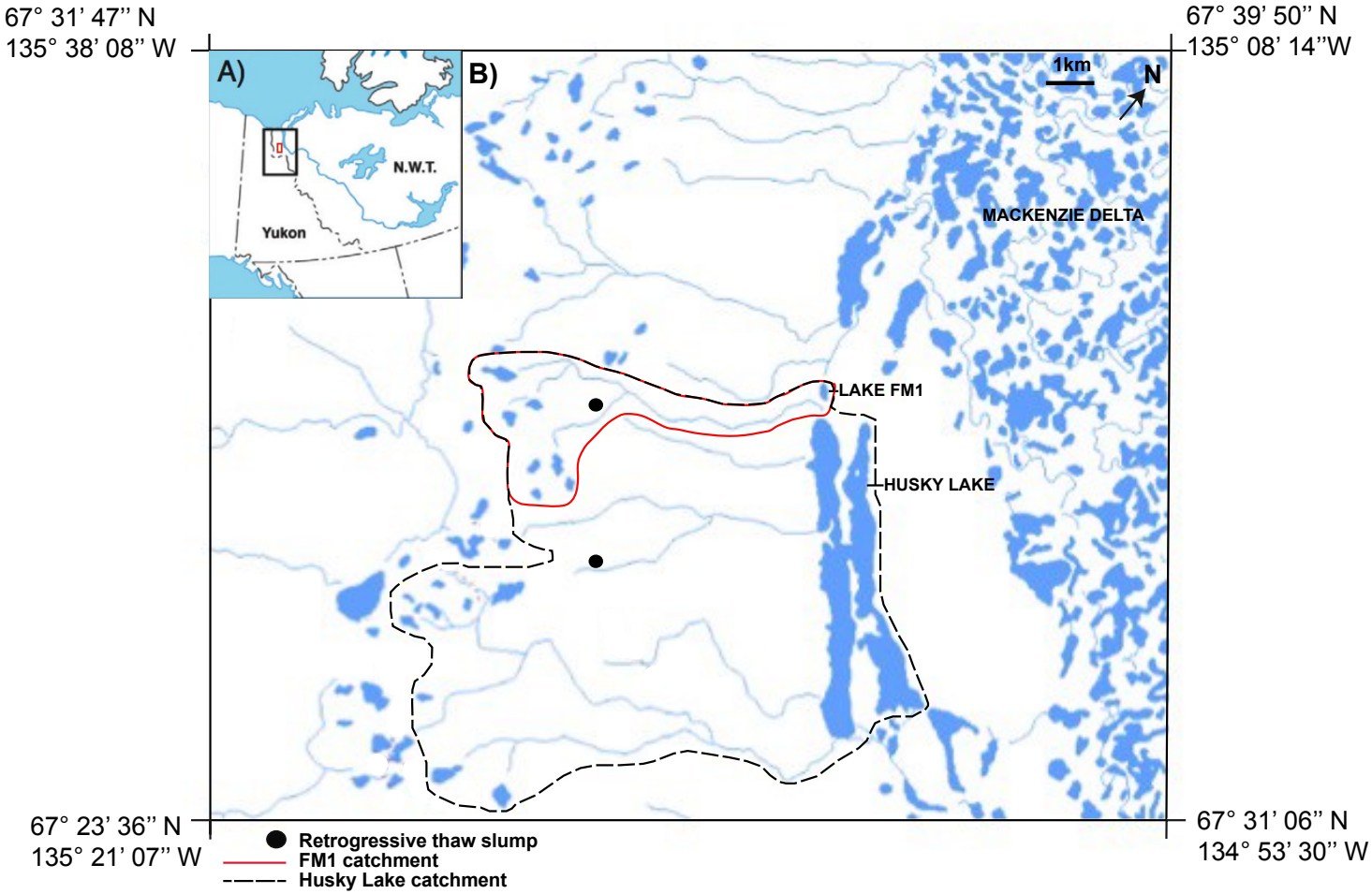

Figure 1.4: Map of studied systems.

A) The location of the Peel Plateau is outlined by the black rectangle, and the study area indicated by the red dot. B) Husky Lake (895 ha) is located just South of the much smaller lake FM1 (6 ha). The catchment of Lake FM1 (803 ha) is outlined in red and that of Husky Lake (6973 ha) is the black dotted line. Retrogressive thaw slumps are indicated with black circles. The slump affecting the FM1 system is slightly larger (8 ha), than that within the Husky Lake catchment. The uplands of the Richardson Mountains are located to the west of the study site and the Mackenzie Delta to the east.

This research seeks to determine whether similar thermokarst erosional features have occurred in the study area in the past and to place the current thaw activity in a long-term context. This thesis focuses on two primary research questions:

1. Can lake sediment records be used to track the occurrence of thaw slumps in the past? Is there a sedimentological signature contained in the cores that can be attributed to thaw slump activity and can this signature be tracked through time making it possible to assess the frequency of retrogressive thaw slumps in the past?
2. What are the geomorphological impacts of increased sediment loading from retrogressive thaw slumps on nearby and connected aquatic systems? Do the ratios between lake, catchment and disturbance size influence the magnitude of the impacts on these systems?

1.5 ORGANIZATION OF THE THESIS

The thesis is organized in 6 chapters as follows: Chapter 1 has provided background information and context for the research project. Chapter 2 is a literature review of pertinent literature of climate in northwest Canada, paleolimnology and permafrost disturbance. Chapter 3 describes the study area and methods employed in this research. Chapter 4 presents the research findings. Chapter 5 discusses the findings in the context of previous research related to permafrost disturbances and Chapter 6 summarizes the conclusions

and implications of the research and proposes avenues of future research that have developed from the current project.

CHAPTER TWO

LITERATURE REVIEW

2.1 HOLOCENE AND CONTEMPORARY CLIMATE IN THE WESTERN ARCTIC

Maximum summer solar radiation at high latitudes of the Northern Hemisphere occurred at 10,000 yr BP, due to Milankovitch cycles (Ritchie, 1984). This climatic optimum is demonstrated by the development of many thermokarst lakes and a paleoactive layer or Holocene thaw unconformity (Burn, 1997).

Pollen records demonstrate that between 10,000 and 6,000 yr. BP *Picea* dominated the Tuktoyatuk Peninsula, approximately 70 km north of the present treeline and reverted back to tundra ~4,000 yr BP, suggesting that summers during the early Holocene in this region were warmer than contemporary climate (Ritchie, 1984). Air temperatures cooled during the mid Holocene, but remained warmer than today due to high incidence of solar radiation (Lacelle *et al. 2010*; Ritchie *et al.* 1983). A summary of Holocene climate and vegetation conditions in the western Arctic of Canada is presented in Table 2.1.

Modern day temperature increases in the Arctic have exceeded those recorded globally (Serreze *et al.* 2000). As a result of polar amplification, the western Arctic of North America has been one of the most rapidly warming regions on the planet during the last 4 decades (Lantz & Kokelj, 2008; Johannessen *et al.* 2004; Serreze *et al.* 2000). Such amplification can be primarily attributed to radiative forcing associated with increasing greenhouse

Table 2.1: Holocene vegetation and climate in the western Arctic of Canada: Palynological data and vegetation classification based on Spear (1993) and Ritchie (1971). Average ΔTSI (Total Solar Irradiance) is expressed as the difference of TSI from the value of PMOD composite during the solar cycle minimum of the year 1986 AD (1365.57W/m^2) (Steinhilber *et al.* 2009). The PMOD composite is one of three TSI composites currently available and is the only one that has reliable data for solar cycle 21.

Years BP	Pollen	Average ΔTotal Solar Irradiance	Vegetation	Climate
Present-4,000	Decrease in *Picea* cf. *mariana*, increase in *Pinus* (transported from the South by aeolian processes)	-0.17 W/m^{-2}	**dwarf birch heath tundra** Disappearance of arboreal cover, replaced by dwarf-birch heath tundra on all sites except those with extremes of moisture condition	Modern conditions
4,000-5,500	Increase in *Picea cf. mariana*, *Betula* dominates but declines	-0.06 W/m^{-2}	**tall shrub tundra** Invasion by alder, forming extensive tall shrub thickets; only scattered spruce; heaths and herb communities confined to exposed sites	Modern conditions
5,500-8,500	*Betula* dominates*;* increase in *Alnus* cf. c*rispa*	-0.27 W/m^{-2}	**closed-crown spruce-birch forest** Continuous spruce forest, with associated tree birch	Warm, moist Pacific air. Summer temperatures ~ 5° C warmer than at present; growing season ~ 30 days longer
8,500-11,600	*Betula, Salix*, *Artemesia*, Chenopodiaceae/ Amaranthus, Rosaceae,Cruciferae, Cyperaceae, Gramineae, Ericaceae, *Myrica*, *Typha latifolia, Shepherdia canadensis*, *Picea* & *Pinus*	-0.13 W/m^{-2}	**forest tundra** Invasion by spruce, forming a forest-tundra	Warmer temperatures than present
11,600-12,900	*Betula, Salix, Shepherdia canadensis, Juniperus, Gramineae, Artemisia and Cyperaceae*	n/a (data not available)	**dwarf birch tundra** Tundra, dominated by dwarf birch and *Shepherdia canadensis* with abundant local herb-dominated communities on open sites (similar to modern shrub tundra)	Younger Dryas (return to glacial conditions, decrease in temperature)

gases and changes in albedo (Chapin *et al.* 2005). Recent dendroclimatological studies from northwest Canada indicate recent warming exceeds most periods during the past ~500 to 1000 years (Porter *et al.* 2014).

2.2 THERMOKARST TERRAIN & RETROGRESSIVE THAW SLUMPS IN THE WESTERN ARCTIC

Approximately 24% of the ice-free land area in the northern hemisphere is currently underlain by permafrost (Zhang *et al.* 1999). Permafrost is ground that remains frozen (at or below 0 °C) for at least 2 consecutive years; it can form epigenetically (after the emplacement of a ground medium) or syngenetically (simultaneous with the positioning of ground medium) (Zhang *et al*. 2008). The most significant contributing factor to the presence and maintenance of permafrost is the climate. Amplified climate warming in the western Arctic has led to increases in ground temperatures (Smith *et al.* 2010). Increases in ground temperatures may lead to the degradation of permafrost, which may form a number of landscape features collectively known as thermokarst terrain. Thermokarst terrain refers to the local or widespread collapse, subsidence, instability, or erosion of the ground surface due to the thaw of permafrost (French, 2007). As permafrost temperatures continue to rise in response to contemporary climate warming in this region, the frequency and magnitude of terrain disturbances associated with thawing permafrost are increasing (Kokelj *et al.* 2009). It has been estimated that within the next century, 25-90% of areas with near-surface permafrost will transition to seasonally frozen ground

(Lawrence *et al.* 2008; Jafarov *et al.* 2012; Belshe *et al.* 2013); however, these estimates span a wide range of values and therefore contain significant uncertainty.

There is a wide diversity of thermokarst features. The spatial distribution and extent of such features varies depending on several local geomorphic factors including: permafrost and ground ice conditions, hydrology, surrounding vegetation, landscape position and soil texture (Belshe *et al.* 2013; Jorgenson and Osterkamp, 2005). Thermokarst formation in areas of low relief usually results in an increase in water storage, changes to vegetation, and active layer deepening, the latter leading to increased activity in nutrient pools and soil carbon (Jensen *et al.* 2014). When thermokarst forms on hillslopes the results are much more dramatic, as terrain degradation has the potential to lead to thermal erosion and slumping, which typically lead to a multitude of cascading effects (Jensen *et al.* 2014; Kokelj and Jorgenson 2013). When the active layer is stripped away from the land, the underlying frozen ground is susceptible to thaw and a retrogressive thaw slump may initiate. Once initiated, thaw slumps remain active as long as massive ground ice within the headwall is exposed (Lacelle *et al.* 2010). For this reason, retrogressive thaw slumps are typically more abundant and larger in ice-cored terrain, which is widespread in the glaciogenic landscape of the western Arctic of Canada (Kokelj *et al.* 2013). As the ground ice ablates, the ice-rich headwalls progressively collapse and the thaw slumps grow (Kokelj *et al.* 2013; Lewkowicz, 1987). The thaw of the ground

ice also allows for the supply of water necessary to maintain mudflows on the slump floor, removing debris from the slump scar.

Within the Peel Plateau, 'mega slumps' have developed (Figure 1.3), some as large as 40 ha in area, with headwalls reaching 25 m in height (Kokelj *et al.* 2013). Kokelj *et al.* (2013) distinguish 'mega slumps' from normal thaw slumps using the following criteria: 1) >5 ha in area; 2) bare headwalls higher than 5 m; 3) possess debris flows leading to stream valleys; and 4) may have regressed beyond the slope of the valley. Kokelj *et al.* (2013) mapped thaw slump occurrence within the Stony Creek watershed of the Peel Plateau (Figure 1.1) and found more than 60 thaw slumps, 9 of which were classified as mega slumps.

Lacelle *et al.* (2010) investigated the climatic and geomorphic factors affecting contemporary (1950-2004) activity and initiation of retrogressive thaw slumps on the Aklavik Plateau, NWT, using aerial photograph analysis. The Aklavik Plateau is located within the ranges of Richardson Mountains and the slumps investigated by Lacelle *et al.* (2010) were all located on glaciated terrain within the maximum westward limits of the Laurentide Ice Sheet. Slumps on the Aklavik Plateau are comparable to those investigated within this thesis, with a near-vertical headwall, a low gradient slump floor and a steeply sloping evacuation channel leading to a fluvial system. Lacelle *et al* (2010) found an almost two-fold increase in slump initiation from the 1954-1971 period to the 1985-2004 period; however a decrease in the total number of active mature slumps from 46 in 1950 to only 24 in 2004. Since retrogressive thaw slumps

typically remain active for 30-50 years (French and Egginton, 1973), and the annual and summer air temperatures in the decades prior to 1950 were cooler than those recorded between 1970-2000, the presence of thaw slumps could not be directly and solely associated with warmer air temperatures. Lacelle *et al.* (2010) found that the decrease in the number of active slumps could be more closely associated with the 10-year running average rainfall data within the region. Precipitation was therefore linked to the maintenance of the activity of thaw slumps, as it allows the ice to remain exposed in the slump headwalls by transporting sediment out of the slump floor in mudflows. Lacelle *et al.* (2010) infer that the activity of thaw slumps in upland regions could increase should rainfall also increase, by triggering mass-wasting processes such as active layer slides.

2.3 KNOWN EFFECTS OF THAW SLUMPS ON HYDROLOGICAL SYSTEMS

Terrain disturbance due to permafrost thaw presents substantial changes in surface water chemistry and soils (Kokelj & Burn, 2003), since near-surface permafrost is typically rich in solutes. Upon the initiation of disturbance, solutes are transported to lacustrine environments via surface runoff. Kokelj *et al.* (2005) investigated the influence of permafrost disturbance on the water quality of numerous small upland lakes in the Mackenzie Delta region. The study involved 22 lakes, 11 of which were impacted by thaw slumps, while the remainder were in pristine condition. Kokelj *et al.* (2005) found that mean dissolved organic carbon (DOC) levels were much lower in lakes affected by thaw slumps (10.5

mg/l) compared to unimpacted lakes (16.3 mg/l). More striking was the difference in mean concentrations of calcium (72.6 mg/l; 9.2 mg/l), magnesium (26.8 mg/l; 3.6 mg/l) and sulphate (208.2 mg/l; 11.1 mg/l) between the disturbed and undisturbed systems. Kokelj *et al.* (2005) concluded that terrain disturbances occupying as little as 2% of a lake's catchment have the potential to alter the water chemistry not only at the time of disturbance initiation, but for decades following the initial disturbance. In a larger study, Kokelj *et al.* (2009) analyzed water chemistry of 39 undisturbed and 34 slump-affected lakes within a larger area of the tundra uplands. Kokelj *et al.* (2009) once again found a correlation with increased ion concentration and retrogressive thaw slumping. However, organic carbon concentrations were more highly influenced by the surficial deposits of the landscape.

Kokelj *et al.* (2013) investigated increases in stream sediment and solute flux across the Stony Creek watershed (11,000 km^2) of the Peel Plateau, caused by the thawing of massive ground ice in mega slumps. This study is pertinent to this thesis as it investigates the effects of thaw slumps on aquatic systems within the Peel Plateau, but focuses on water quality parameters at a watershed scale. Kokelj *et al.* (2013) hypothesized that thaw slump activity within their study area would have a whole watershed impact through increases in stream sediment and solute concentrations. In addition, they hypothesized that the flux of such material in streams would be controlled by diurnal ground-ice thawing. Kokelj *et al.* (2013) found diurnal water levels in slump-impacted streams to lag peak net radiation by several hours. They also found mega slump activity affected the

timing and magnitude of fine-grained sediment transport in nearby streams. Turbidity and total suspended sediment concentrations in the disturbed streams were 1-3 orders of magnitude higher than those in unaffected streams. Turbidity in these streams sometimes exceeded the instrumental maximum of measurement 2-3 hours after maximum daily solar radiation, whereas in unimpacted streams turbidity levels only exceeded peak measurement capabilities during extreme rainfall events. Specific conductivity was also found to be greater in streams affected by large slumps, which spiked diurnally and during rainfall events. In the Peel Plateau, soluble SO_4 levels in permafrost can be up to two orders of magnitude greater than in the overlying active layer (Kokelj *et al.* 2013; Kokelj and Burn, 2005). Kokelj *et al*. (2013) found concentrations of sulphate in slump runoff to be more than 10 times greater than that of the undisturbed surface waters. Trends of elevated sulphate concentrations within the Peel River are also evident, having doubled over the last 40 years, likely due to dramatic geomorphic processes such as thaw slumps occurring on the terrain (Kokelj *et al.* 2013).

Kokelj *et al.* (2013) also measured the mass-wasting associated with the development of a mega slump to assess the release of sediment from a mega slump. In one instance, a debris flow associated with a mega slump extended 500 m down valley in the span of 3 years. Most of this growth occurred during the summer of 2010, which Kokelj *et al.* (2013) emphasized was the season when measured precipitation (245 mm) was the highest in the entire instrumental

record (1920-2010). Kokelj *et al.* (2013) found no evidence of debris flows of this extent in the aerial photographs examined within their study (1970 & 1972).

Overall, Kokelj *et al.* (2013) were correct in their hypotheses and the catchment scale to which the influence of thaw slumps was discernable was 10^3 km^2. The authors suggested that should summer rain events remain frequent and/or intense, geomorphic activity will increase in glaciogenic landscapes in the future. Malone *et al.* (2013) elaborate on these findings by examining the geochemical evolution of slump runoff to the streams. Malone *et al.* (2013) found that permafrost positioned below the early Holocene thaw unconformity has solute concentrations nearly 100 times higher than those measured in the top 1-2 m of ground. They found that solute concentrations in the runoff from both active and stable slumps are one order of magnitude higher than in undisturbed systems, which can be attributed to lower stratigraphic layers of permafrost exposed in the headwalls of the thaw slumps. Since the thaw slumps degrade permafrost to depths of 10 m or more, their impacts are elevated in comparison to shallow active layer disturbances such as active layer detachment slides.

As ground temperatures in permafrost terrain rise, microbial activity increases leading to the release of greenhouse gases such as CO_2 and methane (CH_4) to the atmosphere (Schuur *et al.* 2008, 2009; Schuur & Abbott 2011; Jensen *et al.* 2014). Though several studies have shown that CO_2 and CH_4 production increase as thermokarst matures on low topography and relief landscapes, little is known of carbon fluxes within large degradational features such as thaw slumps. Jensen *et al.* (2014) conducted studies on a mega slump

in northwestern Alaska, which used a 'space-for-time' substitution they termed, "thaw slump chronosequence", to compare the flux of CO_2 during peak growing seasons of undisturbed terrain, an active thaw slump and an inactive slump. Jensen *et al.* (2014) measured soil organic matter, temperature, moisture and bulk density from each of the three chronosequence stages. The authors found that temperature and moisture content do not largely affect the CO_2 flux to the atmosphere, but rather it is the physical and chemical properties, which are strongly related. The authors found that since retrogressive thaw slumps typically occur in conditions with low organic matter, low vegetation coverage and high bulk densities, the flux of CO_2 is quite limited despite the exposure and elevated temperature of the soil. This study, by Jensen *et al.* (2014), places emphasis on the amount of knowledge yet to be gained on these large terrain disturbances, as the changes in climate continue to accelerate the areal extent of thermokarst features in this environment.

2.4 EXAMINING DISTURBANCE IN LACUSTRINE SEDIMENTS

Determining the frequency and magnitude of geomorphic events is an important area of research in geomorphic studies and may be of increasing significance under a rapidly changing climate (Gilbert, 2006). Earth-surface processes are occurring at larger and more frequent extremes and such changes must be recognized while observing proxies in order to understand their impacts in comparison with average or standard processes (Lamoureux *et al.* 2001).

Comparable lacustrine studies of large-scale geomorphic events have been conducted, but only recently do they include retrogressive thaw slumps. Gilbert *et al.* (2006) investigated the record of an extreme flood in the sediments of a montane lake in British Columbia. The study involved the extraction of cores taken from 7 different locations throughout the lake, with replicate cores taken from several of the locations to confirm that those analyzed sufficiently represented deposition at their locations. The sediment deposited in the lake as a result of the flood was clearly distinguishable throughout the cores through the analysis of physical characteristics such as texture, colour, magnetic properties, organic content and grain size stratigraphy. Gilbert *et al.* (2006) determined that as much as 8-12 times more sediment was deposited in the central portion of the lake that year due to the short-lived, but extreme flood event. Such observations highlighted the importance of high magnitude events within environmental systems. However, Gilbert *et al*. (2006) emphasize that the character of the deposits varied by location within the lake basin, as they demonstrated that in some core sites the flood record was not as pronounced and in others the record was completely absent. Therefore, without an appropriate sampling strategy, the significance of major events can easily be overlooked. Gilbert *et al.* (2006) concluded that in order to successfully characterize catastrophic events and assess their importance using paleolimnological methods two elements are crucial, (1) replicate sampling (stratified by depositional environment) and (2) an understanding of the sedimentary processes that produced, delivered and created the deposits.

Lamoureux and Lafrenière (2009) examined widespread active-layer detachments (a total of 25) across a watershed caused by the combination of continuous high temperatures and rainfall at Cape Bounty, Melville Island. The study found that the immediate impacts of the detachments were abrupt and short-lived increases in the turbidity of affected rivers with continuous and gradual increases in discharge and overall turbidity. Pulses of high sediment volume were also observed, which amounted to 18% of seasonal yield within one week (Lamoureux and Lafrenière, 2009). Lamoureux and Lafrenière (2009) concluded that while the active-layer detachments had a significant and immediate impact on the fluvial conditions, the erosion of unstable material caused by the detachments had a continuous impact on sediment fluxes within the watershed for several years or decades. Despite the fact that the authors did not utilize paleolimnological methods within their research, the implications of their study are still significant to this research. It would be reasonable to assume that the effects of the occurrence of a retrogressive thaw slump may be observed long after the slump has stabilized, as seen in the active-layer detachments. This may pose significant challenges in effectively distinguishing the stratification of the sediment core during which the slump occurred and was active, from when it became stabilized but remaining unstable material was being deposited. Such a challenge highlights the importance of understanding the full system prior to conducting analysis and drawing conclusions. External, erosional processes must be determined in order to efficiently characterize the impacts on downstream sediment records.

Thienpont *et al.* (2013) examined the response of aquatic systems to permafrost degradation using paleolimnological methods. The study examined thaw slump disturbance directly. The authors looked at the impact of thaw slumping on Arctic freshwater ecosystems using diatoms. They found that slump-affected lakes displayed greater biological change than undisturbed systems. Although diatom response was variable due to factors such as severity and extent of disturbance, the overall findings established that retrogressive thaw slumps can alter the limnology of lakes, placing stress on their biological communities. It is unclear, however, if these results reflect solely the influence of the thawing permafrost slumps, or also the impacts of a warming climate. Due to natural variability in lake ecosystems, it is difficult to precisely define the effects of thaw slumps on aquatic biota. The paloelimnological analyses by Thienpont *et al.* (2013) revealed that there are a number of biological changes to aquatic systems that arise from permafrost degradation and these changes reflect the magnitude of the disturbance as well as the nature of the affected area.

A large storm surge led to a major saltwater intrusion on a coastal ecosystem of the northern Mackenzie Delta, adjacent to the Arctic Ocean in 1999 (Kokelj *et al.* 2012). This low frequency, high magnitude event was thoroughly investigated using paleoecological techniques (Pisaric *et al.* 2011; Thienpont *et al.* 2012; Deasley *et al.* 2012; Vermaire *et al.* 2013). Pisaric *et al.* (2011) utilized paleoecological techniques to determine the frequency and magnitude of such large-scale events, historically and contemporarily and their associated impacts. Annually resolved dendrochronological and decadally resolved subfossil diatom

records revealed that a flood of the magnitude and ecological impact of the 1999 storm surge had not occurred during the past millennium. Using Pb-210 dating, the timing of a major shift between freshwater and brackish water taxa of diatom assemblages was identified to be consistent with the 1999 storm surge displaying the immediate and remarkable impact of the inundation on the local ecology. Furthermore, Pisaric et al. (2011) document a continued abundance of brackish water taxa and high lake water salinity, suggesting that the ecosystem has not yet recovered from this event.

Pisaric *et al.* (2011) demonstrate the importance of understanding low frequency and high magnitude events in Earth System science, as their effects may be of consequence for unknown periods of time. The authors highlight the importance of an understanding of events of this nature to effectively predict and monitor ecosystem changes in association with a changing climate.

2.5 SUMMARY OF RELEVANT LITERATURE

Amplified climate warming in the western Arctic has lead to increases in ground temperatures (Smith *et al.* 2010), degradation of permafrost, and the development of thermokarst terrain. Retrogressive thaw slumps represent one of the most rapid erosive features in present-day periglacial environments (French, 2007). Thaw slumps remain active as long as ice within the headwall is exposed and precipitation available to transport sediment out of the slump floor (Lacelle *et al.* 2010). There are many known effects of thaw slumps on hydrological systems. Changes in water quality include increases in turbidity, total suspended

sediment concentrations and solutes; decreases in mean DOC levels and increases in specific conductivity and sulphates. Kokelj *et al.* (2013) found that these effects may be felt at a watershed scale and may be observed long after the thaw slump has stabilized.

As climatic changes persist, the importance of understanding low frequency and high magnitude events (such as large disturbances) in Earth System science increases. With appropriate sampling strategies, paleolimnological methods may be applied to examine landscape disturbances in lacustrine sediments. However, in order to do so efficiently, an understanding of the sedimentary processes that produced, delivered and created the deposits is crucial.

CHAPTER THREE

STUDY AREA AND METHODS

3.1 NATURE OF THE TERRAIN

The Peel Plateau consists of the rolling uplands along the eastern fringes of the Richardson Mountains in the Northwest Territories, covering an area of about 24,000 km^2. The Plateau itself is an erosional remnant of Cretaceous origin with resistant sandstone platforms exceeding 900 m in elevation (Pyle *et al.* 2006). These Cretaceous terraces are underlain by a succession almost 2,000 m in thickness of Devonian- Carboniferous origin, which in turn is underlain by Proterozoic sedimentary rocks (Government of the Yukon, 2000). The area is bordered by the Richardson Mountains to the west, the Mackenzie Mountains in the south and the lower lying Peel Plain to the east (Figure 3.1).

Richardson Mountains formed the western boundary of ice cover during the Wisconsinan glaciation. The region was largely covered with Laurentide ice throughout this period, which reached its maximum extent about 30,000 B.P (Murton, 2009). Glacial retreat began around 15,000 B.P and the area is estimated to have been ice-free within approximately 2,000 years (Dyke *et al.* 2004). Surficial deposits in the Peel Plateau are therefore mostly glacial in origin. These glaciofluvial, glaciolacustrine and morainal sediments may be characterized as mixed, fine-grained and ice-rich (Dixon *et al.* 1992). The remaining deposits constitute postglacial alluvium and colluvium, the latter

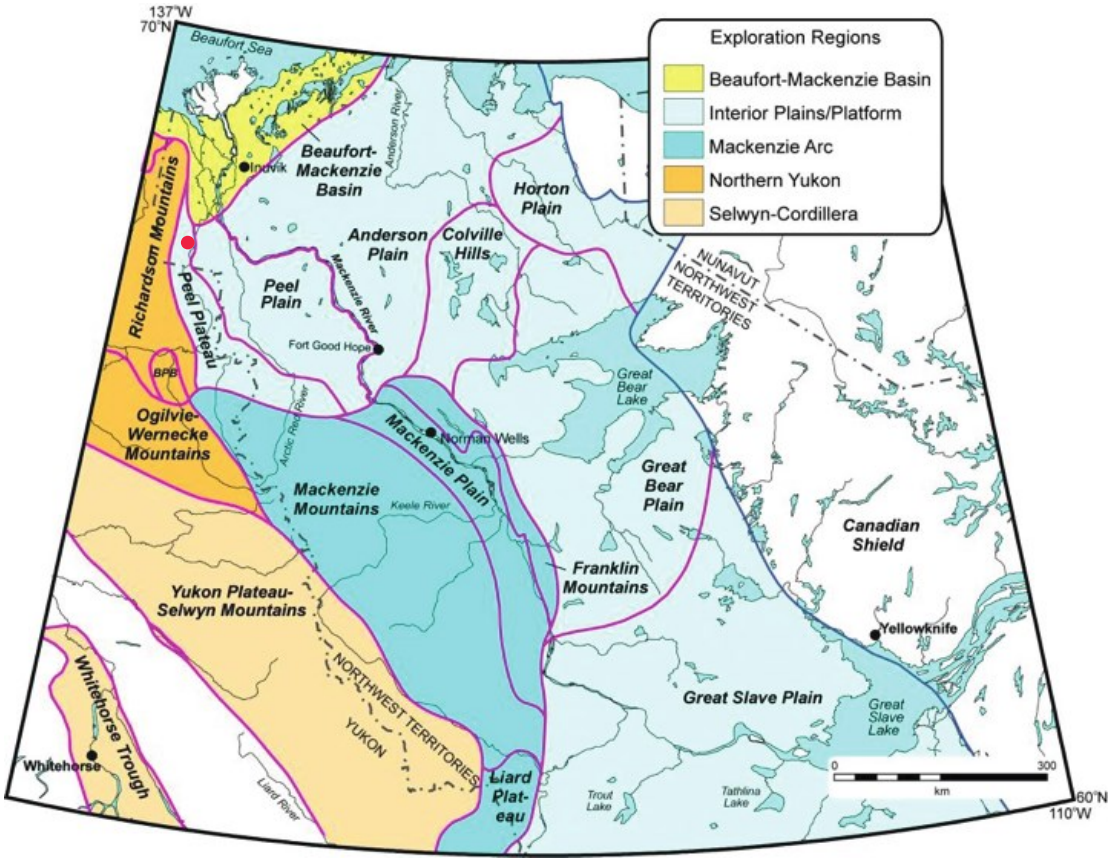

Figure 3.1: Location of the Peel Plateau.
The Peel Plateau (upper right) spans the border between Yukon and the Northwest Territories, east of the Richardson Mountains and north of the Mackenzie Mountains. The Peel Plateau is part of the Interior Plains Platform ecoregion and the study site is indicated by a red dot (Northwest Territories Geological Survey, 2014).

located on valley sides and foothills and the former primarily along streambeds (Government of Yukon, 2000).

Sedimentary rocks dominate the landscape, releasing large amounts of carbonate into the hydrological system. Over the past 40 years, the concentration of dissolved calcium, sulphate and magnesium have increased in the Peel watershed during all seasons (Stantec, 2012). This indicates changes in the landscape of the watershed and that previously unweathered and unexposed material has become available to be carried from the land to the water by runoff events (Stantec, 2012).

Due to former glaciation, a variety of parent materials were available for soil formation in the area, the majority derived from shield bedrock to the east. Soils are generally classified as Orthic or Brunisolic Turbic Cryosols and vary in texture depending on the parent material (Smith *et al.* 2004). Those of glaciolacustrine origin in locations of ancient glacial lakes tend to be more fine grained and moist with Gleysolic development, whereas soils with glaciofluvial or morainal parent material have larger grain sizes and in turn support different types of vegetation due to better drainage (Smith *et al.* 2004).

3.2 PRESENT ECOLOGY

Fine-textured poorly drained tills are characteristic of *Picea mariana* (black spruce) dominated forests with *Larix laricina* (larch), *Salix sp.* (willow), *Vaccinium vitis-idaea* (mountain cranberry), *Rubus chamaemorus* (cloudberry),

Rhododendron tomentosum (syn. Ledum palustre) (Labrador tea), *Arctostaphylos uva-ursi* (bearberry) and lichen occurring on these substrates. In more efficiently drained soils on alluvial terraces, slopes and along rivers, growth conditions are more favorable and *Picea glauca* (white spruce) stands dominate with *Alnus viridis subsp. crispa (A. crispa)* (mountain alder), *Equisetum* (horsetail) and a variety of mosses (Smith *et al.* 2004). Higher elevations are dominated by shrub communities and are associated with hummocky terrain containing *Betula nana* (dwarf birch), Labrador tea, cloudberry, *Vaccinium uliginosum L.* (alpine blueberry), mountain cranberry, mosses, sedges and lichen (Stanek *et al.* 1981). Hummocks are common on the terrain of finer-grained soils such as turbic cryosols and are the product of severe frost churning or cryoturbation.

Wildlife on the Plateau is diverse and includes mammals such as *Ovis dalli* (sheep), *Rangifer tarandus granti* (porcupine caribou), *Ursus americanus* (black bear), *Ursos arctos horribilis* (grizzly bear), *Lynx canadensis* (lynx), *Canis lupus* (wolves), *Puma concolor* (cougars) and *Gulo gulo* (wolverines). The Peel watershed is home to over 24 species of fish, including but not limited to, *Coregonus nasus* (broad whitefish), *Coregonus clupeaformis* (lake whitefish), *Thymallus arcticus* (arctic grayling), *Sander vitreus* (walleye), *Salvelinus namaycush* (lake trout) and *Esox lucius* (northern pike) (Stantec, 2012).

3.3 LOCAL HYDROLOGY

The Peel River runs through Peel Plateau parallel to Richardson Mountains and originated as a meltwater channel of receding Laurentide Ice

(Smith *et al.* 2004). The river has cut a 30 m canyon into the landscape at points within this area and drains an area of approximately 77,000 km^2 (Figure 1.1). The Peel River is a tributary of the Mackenzie River and its tributaries within the Plateau include Trail, Road, Vittrekwa and Caribou rivers, all of which originate in Mackenzie Mountains. At its headwaters, the Peel is fed by much larger systems such as the Ogilvie, Blackstone, Snake, Wind, and Bonnet Plume rivers (CPAWSYukon.org, 2014). A recent report by Stantec produced for Aboriginal Affairs and Northern Development Canada (AANDC) reported a gradual warming within the watershed over the past 40 years. This warming has been manifested as increased flow rates of the Peel River during the winter season, with averages from 2005-2010 (150 m^3/s) doubling those recorded in the 1970's (75 m^3/s). Flow rates are continuously higher later into the fall, while flow rates have decreased in the month of June, as there is less sustained flow during early summer.

High runoff due to the morphology of the landscape produces continuous changes in flow rates of the Peel watershed hydrological system. An increase in water flow coincides with an increase in suspended sediment within the water column. The sand, silt and clay within the Peel River contain metals, which during periods of high flow are well above government standards for the well being of aquatic species, however since this is due to natural processes it is assumed that the native species have adapted (Stantec, 2012). For example, at peak flow levels of copper approach 40 µg/L (guideline value: 3-4 µg/L); levels of aluminum reach 12800 µg/L (guideline value: 100 µg/L); and zinc reaches 198

µg/L (guideline value: 30 µg/L). As mentioned previously, the Peel watershed contains high amounts of potassium, chloride and sodium (Stantec, 2012). The quantity of major dissolved ion concentrations also vary with changes in seasonal flow, with most being at their lowest levels during the spring, increasing throughout the summer and peaking during the winter months.

Numerous small lakes and ponds dot Peel Plateau. The scarcity of wetlands and presence of continuous permafrost limit the storage of melt-water resulting in a spring freshet that varies in initiation time every year (typically occurring during the month of May or early June) (Stantec, 2012). Streamflow peaks a few weeks following snowmelt, which can sometimes be surpassed by summer rain events, depending on stream size (smaller streams reach peak flow due to rainfall events more commonly).

3.4 RECENT CLIMATE

Continuous permafrost underlies this area, and ice-rich ground is common in the near-surface layers (Smith *et al*. 2004). The thickness of permafrost extends to 300 m in the nearby Richardson Mountains and 100 m at Inuvik (Smith and Burgess, 2000). The most significant contributing factor to the presence and maintenance of permafrost is the climate. The region has long cold winters and short summers. Mean annual air temperature at Fort McPherson (1986-2007) was -6.2 ˚C and total annual precipitation at Fort McPherson from 1986 to 2007 averaged 306 mm (Figure 3.2), of which more than half fell as rain. Large summer rainstorms can also occur and maximum

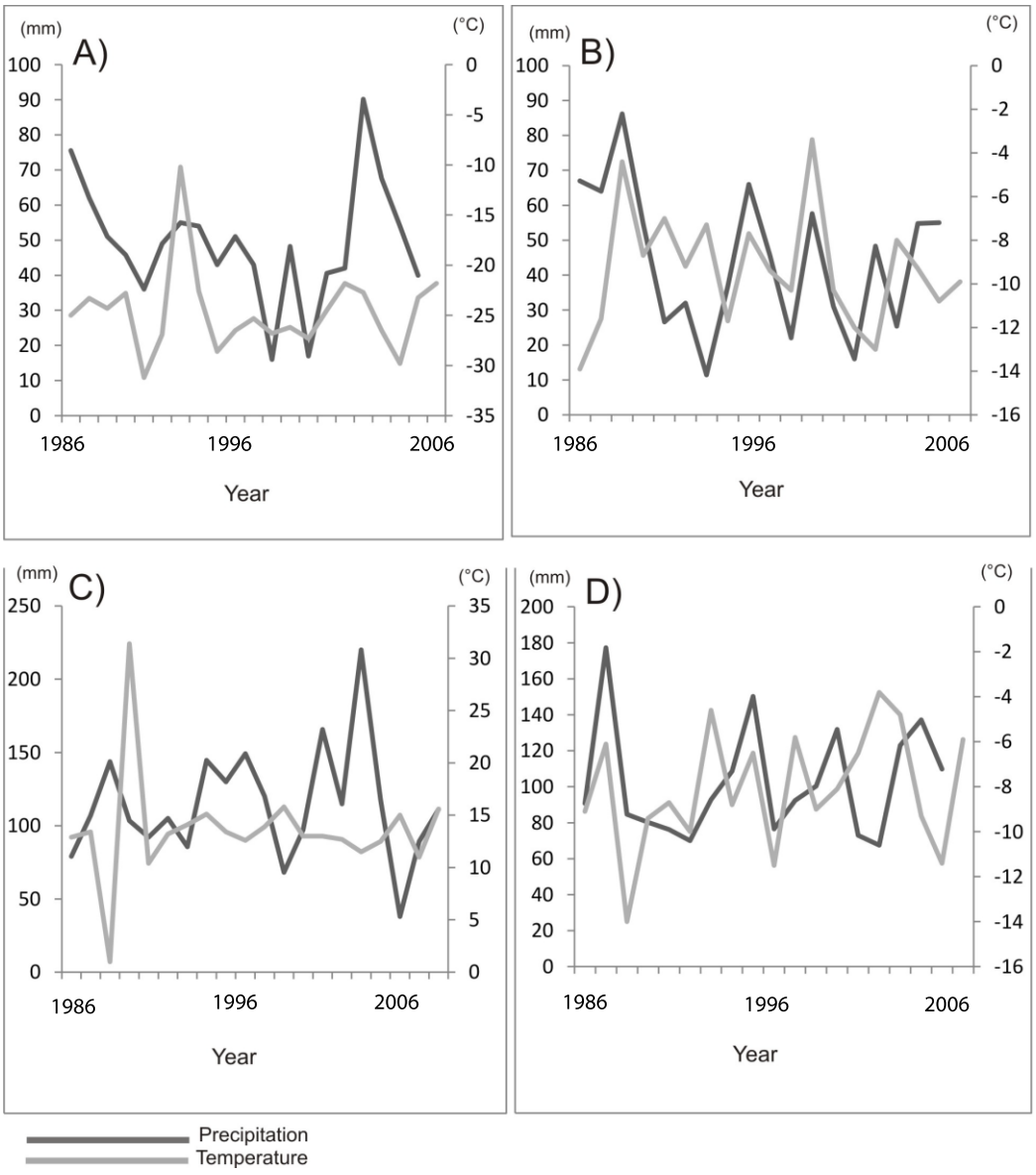

Figure 3.2: Seasonal climographs for Fort McPherson, Northwest Territories.

A) Winter (DJF); B) spring (MAM); C) summer (JJA); D) autumn (SON). Temperature data (°C) is displayed as seasonal averages (light grey line) shown on the right (secondary) vertical axis and mean seasonal precipitation (mm) (dark grey line) is measured by the left (primary) vertical axis. Missing data was omitted rather than interpolated. The coldest season recorded within this time frame (mean air temperature: -31.2°C) was in the winter of 1990, while the warmest (mean air temperature: 30.4°C) was the summer of 1990.

annual rainfall can approach 250 mm (Kokelj *et al.* 2013). The past decade has seen three of the five wettest summers since 1920 (Kokelj *et al.* 2013).

3.5 SITE DESCRIPTION

Lake selection for the current study was based on previous research at a small lake informally named FM1 (67˚ 33' 12"N, 135˚ 12' 14"W) (Figure 1.4). This previous work examined a short, 24 cm long surface core (FM1-KB2) from lake FM1 and was completed as part of my undergraduate thesis in 2011, under the supervision of Dr. Michael Pisaric. ^{210}Pb dating was conducted on 15 samples selected throughout the FM1-KB2 sediment core (Appendix I). Results of the ^{210}Pb dating were inconclusive since background levels were not reached in the deepest sediment samples that were submitted. Therefore, other means of dating the sediment cores and thaw slump activity had to be explored. The current project has expanded to include a longer record from FM1 and a study on Husky Lake (67˚31'33"N, 135˚08'14"W) (Figure 3.3), which is located immediately south of lake FM1 (Figure 3.4). Both lakes are surrounded by open, stunted stands of black spruce, white spruce, dwarf birch, willow and mountain alder.

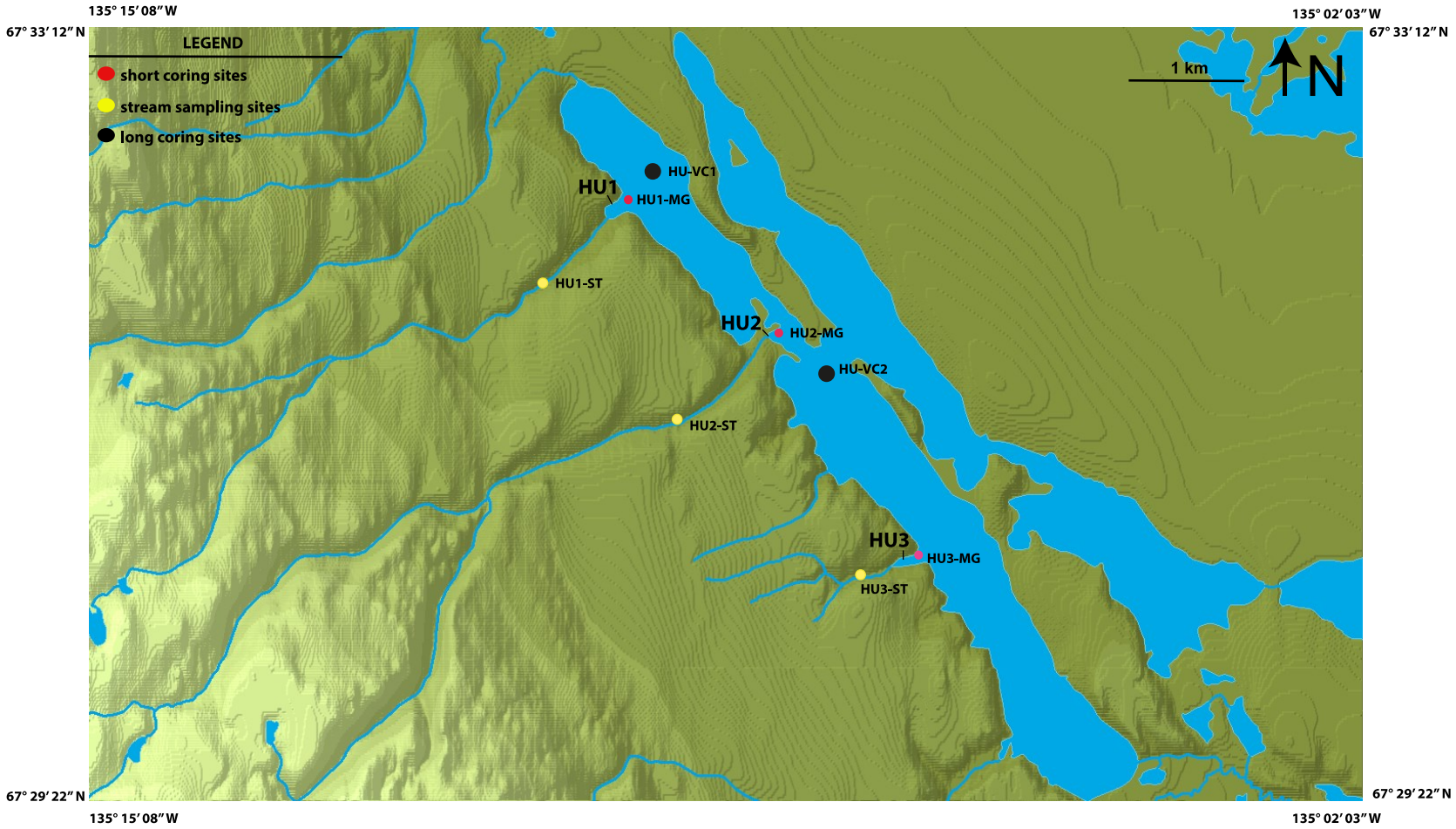

Figure 3.3: Map of study area- Husky Lake.
All studied basins of Husky Lake are labeled: HU1, HU2 & HU3; along with the stream sampling sites HU1-ST; HU2-ST & HU3-ST. The locations of long cores are labeled with black circles and short cores with red circles. HU1 & HU3 are undisturbed stream and lake basins, whereas HU2 is impacted by a thaw slump. The elevation ranges from 17m a.s.l at the lake and ~280m a.s.l in the upper ranges to the west.

Figure 3.4: Aerial view of lake FM1 and the northern tip of Husky Lake. The view is looking towards the southeast; FM1 is in the foreground and the west arm of Husky Lake is at the right of the photograph. The sediment-loaded waters of FM1 are clearly visible. A Crow's Foot delta can be seen jutting into the west arm of Husky Lake near the top right of the photograph. Photograph courtesy of Michael Pisaric.

The FM1 study area includes a very large retrogressive thaw slump (~10 ha; Table 3.1) with a debris flow that has infilled about 1 km of stream valley within the upper catchment of the lake (Figure 3.5). Several small slumps have also initiated along the infilled valley due to mechanical erosion by the stream pushing up against the valley side, causing further slope erosion and slump expansion (Figure 3.6). The primary thaw slump (67° 31' 10" N, 135° 18' 16"W) is located approximately 8.5 km upstream from the lake at an elevation of approximately 265 m a.s.l.. The slump is increasing in size, loading thawed material into the small stream, which is as a result, subject to occasional small-scale damming (Figure 3.7). The sediment-loaded stream flows down through the valley and into FM1, where the sediment is ultimately deposited. Based on aerial photographs, the slump affecting FM1 became active between 1969 and 1990. Though the slump is not visible in airphotos from 1969 or 1990 (Appendix II), the difference in the colour of FM1 waters between the two airphotos is striking and indicates an increase in sediment input to lake FM1. Lake FM1 has a surface area of ~6 ha (Table 3.1) and has a maximum depth of 1.2 m.

Husky Lake is much larger in comparison (Figure 3.8), with an approximate area of 895 ha. Due to the morphology of the lake and the purpose of this research, only the western arm of the lake was investigated, as it lies adjacent to the uplands of the Peel Plateau from which streams flow into the small basins of the lake.

Figure 3.5: Infilled stream valley at the FM1 study site
Photograph courtesy of Michael Pisaric shows the extent of sediment transport from the retrogressive thaw slump upstream from lake FM1. Sediment from this valley infill is flowing downstream into the lake. In the left of the photo, the outlets of the secondary slumps can be seen.

Figure 3.6: Retrogressive thaw slump at the FM1 study site.
The thaw slump affecting lake FM1 can be seen in this photograph courtesy of Michael Pisaric from 2012. To the left the stream valley with the secondary thaw slumps are present and at the bottom a small lake is present very close to the primary disturbance.

Figure 3.7: Aerial view of the slump and debris flow at the FM1 site. Photograph from August 2011 displays the primary slump in the top right, the 2 secondary slumps to the left and the debris flow moving down the small valley.

Figure 3.8: Aerial view of Husky Lake.
Photograph of Husky Lake looking towards the southeast. The basin of the undisturbed site HU1 is visible in the bottom and the Crow's Foot delta of the disturbed site of HU2 can be seen jutting into the western basin of Husky Lake in the right-centre of the photograph.

Table 3.1: FM1 & Husky Lake morphometrics.
Lake FM1 is smaller than the disturbance within its upper catchment. The lake consists of a much smaller portion of the catchment in comparison to the Husky Lake system, however the disturbance size is much greater in relation to catchment size than that of Husky Lake.

STUDY SITE	CATCHMENT AREA (ha)	LAKE AREA (ha)	DISTURBANCE AREA (ha)	LAKE TO CATCHMENT RATIO	LAKE TO DISTURBANCE RATIO	DISTURBANCE TO CATCHMENT RATIO
FM1	803	6	10	1: 133	1:1.7	1: 80
HUSKY	6973	895	6	1: 7.8	149:1	1: 1,162

Three of these streams and their respective basins were investigated for this study, two of which are undisturbed systems and one of which has a thaw slump in its upper catchment. The undisturbed systems were labeled HU1 (north Husky) and HU3 (south Husky). The disturbed system with the thaw slump within its upper catchment was labeled HU2 (Figure 3.3). This slump is located approximately 6.5 km upstream from the lake basin at an elevation of 277 m above sea level. A Crow's Foot delta has formed at the mouth of the impacted stream in the lake basin (Figure 3.8). According to bathymetric profiling, Husky Lake appears to have formed from an old river channel, which was likely the remnant of an old meltwater channel formed during the recession of Laurentide ice. The maximum depth of this presumed former channel is ~16 m and it vertically dissects the western portion of the lake from North to South (Figure 3.9).

3.6 FIELD METHODS

Fieldwork for the current research took place at FM1 and Husky Lakes in 2011 and 2012. The lakes were visited in the summers of 2011 and 2012 to deploy sediment traps and carry out bathymetric surveys of the lake bottoms. In April 2012, both lakes were visited to collect sediment samples using the ice cover as the coring platform.

3.6.1 BATHYMETRIC PROFILING

A bathymetric survey of the studied portion of Husky Lake was conducted in June 2012. This was completed with the use of a depth sounder, a timer and a GPS unit. Travelling in a 15 ft Lund boat, a zig-zag pattern was made across the western side of the lake. Depth, GPS coordinates and time were recorded every 5 seconds in order to profile the bathymetry of the lake bottom (Figure 3.9).

3.6.2 SEDIMENT TRAPS

Sediment traps were deployed to characterize the type and quantity of sediment entering the study lakes from streams with and without active thaw slumps in their catchments. The sediment traps were deployed over the winter of 2011-12 and during the summer of 2012. The purpose of using sediment traps was to provide insight into seasonal (short-term) sediment deposition in the lakes. Kokelj *et al.* (2013) found that total suspended sediment concentrations in slump affected streams were 1-3 orders of magnitude higher than that within unimpacted streams. The design of the sediment traps followed that of Cockburn and Lamoureux (2008) and consisted of the elements illustrated in Figure 3.10. Upon deployment, water depths were measured from the surface of the lake in order to ensure that the sediment trap line was an appropriate length to accommodate for the ice accumulation throughout the winter season; however short enough that the line would be sufficiently taut to avoid being tipped horizontally.

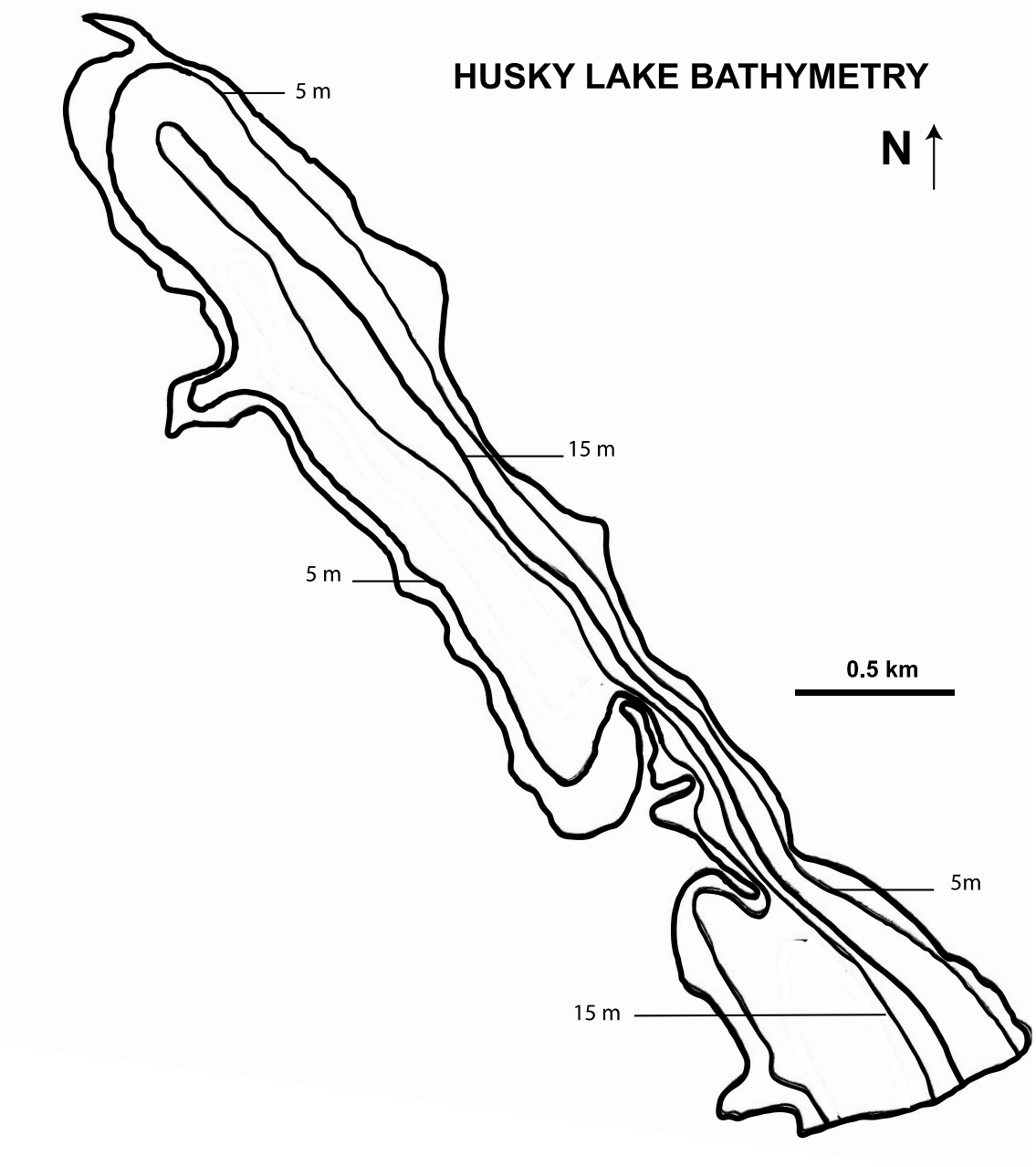

Figure 3.9: Measured bathymetry of the western arm of Husky Lake.

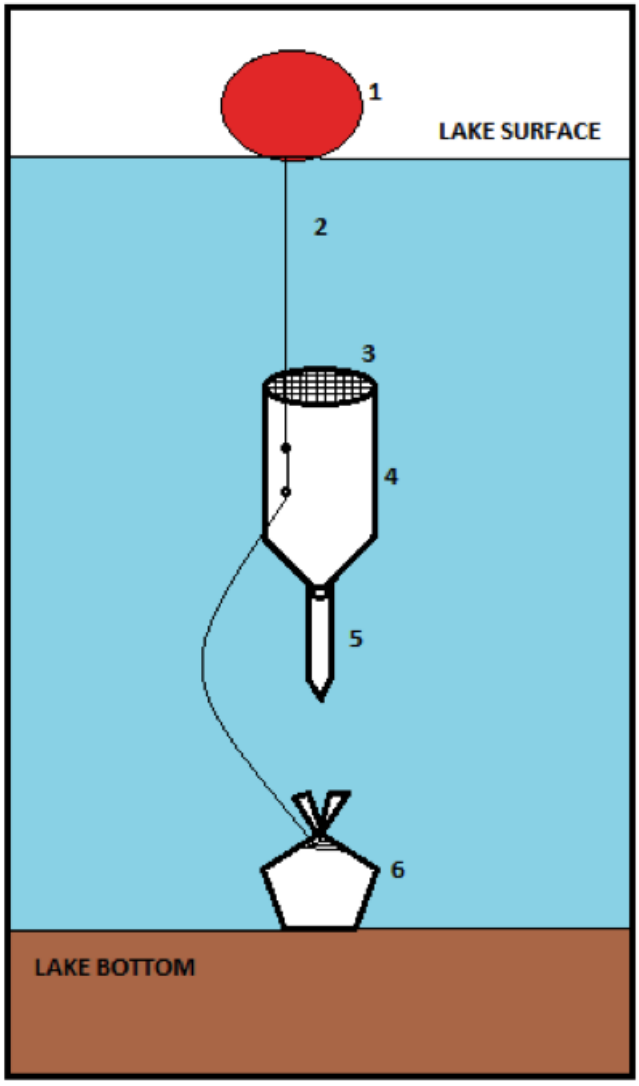

Figure 3.10: Diagram of sediment trap design.
The sediment trap consisted of six main parts: 1) buoy to keep the sediment trap upright in the water column; 2) wire line to attach the buoy, sediment trap and weight; 3) chicken wire grid cut to fit the opening in the top of the trap to prevent any large debris from entering and plugging the sediment collection tube; 4) 2 litre bottle with the bottom cut off to act as a funnel. The open top of the funnel collects sediment into the collection tube at the bottom of the sediment trap; 5) plastic centrifuge tube that acts as the sediment collection tube; and 6) large rocks wrapped in a feedbag to keep the sediment trap anchored in place.

Five sediment traps were deployed throughout Lake FM1 on August 29th 2011 (Figure 3.11) and collected on June 9th 2012. Due to uncertainty in the scope of the research at the time of trap deployment in August 2011, no traps were deployed in Husky Lake for the winter season. The samples from the winter season sediment traps deployed at FM1 were lost and will not be considered further. Summer season sediment traps were deployed in Husky Lake and FM1 on June 9th, 2012 and successfully retrieved August 24th, 2012. The traps were deployed at the coordinates listed in Table 3.2. Water was removed from the trap and Zorbitrol was applied to the top of the sediment to absorb any water and seal it for transport (Tomkins *et al.* 2008). The traps were transported back to Carleton University upon return from fieldwork.

3.6.3 CORE COLLECTION

Sediment cores HU-VC1 and HU-VC2 were collected from the surface of the ice on Husky Lake using a vibracorer (Figure 3.12) in April 2012. HU-VC1, measuring 180 cm in length, was collected from the northern portion of Husky Lake (Table 3.2, Figure 3.3). HU-VC2, measuring 205.5 cm in length, was collected from the central portion of Husky Lake (Table 3.2, Figure 3.3). The vibracorer consisted of a concrete vibrator powered by a small generator and mounted onto an aluminum core tube. A 1 m^2 hole was cut through the ice (ice thickness ~1.8 m) using an ice auger and ice blocks were removed from the hole using ice screws. The corer was then submerged into the water and secured to the surface by a cable attached to a metal frame with a winch for extraction.

Figure 3.11: Photograph of a sediment trap.
Stephen Tetlichi (resident of Fort McPherson, field assistant and wildlife guide) is seen in this photograph displaying one of the sediment traps deployed in lake FM1 in August of 2011.

Table 3.2: Sediment trap and core locations.
Geographic coordinates of the sediment traps deployed in FM1 and Husky Lake. The condition of the site is listed as either disturbed or undisturbed.

FM1 trap IDs (winter & summer season)	Sediment Trap Coordinates
FM1-SED1 (disturbed)	67° 33' 16" N 135° 12' 13" W
FM1-SED2 (disturbed)	67° 33' 13" N 135° 12' 09" W
FM1-SED3 (disturbed)	67° 33' 11" N 135° 12' 04" W
FM1-SED4 (disturbed)	67° 33' 10" N 135° 12' 10" W
FM1-SED5 (disturbed)	67° 33' 13" N 135° 12' 17" W
Husky Lake trap IDs (summer season)	
HU1-SED1 (undisturbed)	67° 32' 14" N 135° 11' 7" W
HU1-SED2 (undisturbed)	67° 32' 14" N 135° 11' 7" W
HU1-SED3 (undisturbed)	67° 32' 14" N 135° 11' 6" W
HU1-SED4 (undisturbed)	67° 32' 26" N 135° 10' 40"W
HU2-SED1 (disturbed)	67° 31' 38" N 135° 8' 56" W
HU2-SED2 (disturbed)	67° 31' 25" N 135° 8' 56" W
HU2-SED3 (disturbed)	67° 31' 38" N 135° 8' 54" W
HU3-SED1 (undisturbed)	67° 30' 29" N 135° 7' 33" W
HU3-SED2 (undisturbed)	67° 30' 30" N 135° 7' 31" W
HU3-SED3 (undisturbed)	67° 30' 49" N 135° 7' 29" W
HU3-SED4 (undisturbed)	67° 30' 39" N 135° 6' 48" W
Husky Lake & FM1 core IDs	**Core Coordinates**
HU-VC1 (undisturbed)	67˚ 32' 23" N, 135˚ 10' 28" W
HU-VC2 (disturbed)	67˚ 31' 44" N, 135˚8' 56"W
HU1-MG (undisturbed)	67° 32' 13" N, 135° 11' 07" W
HU2-MG (disturbed)	67° 3' 39" N 135°08' 53" W
HU3-MG (undisturbed)	67° 30' 30" N, 135° 07' 29" W
FM1 (disturbed)	67˚33'13" N, 135˚12'11" W

Figure 3.12: Vibracorer coring device.
This photograph (courtesy of Dr. Scott Lamoureux, Queens University) shows the concrete vibrator mounted on the top of an aluminum core tube. The metal frame with the winch used for extraction can be seen in the top right of the photograph.

A vibracorer operates as its name implies. High frequency, low magnitude standing waves vibrate down the length of the tube, which liquefy a thin layer of sediment at the sediment-water interface and allow the tube to penetrate the sediment column with little force (Glew *et al.* 2001). The weight of the concrete vibrator on the aluminum tube also eases this process. The corer is pulled out of the sediment by winding up the cable using the winch then sealed at each end by dusting Zorbitrol® over the sediment to absorb remaining water and capped using core plugs (Tomkins *et al.* 2008). Once back in the laboratory, core tubes were cut in half using a skill saw with an abrasive blade and the sediment was subsampled at 0.5 cm intervals and stored in Whirlpak® bags at the Carleton University Paleoecology Laboratory in a walk-in cooler at 4°C until further analysis. The vibracorer was selected as a tool for core collection since it can be used to sample a wide variety of sediment types, can penetrate the sediment to sufficient depths (typically 1 – 15 m) (Last and Smol, 2001) and was readily available for use in this research. The primary downfalls of using a vibracorer are the disturbance of the sediment in the top few centimetres of the core near the sediment-water interface (due to the vibration mixing the watery sediment) and sediment compaction downcore.

The sediment core from FM1 was collected in April, 2011 from the centre of the lake (Table 3.2) using a PVC pipe and core catcher. The core measured 78 cm in length and was kept frozen to be later extruded using a table saw and subsampled at 0.5 cm intervals using a bandsaw. Subsampled material was

stored in Whirlpak ® bags at 4°C at the Carleton University Paleoecology Laboratory until analysis.

Three shorter cores were collected from Husky Lake in August 2012 using a Maxi-Glew Corer (Glew *et al.* 2001): HU1-MG, HU2-MG, & HU3-MG (Table 3.2). These cores were collected from the middle of each basin in order to characterize the surface sediments without the difficulties in preserving the sediment-water interface that are common when using other coring devices such as the vibracorer. These cores were subsampled at 0.5 cm intervals in the field using a core extruder (Glew *et al.* 2001) and transported to Carleton University for analysis.

3.6.4 WATER QUALITY

Large retrogressive thaw slumps and their concurrent debris flows cause significant increases in concentrations of solutes and suspended sediment in the streams they impact (Kokelj et al 2013). Such increases in solute concentrations can be seen within the Peel River due to large-scale slump disturbances within its catchment, which encompasses approximately 70,000 km^2 (Kokelj *et al.* 2013).

In order to examine the impacts of thaw slumping on water quality in FM1 and Husky Lake, various monitoring efforts were conducted. This was done in order to gain a full system understanding of the two studied lakes. YSI Multiparameter Sondes (600OMS) were deployed within the three studied basins at Husky Lake (HU1, HU2, HU3; 67° 32’ 14.6” N, 135° 11’ 07.1” W; 67° 31’ 39.1”

N, 135° 08’ 55.6” W; 67° 30’ 30.9” N, 135° 07’ 29.2” W, respectively) during the months of June- August 2012 (inclusive). These water quality loggers are equipped with water level, specific conductivity, pH and turbidity sensors. The range of the conductivity sensor is 0-100,000 μs/cm with an accuracy of +/- 0.5%. The accuracy of the water level sensor is +/- 0.003 m and the turbidity sensor has an accuracy of +/- 2% and a range of 0-1000 nephelometric turbidity units (NTU) (Kokelj *et al.* 2013). The YSIs were anchored with cinderblocks and secured using cable to 2 buoys per unit, in order to record parameters of water chemistry, quality and changes in sediment influx from stream flows. The multi parameter sondes were set to record data every hour to obtain data on a diurnal resolution. Upon the collection of the YSI units in August 2012, the YSI at HU2 (disturbed site) was found on the adjacent shore of the lake. Due to the fact that this unit was displaced and that the primary purpose of using the YSI was to gather data to compare the disturbed site’s water quality to that of the undisturbed, this data was not included in this thesis.

The three examined streams of Husky Lake (HU1-ST, HU2-ST, HU3-ST) were also monitored during field sessions through the collection of water samples and the calculation of velocity profiles of stream flow at the determined sampling sites (Figure 3.3).

Water quality parameters were also monitored through the collection of samples at the sediment trap sites within Husky Lake using a Van Dorn Sampler. Such sampling was primarily implemented in order to examine the difference between water chemistry within the proximal and distal sections of the lake, or

more specifically, the impact of the sedimentary effects of the thaw slump on the lake. The use of the Van Dorn Sampler also allowed for the examination of water quality at differing depths within the lake. Samples were taken from these sites at every 3 m depth providing data on stratification within the water column.

Water quality monitoring was also conducted at FM1; however since the effects of the FM1 slump were visibly evident given the colour of the lake (Figure 3.4) and accessibility was limited due to distance from the field campsite; the sampling methodology had to be less extensive and limited to the collection of random water samples.

3.7 LABORATORY METHODS

Several methods have been developed for laboratory analysis of lacustrine sediments and are used in order to analyze changes in sediment strata. Analyses are done throughout the depth of the sample to interpolate changes to the outer controls and processes of the environmental system.

3.7.1 LOSS-ON-IGNITION

Loss-on-ignition (LOI) has become a widely used method in paleoecological studies to provide an estimate of the organic and carbonate content of sediments. The results of calculated mass LOI of organic matter from lake sediments are largely controlled by changes in sediment composition and the patterns of sediment accumulation within the lake environment. Lake productivity, inorganic inputs, decomposition, basin morphology and water levels

can all impact organic and carbonate content of sediment; however at a larger scale, climatic changes influence all such factors (Shuman, 2003). Rowan *et al.* (1992) illustrate that inorganic inputs play a large role in sediment composition that often outweighs the influences of lake trophic status. Such inorganic inputs are often the result of shoreline erosion or, as applied to this study, upland inputs caused by erosional events (Brown *et al.* 2000).

LOI was conducted on cores HU-VC1, HU-VC2 and FM1 at 0.5 cm resolution; cores HU1-MG, HU2-MG, and HU3-MG at 1.0 cm resolution and on random samples from the sediment trap material. The methods used were based on those of Heiri *et al.* (2001). 1 cm^3 wet samples were weighed (W_{wet}) then dried at 110˚ C for 24 hours in a drying oven then weighed again (DW_{110}). The samples were ignited at 550˚ C for 4 hours using a muffle furnace, cooled in a desiccator and weighed (DW_{500}). The samples were then re-ignited at 950˚ C for 2 hours in the muffle furnace, cooled in the desiccator and reweighed (DW_{950}). Percent water, organic matter, carbonate and siliciclastic content were determined using the following equations:

$$\% \text{ water} = 100(W_{wet} - DW_{100})/(W_{wet}) \quad (1)$$

$$\% \text{ organic matter} = 100(DW_{100} - DW_{500})/(DW_{100}) \quad (2)$$

$$\% \text{ carbonate} = 100(DW_{500} - DW_{950})/(DW_{500}) \quad (3)$$

$$\% \text{ siliciclastics} = 100 - \% \text{ organic matter} - \% \text{ carbonate} \quad (4)$$

3.7.2 MAGNETIC SUSCEPTIBILITY

All soils possess magnetic properties to some degree due to the iron compounds found within their mineral component. Magnetic susceptibility is the degree of magnetization of sediment in response to an applied magnetic field. Lake sediments may provide magnetic information through the analysis of the composition and properties of their materials (Bartington Instruments, 2009). Changing magnetic susceptibility throughout lake sediment cores appears to be positively correlated with variations in the amount of inorganic allochthonous material present (Thompson *et al.* 1975). Analysis of the downcore variations in magnetic properties is often used alongside other paleolimnological methods as a tracer for erosional inputs of material as a response to climatic changes (Hirons & Thompson, 1986).

Volume magnetic susceptibility (k) measures, in dimensionless units, the total magnetic attraction of the various constituents of the sediment when exposed to a magnetic field (Dearing, 1999). It is defined as:

$$k = M \times H^{-1} \quad (5)$$

Where M is the magnetization per unit volume and H is the magnetic field strength or magnetizing force applied (Moskowitz, 1995).

Variations in susceptibility profiles indicate changes throughout time in processes including sediment transport, flux, erosion and deposition within the lake basin and catchment (Nowaczyk, 2001; Zolitschka et al. 2001). Analysis of magnetic susceptibility was conducted at 0.5 cm resolution on cores HU-VC1,

HU-VC2, FM1, HU1-MG, HU2-MG and HU3-MG using a Bartington MS2E Magnetic Susceptibilty Meter (Bartington Instruments, 2009).

The Bartington MS2E Magnetic Susceptibility Meter operates by generating a low frequency, low intensity AC magnetic field around its sensor. The sensor provides readings to a resolution of 2×10^{-6} SI units and was used for split core logging at every 0.5 cm along the length of the cores using a meter stick as a guide. Prior to taking readings, the split core was laid on a flat surface, covered in a thin layer of plastic wrap and allowed to warm to room temperature. Corrections were applied to all measurements for an assumed linear measurement drift using the method developed by Dearing (1999).

3.7.3 PARTICLE SIZE DISTRIBUTION

Through the analysis of particle size of sediment samples, information may be gained pertaining to sediment source, transport mechanisms, energy, depositional conditions and paleoclimatic conditions (Last and Smol, 2001). Particle size distribution analysis was done on all cores and sediment trap material for this research. Sediments of core HU-VC2 were subsampled (1 cm^3) at 0.5 cm intervals whereas those of HU-VC1, FM1, HU1-MG, HU2-MG and HU3-MG were sampled every 1 cm. Random sediment trap samples were also analyzed for particle size distribution. The sediments were placed in test tubes with deionized water. Approximately 10 ml of 35% hydrogen peroxide was then added daily (to eliminate all organic material) until no reaction with the samples was observed. Samples were then placed in a hot water bath (~80˚C) for 3

consecutive days and 35% hydrogen peroxide and deionized water were continuously added as needed. A small amount of dispersant, ~15 mL of CALGON®, was added for disaggregation of clay particles. Samples were then processed using a Beckman Coulter LS13 320 laser particle size analyzer following the protocols developed by Colin Courtney Mustaphi and Jesse Vermaire. From the distribution data obtained, the percentages of sand, silt and clay were determined and plotted for the length of the core.

3.7.4 RADIOCARBON DATING

The radioactive decay of carbon-14 is useful for the dating of organic matter in lacustrine sediments. The half-life of this isotope is 5,730 years and the method can be applied back to ~40,000 years. Due to varying atmospheric ^{14}C content, fossil fuels combustion, and measurement uncertainties, the technique cannot be applied for the last few hundred years (Björk & Wohlfarth, 2001).

Organic material throughout the sediments of the cores was sparse, therefore only a few radiocarbon dates could be obtained. Organic material in the form of small twigs located at depths of 155.5 cm and 162.5 cm were extracted from the core HU-VC1 immediately after core extrusion using tweezers. Organic material (including peat and wood) was manually extracted from core FM1 at 61.5 cm depth, using tweezers and a light microscope, to obtain a date for the basal sediments of the smaller lake. Due to the lack of organic matter throughout the cores, subsampling locations were chosen at levels where organic matter was present.

Beta Analytical Inc, (Miami, Florida), using the Accelerator Mass Spectrometry (AMS) technique, performed the radiocarbon dating for this study. Results were calibrated from radiocarbon ages to calendar year ages using CALIB 7.0 Radiocarbon Calibration Program software (Stuiver & Reimer, 1993).

CHAPTER FOUR

RESULTS

4.1 HUSKY LAKE WATER QUALITY

Water quality data collected from Husky Lake is presented in Figure 4.1. The results for Turbidity (Figure 4.1 A) show little variation in median values among the 3 examined sites (HU1, HU2, HU3). However, a much wider range of observations are found at the disturbed site, HU2, which upon closer investigation of the data, are due to elevated values of turbidity from the samples collected at the disturbed inflow stream (Appendix III). Turbidity values of the water samples collected in the disturbed site's inflow stream are more than an order of magnitude higher than all other samples collected within the study area, including the undisturbed inflow streams and the disturbed site's basin (Appendix III).

The results of conductivity (Figure 4.1 B) also show little variability among median values of the 3 sites; however outlier values of much higher levels are seen at the disturbed site (HU2). These values, expressed as outliers in the graph, are samples collected from the disturbed stream, which in some instances double the recorded values of turbidity within the disturbed basin. The lowest values of conductivity were recorded within the undisturbed inflow streams (Appendix III).

Dissolved oxygen shows little variation among the three sites (Figure 4.1 C). Median values of dissolved oxygen for all three sites were between 10 and

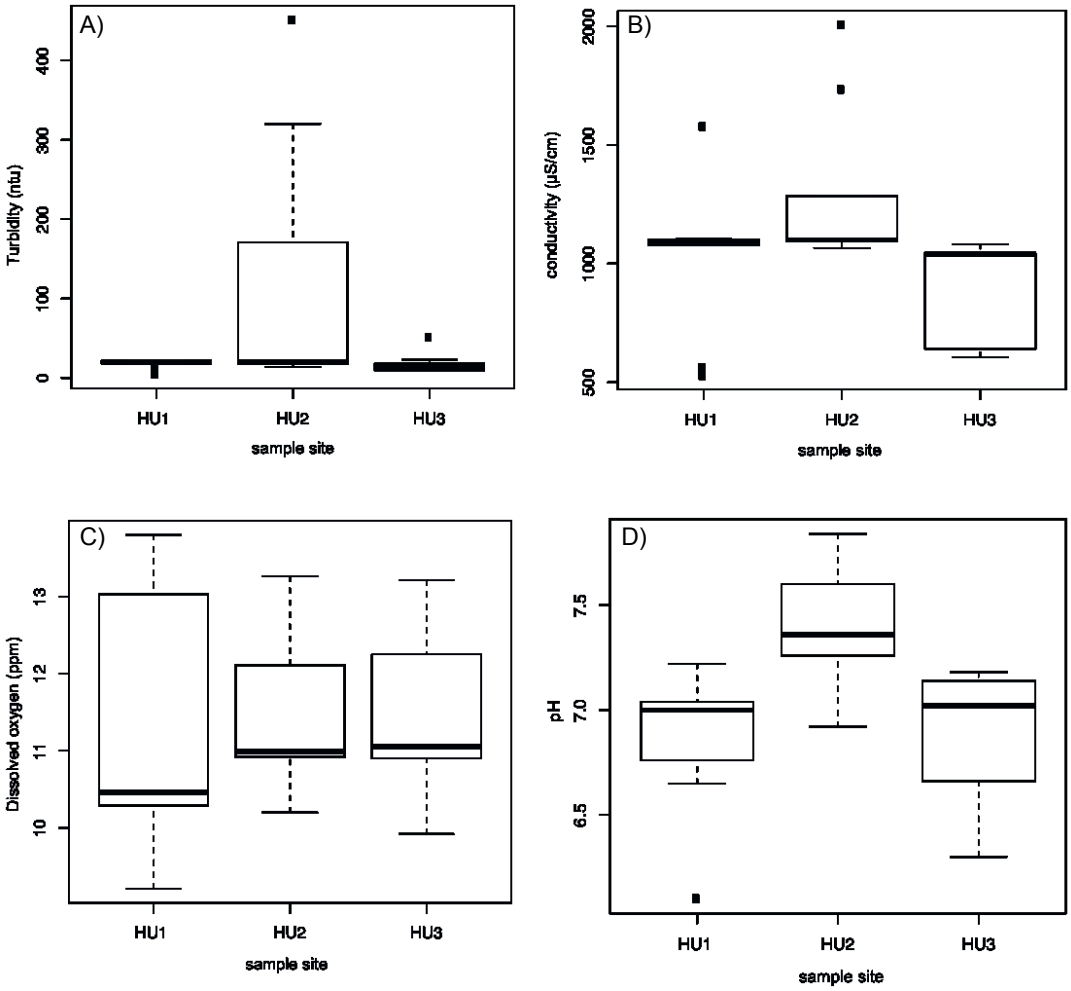

Figure 4.1: Box plots of Husky Lake water quality parameters.
(A) turbidity (ntu); (B) conducitivity (µS/cm); C) dissolved oxygen (ppm); (D) pH. Outlier values are indicated by the black dots and horizontal lines at the end of the dotted lines show maximum and minimum values (excluding outliers). HU1 (n = 9); HU2 (n = 8); HU3 (n = 9).

11 ppm. Minimum (9.2 ppm) and maximum (13.8 ppm) values were both from HU1 (undisturbed system). Water samples examined from the inflow streams at all three sites were consistently higher than that of the basins and from the centre of the lake (Appendix III).

The pH of water at the disturbed site (HU2) has a higher median value than the two undisturbed sites (HU1, HU3) (Figure 4.1 D). The highest values (7.6 to 7.84) are found within the disturbed stream, whereas samples collected at the disturbed basin (6.95 to 7.34) are closer to the median values of the undisturbed sites (Appendix III).

Throughout all sampled sites, temperature varied from 3.2 °C to 10.8 °C; dissolved oxygen varied from 9.2 ppm to 13.26 ppm. Conductivity peaked at 2006 µS/cm within the disturbed stream and was lowest in the undisturbed stream in the northern portion of Husky Lake at 528 µS/cm. Turbidity was also highest at the undisturbed stream at 451 NTU and lowest in the surface water in the central portion of south Husky Lake. The pH of water was highest at 7.84 in the disturbed stream and lowest at 6.1 at the surface of north Husky Lake.

4.2 HUSKY LAKE SEDIMENT TRAPS

4.2.1 LOSS-ON-IGNITION

Twelve sediment traps were deployed in the western arm of Husky Lake near Fort McPherson to determine sediment input into Husky Lake from the adjacent uplands. Three traps were placed in the basin of each site (HU1, HU2,

HU3), two traps in the central portion of the lake (adjacent to the undisturbed sites) and one in the northern portion of the lake. The sediment collected in the trap in North Husky (labeled NH) was omitted from the results, as the physical appearance of the sample was characteristic of that of terrigenous surface material, containing large fragments of surface vegetation throughout the sample due to an anomaly of shoreline erosion. The remainder of the traps contained highly inorganic material, characteristic of thawed sediments that are found in this region. The coordinates of the sediment traps are presented in Table 3.2. The results (Figure 4.2, Appendix IV) show that the percent organic matter was greatest in the sediment collected at the undisturbed sites (HU1 & HU3) and lowest at the disturbed site (HU2). Median values for percent organic matter of the sediment at the undisturbed sites, (HU1: 12.5%, HU3: 13.5%) were approximately double that of the disturbed site (HU2: 6.9%). The maximum value at the disturbed site (13.5%) is equivalent to the median value at the undisturbed site HU3.

4.2.2 PARTICLE GRAIN SIZE

The results of particle grain size analysis (Figure 4.3, Appendix V) do not show much diversity overall, as all sediment collected in the traps throughout Husky Lake ranges from very fine silt to fine silt. However, the median average particle size at the disturbed site (HU2) is almost double (20.4 μm) that of the undisturbed site (10.3 μm) (HU1). The sediment traps that were deployed

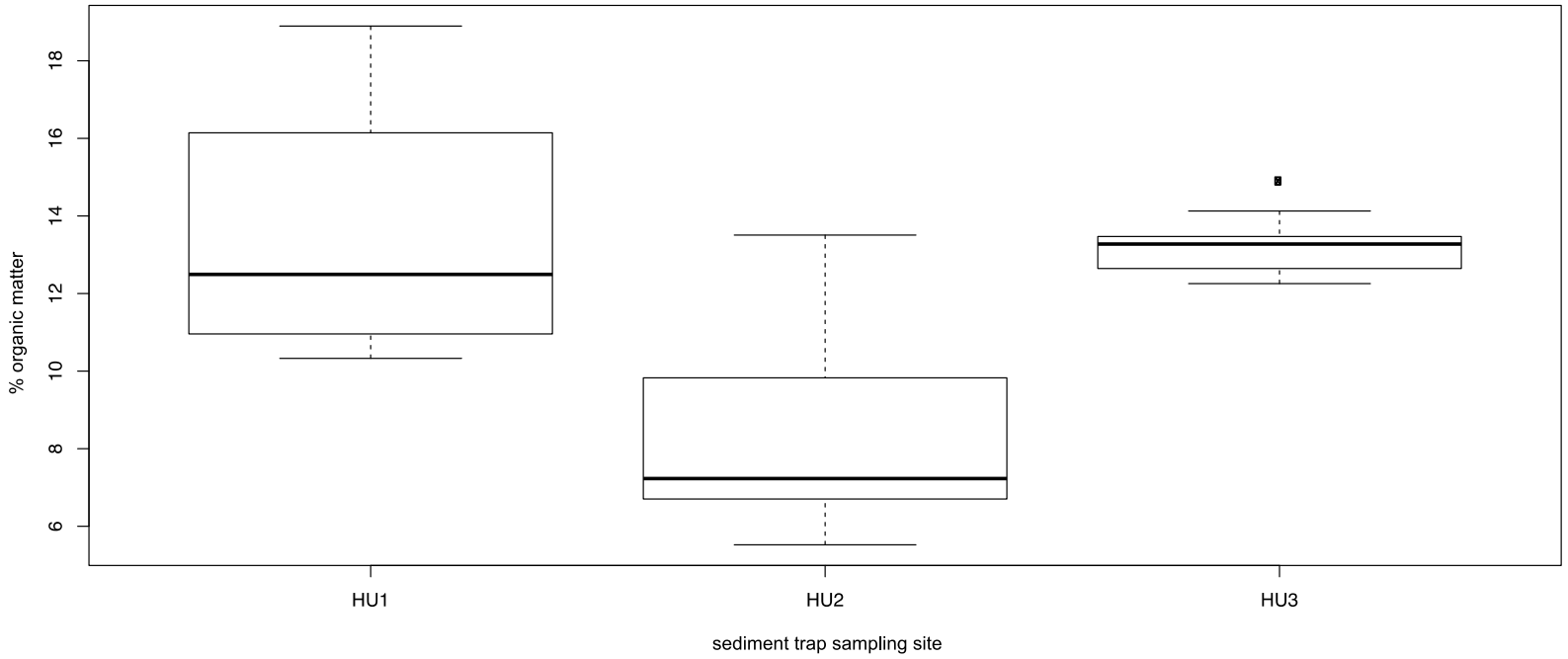

Figure 4.2: Results of loss-on-ignition tests of sediment from Husky Lake sediment traps.
Box plots display the percent organic matter of the sediment collected in sediment traps at the three study sites of Husky Lake. Horizontal bars indicate maximum and minimum values, while outliers are represented by a black dot. HU1 (n = 4); HU2 (n = 17); HU3 (n = 14).

centrally in the lake; adjacent to the undisturbed systems (HU1-SED4 & HU3-SED4) had the smallest grain sizes (very fine silt), whereas those located within the bays display larger grain sizes characterized as silt (Appendix V). The largest grain sizes are found most consistently in the sediment traps of the disturbed basin (HU2). The highest volume of sediment was accumulated within the traps of the disturbed system (HU2), and the lowest in those of the undisturbed site (HU1). The volume of sediment collected in trap HU2-SED3 (336.23 cm^3) was almost an order of magnitude greater than that of HU1-SED1 (5.73 cm^3) (Figure 4.4, Appendix V). The median volume of sediment collected in the traps at HU2 was 83.02 cm^3, whereas the median volumes at the undisturbed sites (HU1 & HU3) were 13.74 cm^3 and 34.64 cm^3, respectively.

4.3 HUSKY LAKE SHORT CORES

A short core was collected from the centre of each studied basin (HU1, HU2, HU3) (Figure 3.3, Table 3.2) in order to describe the sediments at the sediment-water interface without the disruption associated with using a larger coring device or the limitations of sediment traps. These cores were subsampled in the field at 1 cm intervals (Glew *et al.* 2001) and transported to Carleton University for analysis. Since these cores are short in length, the results will be reported as bulk samples, similar to the sediment trap data; however, detailed stratigraphic data of each core is shown in Appendices VI through VIII, which includes written descriptive summaries of each core.

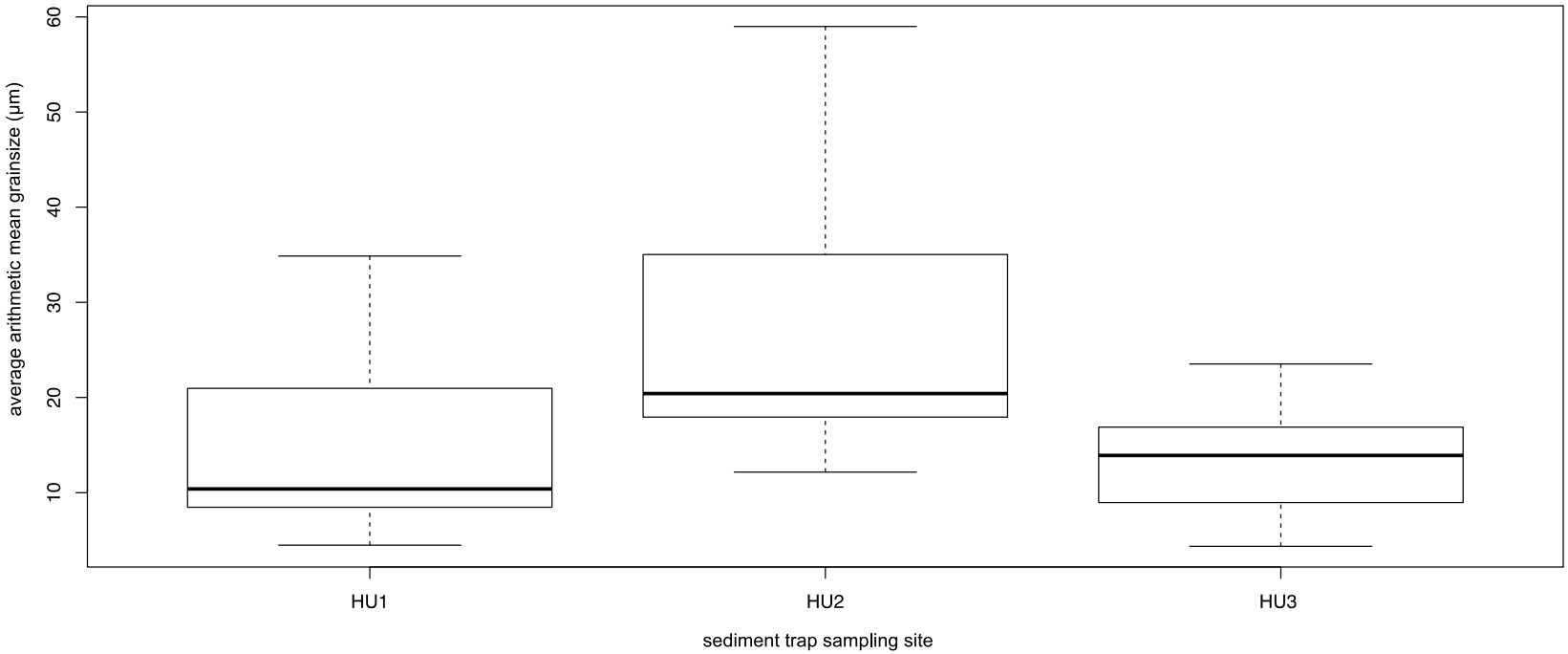

Figure 4.3: Results of particle size distribution tests of sediment from Husky Lake sediment traps.
Box plots display the average arithmetic mean grainsize (µm) of the sediment in the traps deployed at the studied sites at Husky Lake. As the graph displays, median particle size is greater at the disturbed site and lower at the undisturbed sites. HU1 (n = 4); HU2 (n = 15); HU3 (n = 14).

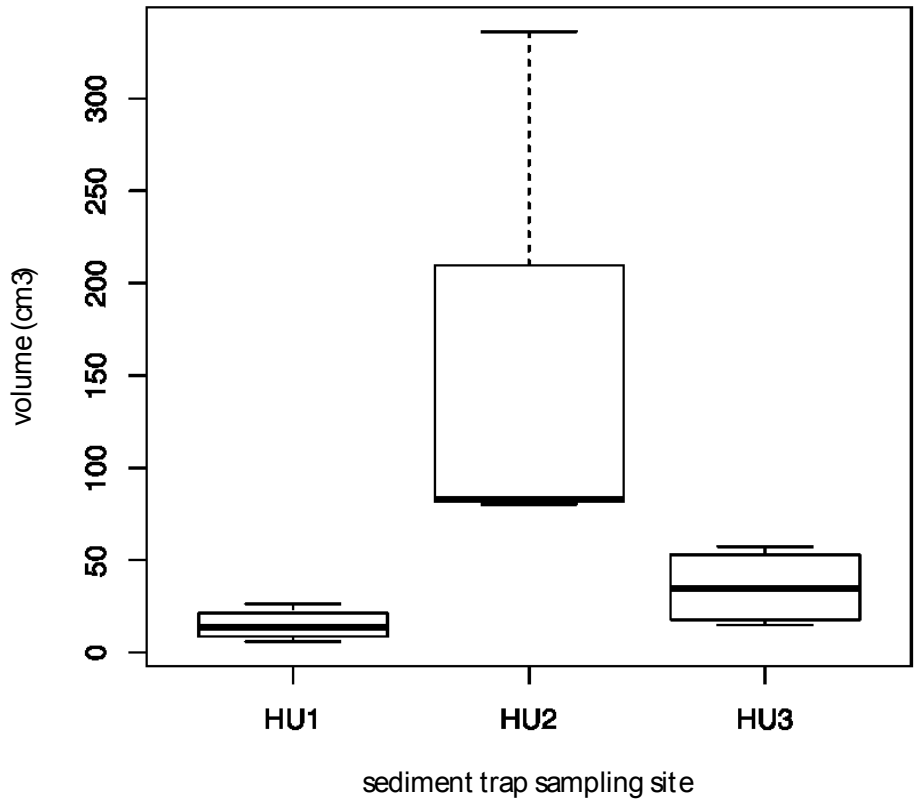

Figure 4.4: Volume of sediment collected in Husky Lake sediment traps. Box plots show the volume (cm^3) of sediment collected in the summer season sediment traps deployed in each of the studied sites at Husky Lake. The traps at the disturbed site (HU2) collected significantly more sediment than those at the undisturbed sites (HU1 & HU3).

The results of loss-on-ignition testing on the short cores collected within the studied basins (Figure 4.5) show that the median values of percent organic matter do not differ significantly between the disturbed and undisturbed systems. Omitting a few outlier values, the sediment at the undisturbed sites is highly inorganic and contains little variance among samples. The disturbed site, in contrast, has a maximum value of 31.2% organic matter and a minimum of 6.8%, displaying greater variability and occurrences of higher organic matter among the samples.

The magnetic susceptibility (Figure 4.6) of the short cores' sediment is overall higher at the disturbed site (HU2-MG) than at the undisturbed sites (HU1-MG, HU3-MG). The median value of the disturbed site (12.8 x 10^{-6} SI units) nearly doubles that of the undisturbed sites (6.4 x 10^{-6} SI units & 6.2 x 10^{-6} SI units) and the minimum value of the disturbed site (8.4 x 10^{-6} SI units) is almost equal to the maximum value of the undisturbed site HU1 (8.5 x 10^{-6} SI units).

Results of particle size distribution (Figure 4.7) show that the median value of the disturbed site: HU2 (24.29 μm), is higher than that of the undisturbed sites HU1 & HU3 (18.39 μm & 17.51 μm, respectively). The undisturbed site HU1 has the greatest range in particle size with a larger percentage of sand (Appendix VI-VIII) than the other cores.

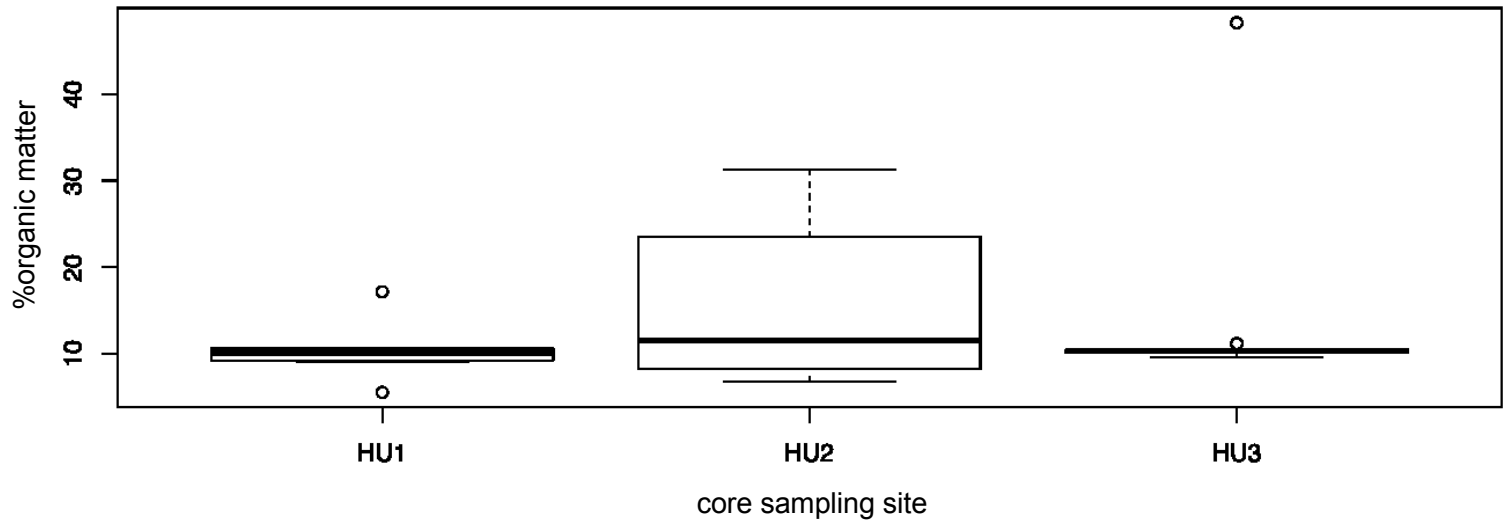

Figure 4.5: Box plots of short core LOI (% organic matter).
Box plots displaying the percent organic matter of sediment collected in short cores of each studied basin in Husky Lake. The disturbed sites (HU1 & HU3) show little variation besides a few outlier values, whereas the disturbed site shows a much wider variation. HU1 (n = 8); HU2 (n = 8); HU3 (n = 9).

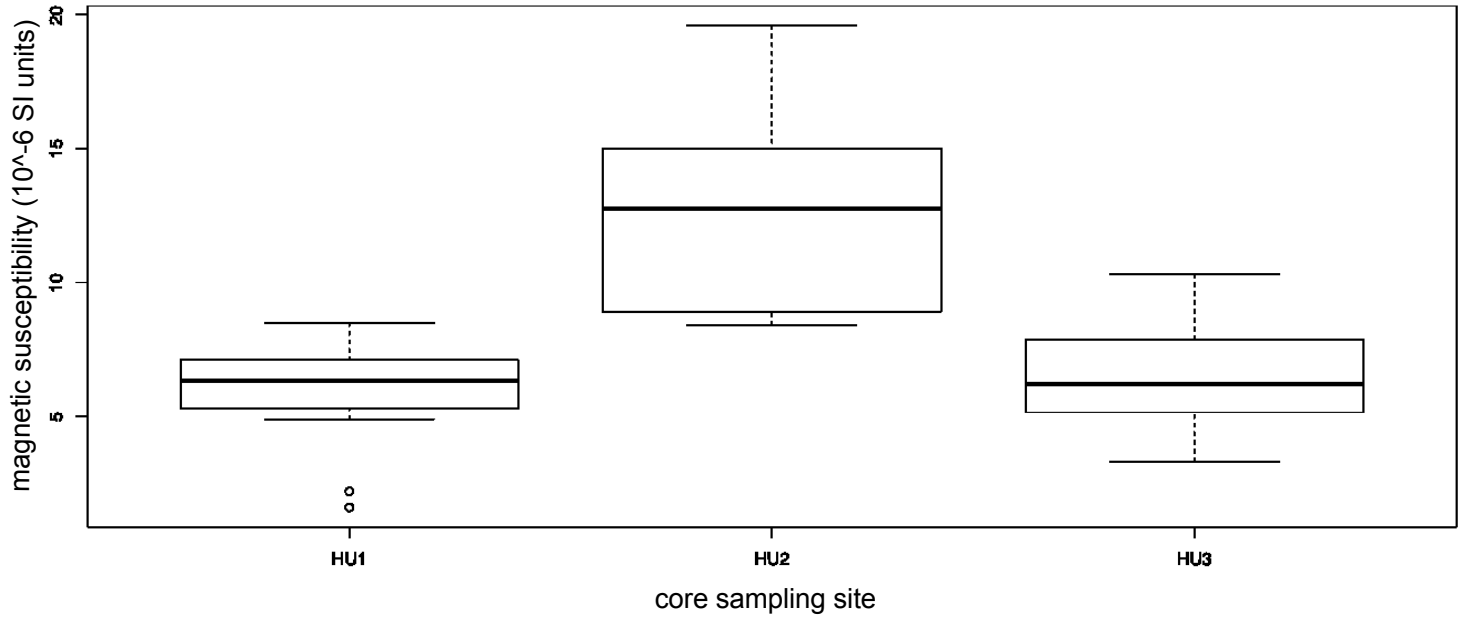

Figure 4.6: Box plots of short core magnetic susceptibility.
Box plots displaying the magnetic susceptibility of sediment from the maxi Glew cores of each basin. The values obtained for the disturbed site (HU2) are overall much higher than those from the undisturbed sites (HU1, HU3).
HU1 (n = 9); HU2 (n= 9); HU3 (n = 10).

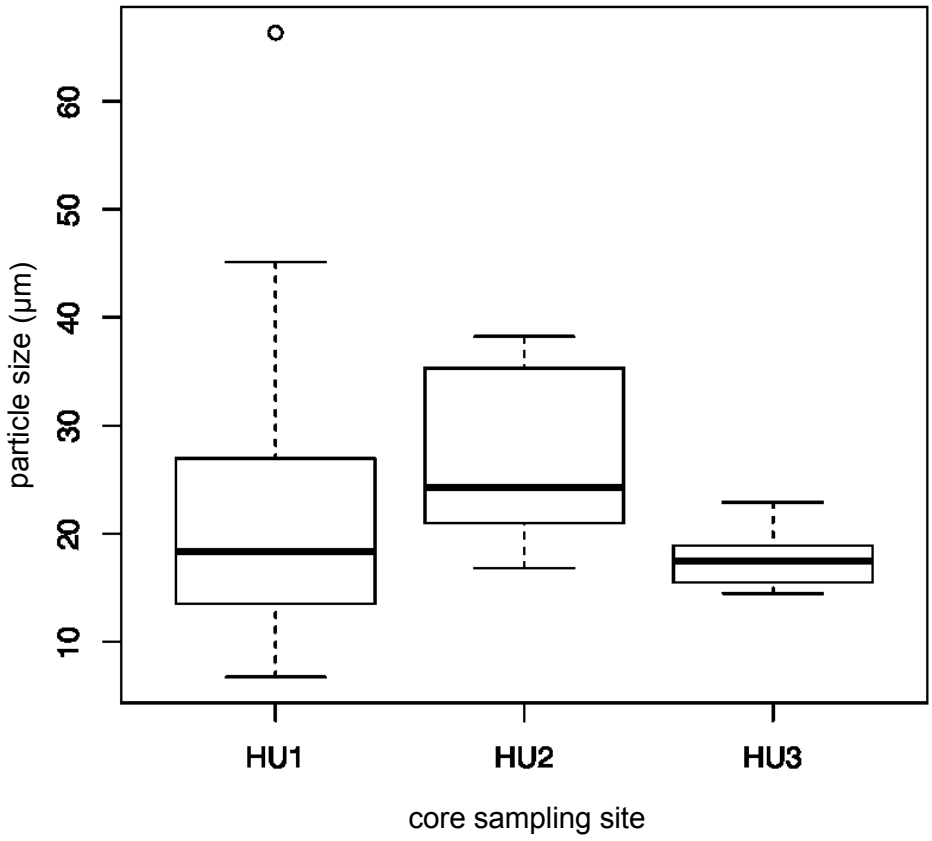

Figure 4.7: Box plots of short core particle size distribution.
Box plots displaying the particle size distribution of the short cores collected from the studied basins of Husky Lake. HU1 (n = 9); HU2 (n = 9); HU3 (n= 10).

4.4 HUSKY LAKE LONG CORES

4.4.1 HU-VC1

Core HU-VC1 measured 180 cm in length (Figure 4.8). The percent organic matter within the core varies from a minimum of 3.2% at 96 cm depth to a maximum of 27.7% at 163 cm depth. The percent organic matter averages ~8% from the top of the core to ~162.5 cm depth. At 162.5 cm, percent organic matter increases and attains the highest values in the core. Carbonate content is low throughout the entire core, averaging ~2%. Siliciclastic material dominates the core, with a maximum of 95% at 96 cm and a minimum of 68% at 163 cm following similar trends to both percent organic matter and carbonate content. The magnetic susceptibility of the core has a minimum of 0.7 x 10^{-6} SI units for the uppermost sample of the core. The maximum value (19 x 10^{-6} SI units) is reached at 25 cm depth. There are fluctuations throughout the core; however the mean value is approximately 12 x 10^{-6} SI units. There is an overall decreasing trend in magnetic susceptibility throughout the core. From 0 – 50 cm depth, magnetic susceptibility averages ~12.8 x 10^{-6} SI units while between 50-100 cm depth it averages ~14.92 x 10^{-6} SI units. The average decreases to 11.7 x 10^{-6} SI units between 100 and 150 cm, then further to 10.8 x 10^{-6} SI units at the bottom portion of the core (150-180 cm).

Mean particle size distribution of each sampled depth ranges from 2.48 μm to 8.80 μm. The mean value of the core is 6.18 μm and there are many fluctuations seen within the data, with several pulses of finer grained material

occurring throughout the depths. These pulses are seen consistently as drops from coarser and medium silt to very fine silts and clays. Overall the core is predominantly silt (73%), with a lower percentage of clay (27%), on average. The radiocarbon dates obtained were measured from twig samples at depths of 155.5 cm and 162.5 cm. The radiocarbon age for sample HU-VC1-155.5 was 2540 +/- 30 BP. The conventional radiocarbon age was 2470 +/- 30 BP. The conventional radiocarbon age represents the measured radiocarbon age corrected for isotopic fractionation (calculated using delta 13C). The calendar-calibrated result was calculated from the conventional radiocarbon age and was determined to be 2433 - 2621 cal BP. For HU-VC1-162.5, the measured radiocarbon age was 2450 +/- 30 BP; the conventional radiocarbon age was 2440 +/- 30 BP; and the calibrated result for calendar years was 2355 – 2544 cal BP. Based on the radiocarbon dates obtained, an average sedimentation rate of ~0.07 cm/year can be assumed for the centre of the lake at the undisturbed site HU-VC1 in North Husky.

4.4.2 HU-VC2

Core HU-VC2 was the longest core collected, measuring 205 cm. The results for this core are displayed in Figure 4.9. The percent organic matter was low throughout this core, with a maximum of only 10.4 % and a mean of 7.1 %. The minimum (5.56 %) occurred at a depth of 115 cm. From 40 cm to 130 cm depth, percent organic matter averages ~6.0 %. Peaks in organic matter occur at ~ 25 cm, 37 cm and from 135 to 150 cm.

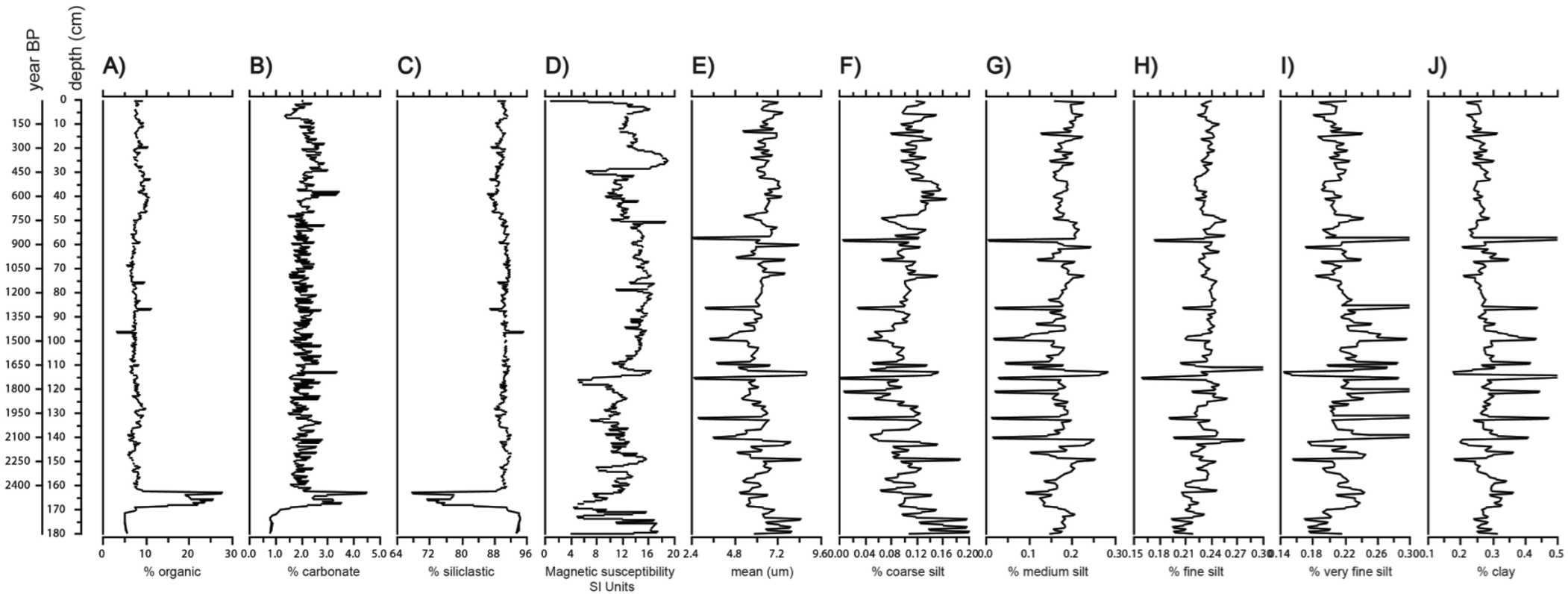

Figure 4.8: Sedimentological analyses of core HU-VC1.
A) Percent organic matter, B) Percent carbonate, C) percent siliciclastic D) Magnetic susceptibility E) mean grainsize (μm), F) Percent of coarse silt material G) Percent of medium silt material, H) Percent of fine silt material I) Percent of very fine silt material, J) Percent of clay material. The primary Y-axis is core depth in centimetres, with a secondary axis of years BP, which was extrapolated based on the radiocarbon dates obtained from samples at depths 155.5 cm and 162.5 cm, assuming based 2400 BP.

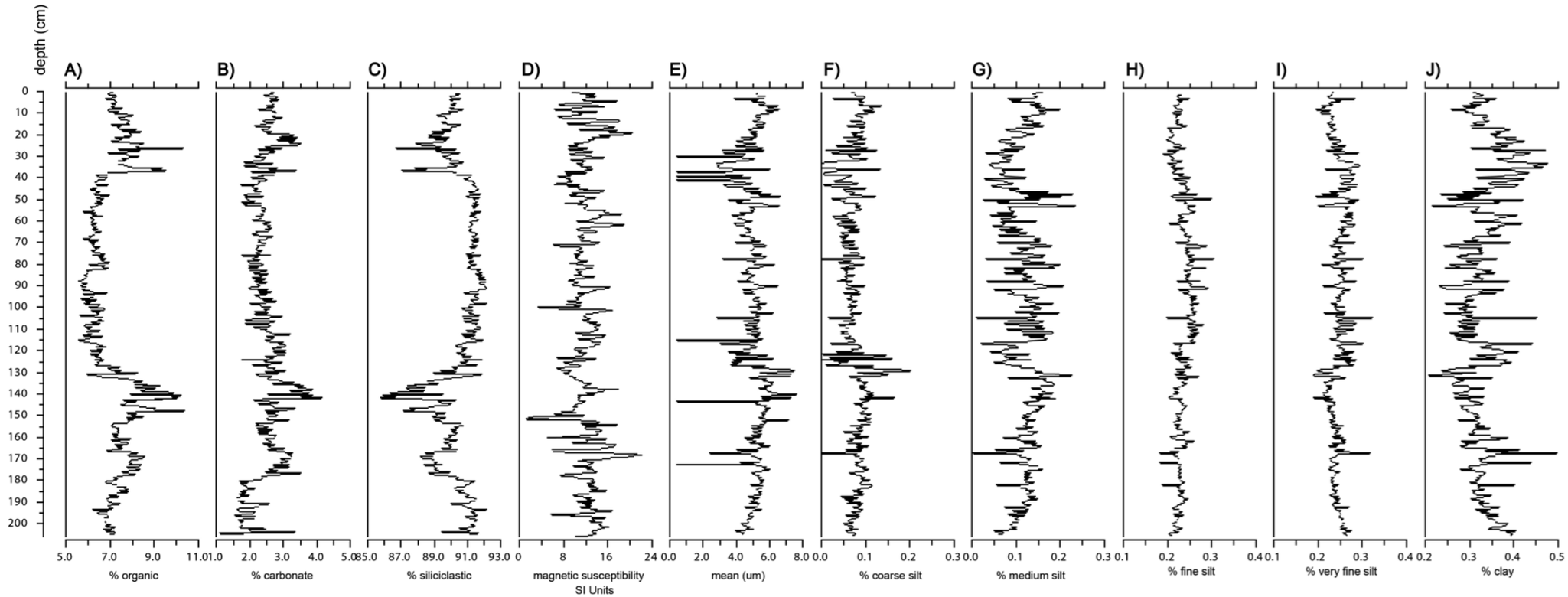

Figure 4.9: Sedimentological analyses of core HU-VC2.
A) Percent organic matter, B) Percent carbonate, C) percent siliciclastic D) Magnetic susceptibility E) mean grainsize (μm), F) Percent of coarse silt material G) Percent of medium silt material, H) Percent of fine silt material I) Percent of very fine silt material, J) % of clay material.

Carbonate content was low within the core as well, ranging from ~1% to 4%. Peaks in carbonate, though minimal appear to correlate with those of percent organic matter at ~ 20 to 25 cm, 37 cm, and from 135 to 150 cm depth, with another peak occurring at the bottom of the core (~ 203 cm). Percent siliciclastics averaged 90.5 % within the core, with a minimum of 85.8 % and a maximum of 92.2%. All major changes that occur in siliclastic matter throughout the core can be seen as declines in concentration, mirroring the peaks of organic matter almost precisely.

The magnetic susceptibility of HU-VC2 averaged 12 x 10^{-6} SI units. This mean remained steady throughout the length of the core, with fairly consistent fluctuations toward lower and higher values (min= 1.3 x 10^{-6} SI units; max= 22 x10^{-6} SI units). The overall trend throughout the core is positive, as the average magnetic susceptibility increases gradually with depth (slope: y=0.0013x + 11.673). Values are generally lower until the bottom quarter of the core where they increase slightly on average. The top 50 cm has an average magnetic susceptibility of 11.7 x 10^{-6} SI units. The average from 50 to 100 cm depth is 12 x 10^{-6} SI units and from 100 to 150 cm: 11.5 x 10^{-6} SI units. From 150 to 205 cm the average magnetic susceptibility increases to 12.3 x x 10^{-6} SI units.
The mean particle size is 4.98 μm, with a minimum of 0.394 μm and a maximum of 7.68 μm. As seen in core HU-VC1, several pulses of finer grained material are evident throughout the core. The largest spikes of finer grained material are seen at depths of ~ 30 to 40 cm; 115 cm; 145 cm; and 172 cm. Smaller spikes

occur at 105 cm and 75 cm. The core is dominated by silty material (fine to very fine silt), with the remainder being clay-sized particles; no sand was present within the core. No radiocarbon dates were obtained for this core due to a lack of organic material.

4.5 LAKE FM1

4.5.1 FM1 WATER QUALITY

Water quality parameters were examined much less extensively for the FM1 system due to sampling limitations. However, in order to determine the state of the system, testing was done upon collection of the summer season sediment traps on August 25th, 2012. Within the lake at 1m depth, the water temperature was 16.5 °C; specific conductivity equaled 1400 µs/ cm; pH was 6.7; turbidity was 217 NTU; and dissolved oxygen measured 77% or 7.51 mg/L. Within the stream of FM1, temperature was 12 °C; specific conductivity equaled 500 µs/ cm; pH was 6.86; turbidity was 704 NTU; and dissolved oxygen was 90% or 9.71 mg/L.

4.5.2 FM1 SEDIMENT TRAPS

Unfortunately due to high amounts of lake overflow (a layer of water between the surface of the ice and the snow pack on a lake), the winter season sediment traps at FM1 were unable to be retrieved in the spring of 2012; therefore retrieval was delayed until June 2012. Sediment traps for lake FM1 were collected on June 11th, 2012. All five sediment traps, which were deployed

in late August of 2011, were successfully retrieved from a zodiac boat. Unfortunately, these samples were lost upon return to CUPL and were therefore unavailable for analysis. However, based on visual observation, the volume of settled sediment within the traps could be estimated as comparable to that of the undisturbed site of HU3 on Husky Lake. On the same day, June 11th, 2012, three more sediment traps were deployed in lake FM1. Due to high rates of sedimentation over the summer months, the summer sediment traps of lake FM1 were unable to be successfully retrieved upon return in late August, 2012. The high amount of unsettled silty-clay sediment within the lake created a dense sludge-like layer of material at the bottom of the lake, which encompassed the sediment traps.

4.5.3 FM1 CORE

Prior to sub-sampling the core, brief notes were made on the visible physical changes in sediment characteristics. From the sediment base to approximately 50 cm in depth the sediments were of lighter colour and appeared to be of finer consistency. Below 50 cm depth, the core sediments were a much darker brown hue, of coarser, denser consistency. When sub-sampling, this highly organic portion of the core tended to 'crumble' when sliced, whereas the layers above it consistently thawed and the core had to be continuously placed back in the freezer to minimize errors in accuracy due to melting and degrading of the sample. Results for the core taken from lake FM1 are displayed in Figure 4.10. Material for radiocarbon dating from the FM1 sediment core was obtained

from near the base of the sediment core at a depth of 61.5 cm. The material recovered from the core consisted of peat and woody debris. The measured radiocarbon age obtained from the peat and wood at 61.5 cm depth was 1030 +/- 30 BP. The conventional radiocarbon age was 990 +/- 30 BP. The conventional radiocarbon age represents the measured radiocarbon age corrected for isotopic fractionation and is calculated using the delta ^{13}C. The calendar-calibrated result was calculated from the conventional radiocarbon age and was determined to be 897- 961 cal BP +/- 64.

The magnetic susceptibility of the sediments of core FM1 ranges from 2.1 x 10^{-6} SI units to 31.1 x 10^{-6} SI units. From 0 – 55 cm depth, mean magnetic susceptibility was approximately 15 x 10^{-6} SI units. Below 55 cm depth, average magnetic susceptibility values trended towards lower values, averaging ~8 x 10^{-6} SI units.

The percent organic matter of FM1 ranges from a minimum of 5% at 6.5 cm depth to 73.3% at 55 cm depth. The percent organic matter is approximately 8% from the sediment-water interface to a depth of 54.5 cm, excluding a slight peak to 27% at 8 cm. At 54.5 cm, organic matter content increases compared to the upper 54.5 cm of the sediment core, reaching values as high as 73% at 57 cm. These values remain consistently higher before slowly decreasing back to the mean value of 8.5% at approximately 75.5 cm. The carbonate content remains fairly low throughout the core, ranging from <1% at 39 cm to 6.2% at 58.5 cm. Besides a few peaks, carbonate content remains fairly low (averaging

~2%) from 0-54.5 cm depth, then consistently peaks to values above 5%, until gradually decreasing back down to lower values at around 70 cm depth.

Siliciclastic material makes up the majority (~90% average) of the sediment from 0 to 54.5 cm depth and then drops down to as low as 22%. The mean particle size ranges from 4.6 μm at 67 cm depth to 49.1 μm, at 60 cm depth, therefore there is no sand throughout the core. From 0 cm to 54.5 cm depth, average particle size is 8.34 μm, with minor fluctuations towards larger grains (up to 19.7 μm) until a drastic spike in mean grainsize is seen from 55 cm depth to 60 cm depth, dropping back down around the average below. This increase in grain size correlates with the depth of the core where dramatic increases in the percent organic matter and carbonate content also occur.

The sediment stratigraphy of the FM1 core captures the onset of current retrogressive thaw slump activity within the catchment of FM1. Based on the physical analyses of the sediment core from FM1 (Figure 4.10), thaw slump material began to accumulate in lake FM1 at 54.5 cm depth. This is evident in the results from analyses of LOI, magnetic susceptibility and particle size distribution. Above 54.5 cm depth in the core, the sediment is characterized as inorganic, silty-clays, representative of the material that makes up the glacial sediment in the area. Below 54.5 cm depth, the sediment is higher in organic content and lower in average magnetic susceptibility.

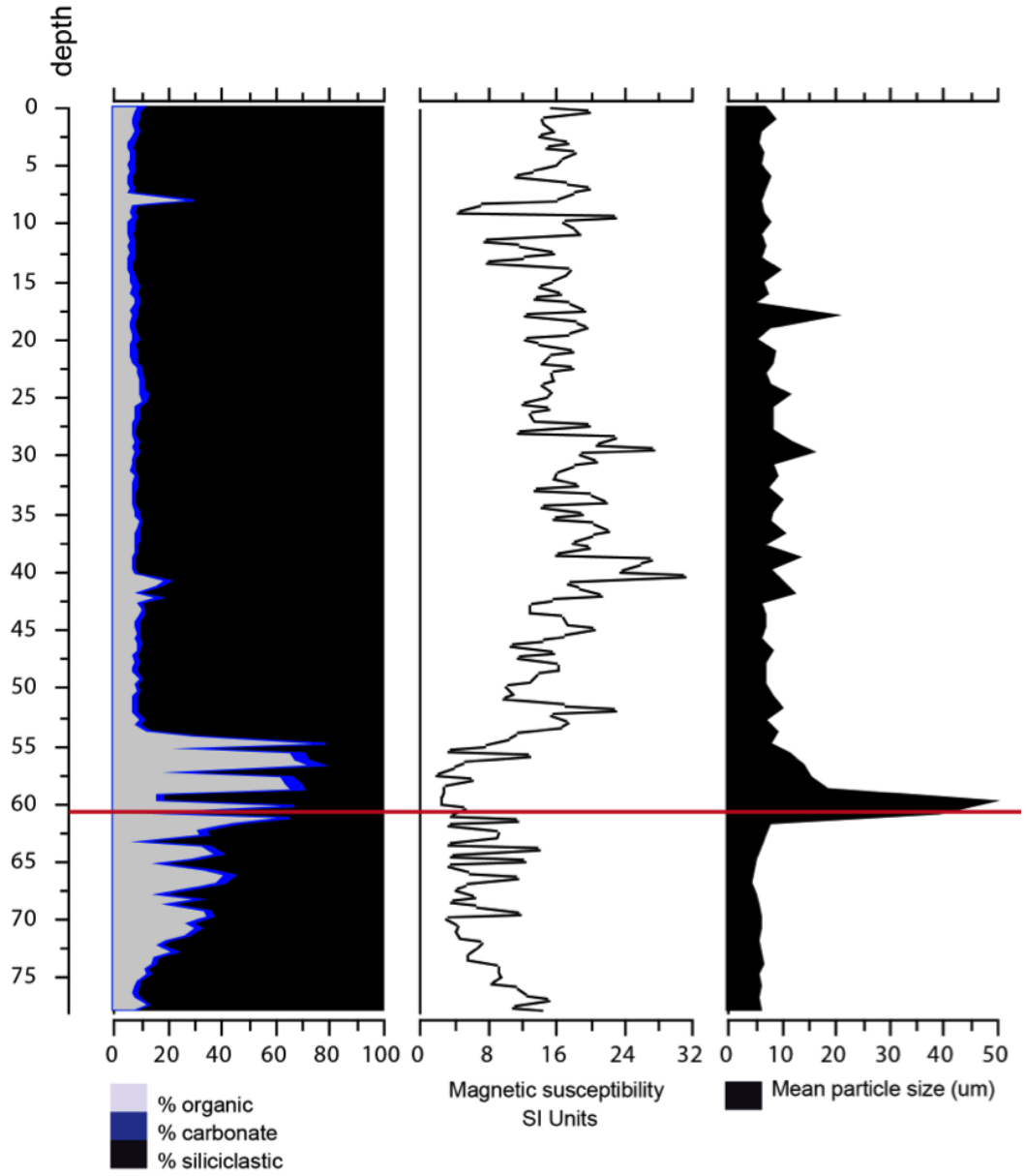

Figure 4.10: Sedimentological analyses of core FM1.
A) Loss on Ignition, B) Magnetic Susceptibility, C) Mean particle size (μm). The red line delineates the calendar calibrated radiocarbon date obtained at 61.5 cm depth (897- 961 cal BP +/- 64).

CHAPTER FIVE: DISCUSSION

5.1 USING LACUSTRINE SEDIMENT RECORDS TO TRACK THE OCCURRENCE OF RETROGRESSIVE THAW SLUMPS IN THE PAST

The first objective of this research was to use lake sediments to determine the timing and frequency of retrogressive thaw slump activity in the past. Due to the high sediment inputs into lake FM1, developing a robust chronology proved difficult, as ^{210}Pb-dating techniques were not successful since background was not reached. ^{210}Pb dating was conducted on 15 samples selected throughout the ancillary FM1-KB2 sediment core (Appendix I). Results of the ^{210}Pb dating were inconclusive since background levels were not reached in the deepest sediment samples that were analyzed. These results suggest a highly elevated rate of sediment deposition, as the half-life of ^{210}Pb is only 22.3 years and the dated core measured just over 20 cm in length. In spite of the dating issues, it is believed initiation of the retrogressive thaw slump impacting lake FM1 occurred in the past 20-40 years.

Aerial photographs are available from the region going back to 1953. Analysis of the available aerial photographs (Appendix II) suggests that the large retrogressive thaw slump within the upper catchment of lake FM1 initiated within the timeframe of 1970- 1990. Lantz and Kokelj (2008) found rates of headwall retreat of thaw slumps within this region increased twofold within this time period.

Radiocarbon dating of organic matter obtained at 61.5 cm depth within core FM1 showed an age of 897- 961 cal BP +/- 64. Based on the sediment

signature of the current slump affecting lake FM1 and the radiocarbon date obtained, it may be interpreted that another thaw slump has not impacted this aquatic system within the past 1000 years. The first research question could not be fully answered for Lake FM1. Although there appears to be a sediment signature in the core that can be attributed to current thaw slump activity, there are no comparable observations present within the core in the past for it to be tracked through time.

Based on the results of laboratory testing of the long cores collected from Husky Lake (HU-VC1, HU-VC2), we were not able to determine whether retrogressive thaw slumps have occurred within the studied area in the past and no sediment signature of current thaw slump activity could be distinguished. However, due to distinct laminations of continuous pulses of finer grained sediment throughout the long cores (Figures: 4.8, 4.9), it is suggested that there has been continuous sediment availability and transport into the Husky Lake system throughout the Holocene and that the regional landscape has been continuously adjusting since the onset of sediment deposition in Husky Lake over 2,400 years ago. Though it is uncertain whether landscape disturbances of this magnitude have been present in the catchment of Husky Lake in the past, the laminations and continuous pulses of changes in sediment grain size within the long cores suggest that this landscape has not been stable within the examined timeline. Such inherent instability in sediment delivery to the receiving waters may be attributed to the numerous valleys that have been incised in the Richardson Mountains, which ultimately drain into Husky Lake. The material

from these valleys has been eroding for some time and eventually makes its way into Husky Lake. Given the consistency of the sediment within the cores collected from Husky Lake, ongoing erosion has been common within the system for several thousands of years.

Since no sediment signature of thaw slump activity was traceable within the long cores collected from Husky Lake, another method would be required in order to determine whether the system has been affected by thaw slumps in the past such as analysis of aerial imagery of the landscape.

5.2 IMPACTS OF RETROGRESSIVE THAW SLUMPS ON NEARBY CONNECTED AQUATIC SYSTEMS

Ice-cored hummocky moraines have the potential to be highly unstable and geomorphically active. When large retrogressive thaw slumps develop due to thermokarst processes, fluvial and lacustrine systems can be significantly altered. The impacts of thaw slump activity on the subarctic lakes investigated for this study were mostly related to increased sediment input.

Evidence of the high amounts of sediment input into lake FM1 is seen in the debris flow transporting thawed sediments downslope (Figure 3.5, Figure 3.7) and the milky brown colour of the lake and stream water (Figure 3.4). The disturbance has visibly grown within the timeframe of this research project. The headwall of the primary slump scar has visibly regressed, enlarging the area of the slump floor and has almost incised into a small lake located just to the west of the disturbance (Figure 3.6). Several small slumps have also initiated along the

infilled valley due to mechanical erosion by the stream pushing up against the valley side, causing further slope erosion and slump initiation.

The deployment of sediment traps in lake FM1 provided further insight to the high rates of sedimentation occurring within this system. Lake FM1 is overwhelmed with the deposition of fine-grained sediments from the degrading slump, as sediment appears to remain in suspension throughout the lake, unable to completely settle to the lake floor. Fieldwork observations determined that the bottom ~30 cm of the water column is saturated with sediment forming a sludge-like material. This material prevented the retrieval of summer season sediment traps, as the sediment did not settle and the dense sludge-like material enveloped the traps.

Laboratory analyses of core FM1 indicate that the uppermost 54.5 cm of the core were deposited as a consequence of sedimentation from the disturbance in its upper catchment within the past 20 – 40 years. Such elevated rates of sedimentation into the lake have affected the lake's water quality (Figure 3.4), as suspended sediment in the water column increases rates of turbidity and specific conductivity of the water. The specific conductivity of sampled water at lake FM1 was 1400 µs/cm. Water that exceeds a specific conductivity of 500 µs/cm may indicate that it is not hospitable to various fish species and macroinvertebrates (United States Environmental Protection Agency, 2012). The turbidity of typical surface waters does not exceed 50 NTU, however that of the affected inflow stream to lake FM1 was measured at above 700 NTU. Based on visual observation and physical parameters it is clear that the water quality of

the lake FM1 system has been impacted by the inflow of thawed sediments, however the magnitude of such impacts is not certain. As previously stated, sediment pulses become disturbances to lakes when the present assemblages of organisms can no longer tolerate or are not able to adapt to the destabilization of the system by the imposed variability (O'Sullivan, 2004). In order to draw substantive conclusions on the impacts of thaw slump activity on the water quality of the FM1 system, a more comprehensive and thorough approach is necessary, including more frequent sampling methods and an examination of the ecological changes in the lake since slump initiation. This was not possible since the FM1 site was not easily accessible for extensive fieldwork.

At Husky Lake, the volume of sediment collected within sediment traps deployed in the bay of the disturbed stream (HU2) was much higher than that collected in the undisturbed streams (Figure 4.4). High sedimentation rates within the disturbed system were expected due to the magnitude of the thaw slump present. The average grain size of the sediment collected in the traps at the disturbed site was slightly larger than those of the undisturbed sites (Figure 4.3), however, the sediment was still dominated by silty clay sized particles similar to particle grain sizes measured from eroded slump material at the FM1 slump (~17 μm). The increase in average particle size examined at the disturbed site may be attributed to higher sediment availability due to the exposed scar in the landscape. The lower percentage of organic matter in the traps of the disturbed site may also be attributed to the exposure of highly erodible glacial sediment.

The short cores collected within the 3 basins of Husky Lake also show larger particle sizes within sediment at the disturbed site, however there were observations of higher percent organic matter that may not have been high enough in suspension to be captured within the traps or may have been deposited as a result of turbulent flows. The magnetic susceptibility of the short core sediment was doubled at the disturbed site compared to the undisturbed site, again indicating the differences in the source material available for transport within the systems.

Larger lakes provide greater opportunities for inflow sorting and dispersion processes (Lamoureux & Gilbert, 2004). As a result, particle sizes have little variability in central and distal deposition sites. The short cores collected from the Husky Lake basins (HU1-MG, HU2-MG, HU3-MG), are largely dominated by silt sized particles with some sand sized particles as well. Conversely, long cores (HU-VC1, HU-VC2) collected from distal positions in Husky Lake were comprised exclusively of silts and clays. The presence of sand grains in proximal sediments could be attributed to high-energy hydrologic events, which carry higher sediment loads down through the stream systems and deposit that material in near-shore locations rather than settling out further upstream.

Hydrological regimes in high latitude catchments are strongly seasonal. In undisturbed systems, as the summer progresses, the amount of sediment transported decreases substantially as active layers deepen and water infiltration into the ground increases (Lamoureux, 2000; Gilbert & Lamoureux, 2004). This is not the case for the Husky Lake or the FM1 system. Laminated sedimentary

structures are most often seen in high latitude regions due to the strong seasonality of sediment yield. Where sediment yield is high, very thin lamina can be produced due to fluvial processes. In catchments where materials are readily erodible and exposed, such as those of the disturbed systems of Husky Lake and lake FM1, laminae seen within lacustrine sediment cores may be produced by major hydrometeorological events (Lamoureux, 2000; Gilbert & Lamoureux, 2004). The long cores collected within the central portion of Husky Lake (HU-VC1 & HU-VC2) contained visually distinct laminae of varying width throughout their entire length (Figure 5.1). The FM1 core was stored in a frozen state and due to the nature of subsampling, it was not possible to determine whether laminae of the same nature were present. However, the previously analyzed core FM1-KB1 displayed similar pulses throughout its length (Appendix IX). This data shows that the sediment delivery to Husky Lake and lake FM1 is to some extent reliant on hydrometeorological events increasing the energy and sediment yield of the system. However, in order to make such deductions with more confidence, precipitation levels would have to be monitored in concurrence with measurement of pulses of sediment.

The water quality of the Husky Lake system was mostly affected in the stream of the disturbed site, with increased levels of turbidity and conductivity observed. Overall, the impacts of thaw slump disturbance within the Husky Lake system were more localized than those seen within the FM1 system.

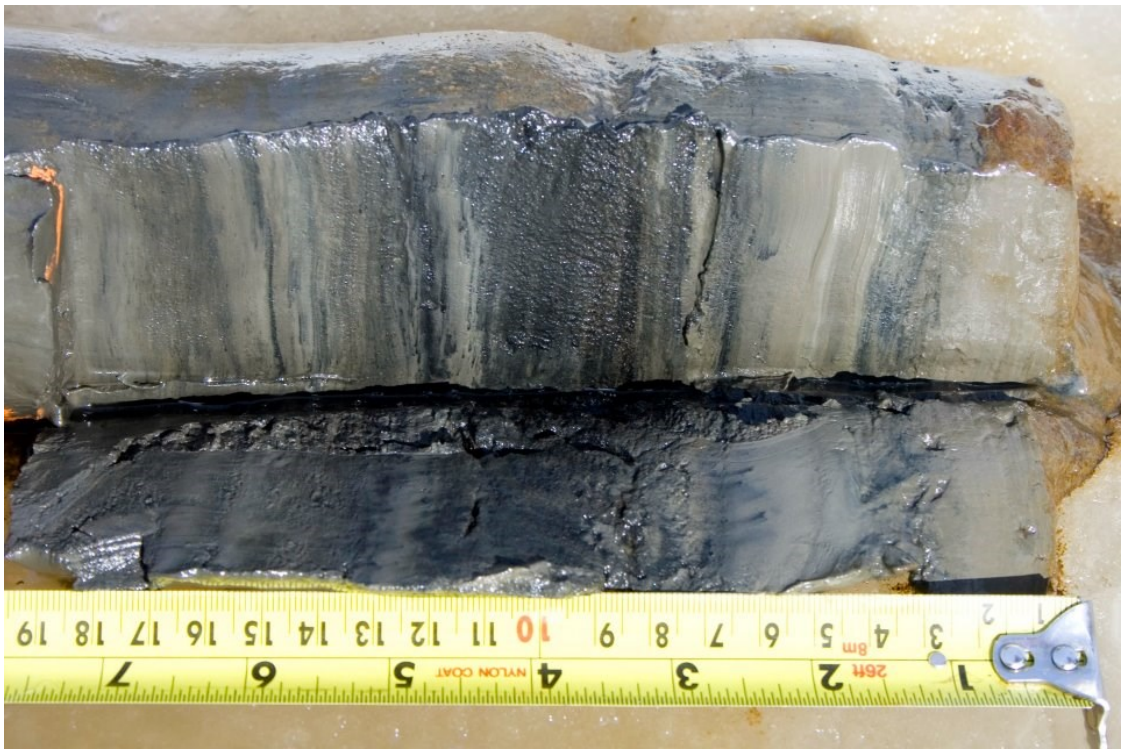

Figure 5.1: Laminations of sediment from Husky Lake.
The sediment from the core pictured was not used for analysis in the results of this project. This core was collected at the same site as HU-VC2 and clearly displays the same type of laminations that are present throughout the long cores collected from Husky Lake.

5.3 LAKE BASIN MORPHOMETRICS AND THE IMPACTS OF LARGE RETROGRESSIVE THAW SLUMP ACTIVITY

The processes that occur within a lake and its catchment influence its physical sedimentary environment. Slope disturbances are key sources of sediments (Lamoureux *et al.* 2014) and allochthonous inorganic fluxes dominate the sedimentary lacustrine deposits in Husky Lake and lake FM1. However, the large size of Husky Lake in relation to its catchment area and the portion of it that is disturbed act as a buffer to the effects of the thaw slump. This is mostly evident through comparing the geomorphic conditions of Husky Lake and lake FM1 (Table 3.1). Though the thaw slump at Husky Lake is similar in size to the one impacting lake FM1 (6 ha and 10 ha, respectively), the effects of the degrading slump are mostly evident solely within the disturbed stream and its basin (site HU2) rather than throughout the entire lake as seen in FM1. The disturbance at Husky Lake is two orders of magnitude smaller than the lake itself, whereas that of lake FM1 is 2 ha larger than the area of the lake. The disturbance to catchment ratio of Husky Lake (1: 1,162) is more than an order of magnitude smaller than that of lake FM1 (1: 80). Husky Lake occupies almost 1/8 of its entire catchment, whereas lake FM1 occupies less than 1% of its catchment. Due to these system morphometrics, the impacts of the disturbance at Husky Lake were minimal in comparison to those of the disturbance at lake FM1. Although the cores taken from Husky Lake were composed almost entirely of silty-clay eroded material from the landscape, the only evidence of the presence of a thaw slump was within the disturbed stream and its respective basin. These results are comparable to that of Dugan *et al.* (2012), who

investigated the impact of permafrost disturbances (active layer detachments) and sediment loading on the limnological characteristics of two high Arctic lakes. Dugan *et al.* (2012) showed that while thermokarst disturbances have potential to generate substantial downstream erosion and high sources of sediment, if a lake is large enough, the impacts of high fluvial sediment loads might be buffered. The lakes investigated by Dugan *et al.* (2012) were much smaller in area (140 ha and 160 ha) than that of Husky Lake, however; they were twice as deep. Although the retrogressive thaw slumps examined within this research are of much larger magnitude than the active layer detachments studied by Dugan *et al.* (2012), a comparison between the two studies should be considered. There are high amounts of sediment input from the disturbed stream into the HU2 basin, however, according to water quality testing at the time of this research, suspended sediment loads must only increase in the basin when the energy of the system is higher. This allows for the effects of current disturbance to remain non-critical in the short term and have no observable effects of the ecological well-being of the lake. Based on the radiocarbon dates, an average sedimentation rate of ~0.07 cm/year can be assumed for the centre of Husky Lake at the undisturbed site HU-VC1. Typical sedimentation rates in pristine Arctic lakes range from an approximate 0.01-0.2 cm/year (Muir and Rose, 2004). This provides further support to the analysis that the size of Husky Lake in relation to its catchment and the size of the disturbance in its catchment act as a buffer to the high sediment supply it receives in its affected basin. Although the

watershed is unstable, and has been inherently unstable and eroding within the examined time period (~2400 years), the lake as a whole remains pristine.

The results found in lake FM1 contrast those of Husky Lake. The calendar year obtained on the radiocarbon-dated material at 61.5 cm depth was determined to be 897-961 cal BP +/- 64. Based on ancillary information (core FM1-KB2 ^{210}Pb: Appendix I, aerial photographs: Appendix II), the thaw slump upstream of lake FM1 was initiated between 24-44 years ago and the uppermost 20.5 cm of sediment was deposited during that time. Based on the stratigraphic characteristics of the sediment within core FM1, it is suggested that the uppermost 54.5 cm of material in lake FM1 has deposited within the last 24-44 years. This places the average rate of sedimentation in the lake since thaw slump initiation at 1.23- 2.27 cm/year. Current sedimentation rates in lake FM1 are, therefore, an order of magnitude higher than in an environmentally stable system (Muir and Rose, 2004). Since the lake to catchment ratio is small in the case of lake FM1 (1:133) and the size of the disturbance exceeds that of the lake (1.7:1), the sediment delivered by the stream is of greater volume and is deposited in a much smaller area, leading to much thicker deposits and less opportunity for inflow sorting and dispersion processes. According to the radiocarbon date obtained at 61.5 cm depth, the sedimentation rate in the lake prior to slump initiation since ~897- 961 BP (from 61.5 – 54.5 cm depth) was ~ 0.01 cm/year, which is indicative of a stable system based on current knowledge.

Kokelj *et al.* (2013) state that high stream sediment loads caused by surface disturbance, high slope sediment availability, delivery of debris to the

floodplain by mass wasting, or perhaps leaching of slump soils by surface runoff will all influence thaw slump disturbed systems for centuries. However, this research shows that the severity of these disturbances and their impacts are dependent upon several factors including the ratio of disturbance to catchment and lake size, local climatic trends and slump activity.

5.4 CURRENT CLIMATE AND FUTURE PROJECTIONS

The dramatic geomorphic transformation of the environmental system of lake FM1 may be attributed to recent climate changes. Since the earliest suggested date of slump initiation (1970), mean annual air temperatures have increased at a rate of 0.77 °C per decade (Kokelj *et al.* 2013; Burn and Kokelj, 2009). Based on precipitation records extending back to the 1920s, three of the five wettest summers on record have occurred in the past decade (Kokelj *et al.* 2013). Such conditions can perpetuate slump growth, as rainfall events evacuate materials from the scar zone, leaving ground ice exposed for further thaw and backwasting. Kokelj *et al.* (2013) suggest that persistence of such climatic regimes will promote polycyclic behavior and growth in disturbance to smaller thaw slumps, evolving into mega slumps.

Retrogressive thaw slumps are becoming more abundant and of larger magnitude on the landscape of the Peel Plateau reflecting landscape instability due to warming permafrost (Kokelj *et al.* 2013, Lantz and Kokelj, 2008). Based on the results presented from the study of lake FM1, Husky Lake and their upper catchments, retrogressive thaw slumps have the potential to drastically impact

the sedimentation and geomorphology of connected lakes. The environmental impact of thaw slumps on downstream lakes depends on factors such as disturbance to catchment and lake to catchment and disturbance ratios, hydrological regimes, thaw slump activity and stream connectivity downslope of the disturbance. Lamoureux *et al.* (2014) examined the erosion dynamic following localized permafrost slope disturbances and found three factors to be critical to the response of lacustrine systems following large-scale sediment erosion: channel density within the disturbance; downstream channel connectivity; and geomorphic evolution of the disturbance. Should recent climatic trends persist, increased temperatures and precipitation patterns will allow for a larger portion of retrogressive thaw slumps to develop into mega slumps by inducing permafrost thaw within the headwalls and washing away accumulating sediment on slump floors downslope (Kokelj *et al.* 2013). Due to current and predicted future climatic conditions, the studied area is likely entering a period of enhanced mass wasting. It is not evident whether large disturbances have occurred within the systems in the past, however it appears that the landscape has been inherently unstable and continuously eroding over a 2,400-year period. It is therefore difficult to predict how such changes in climate will manifest in this landscape. The differing effects of thaw slumps on lake FM1 and Husky Lake show that the degree to which aquatic environments are (and can potentially be) impacted by large disturbances varies depending on the morphologies of each individual system.

CHAPTER SIX

CONCLUSION

6.1 CONCLUSION OF STUDY FINDINGS

Thermokarst activity can lead to significant impacts on fluvial and lacustrine systems. Kokelj *et al.* (2013) reported on the magnitude of the effects of mega slumps on fluvial systems at the watershed scale within the Peel Plateau, NT. This study investigated the localized impacts of thaw slump activity on aquatic systems and focused on the geomorphological changes to a small and a large subarctic lake. Using paleolimnological techniques, the objectives of the research were 1) to determine whether such large-scale disturbance has occurred within these systems in the past; 2) to quantify the current impacts of the disturbance on two very different and connected aquatic systems.

Based on the results of this study it was not possible to quantify whether retrogressive thaw slumps have occurred within the studied area in the past. The long cores collected within Husky Lake displayed an inherent instability within the landscape throughout the period of the late Holocene covered by the collected lake sediment cores. These cores, collected from the centre of Husky Lake near Fort McPherson, NT, were characterized by low percent organic matter, high siliciclastic input and constant input of small particle grain sizes (primarily silts and clays) throughout the entire sediment record recovered. It is suggested that these sedimentary characteristics represent constant input of eroded glacial-deposited sediment from the Richardson Mountains. Although the results

indicate a history of instability within the system, it is not clear whether such disturbance was previously manifested as large-scale permafrost erosional features. In the smaller catchment, FM1, there is an abrupt transition from peat-like sediment at the base of the core to highly inorganic sediment inputs similar to those found through the entire record recorded by the Husky Lake sediment cores. This transition could not be dated accurately using ^{210}Pb dating techniques because background levels of ^{210}Pb were not reached in the 20.5 cm long core previously recovered from the lake (FM1-KB2).

Current effects of thaw slumping on the two studied systems varied greatly, with lake FM1 experiencing sedimentation rates orders of magnitude higher than that of Husky Lake. Based on analyses of airphotos from the study area, it appears the thaw slumping in the catchment of FM1 initiated sometime between 1970 and 1990. Therefore, the sediment deposited in lake FM1 after the abrupt transition from peat-like sediment to highly inorganic sediment likely represents the initiation of this slump and the subsequent transport of eroded material. Almost 55 cm of eroded material has accumulated within the receiving waters of lake FM1 since slump initiation. This substantial accumulation of sediment may be attributed to the fact that the disturbance is greater in size than the lake itself, as well as the small size of the lake in relation to its catchment. The sediment being eroded from the active FM1 thaw slump has minimal area for deposition within the lake basin and is therefore infilling the lake at an overwhelming rate.

The current effects of thermokarst disturbance on Husky Lake were minimal and localized compared to that of FM1. The large size of Husky Lake in relation to its disturbance and the area it covers within its catchment was able to act as a buffer to the effects of the large disturbance. The high sedimentation rates into the disturbed portion of the system were mostly manifested through elevated turbidity and conductivity within the affected inflow stream and increasing sediment accumulation within its concurrent basin.

The observations presented here suggest that ice-rich glaciogenic landscapes are inherently unstable and permafrost disturbance can have significant influence on the geomorphology of surrounding fluvial and lacustrine systems. However, the magnitude of the impacts from such disturbance on these systems may be buffered by individual system morphometrics. Should climatic warming persist and extended melt seasons continue, conditions conducive to the formation of further catchment disturbances of larger scales will place enhanced stress on regional aquatic systems.

6.2 RECOMMENDATIONS FOR FUTURE WORK

It is recommended that future studies further investigate the effects of thaw slumping on the Peel Plateau. Understanding how climate change impacts northern environments and its role in environmental changes such as retrogressive thaw slumping is crucial to sustainable management of natural ecosystems and infrastructure in this region. It is recommended that the FM1 and Husky Lake systems be further studied. A deeper investigation into the past

conditions of these systems should be undertaken through the examination of aerial imagery of the catchments. Efforts to further date the sediment cores should be made and more sediment traps deployed and closely monitored in order to further understand sedimentation rates in these systems and obtain more quantitative data. Changes in disturbance size and activity should also be monitored using aerial imagery or field observations and examined alongside local temperature and precipitation data in order to further understand the dynamics of these systems. Water quality parameters should be more extensively monitored in order to further understand the ecological impacts of the disturbances on the systems. Dr. Roberto Quinlan (York University) is currently examining the ecological impacts of the disturbance in the FM1 through the study of chironomid assemblages from the FM1 core. Of upmost importance is the monitoring of the growth of the thaw slump in the FM1 catchment, as it is rapidly encroaching on a lake. Should erosion of the slump headwall persist, the lake will catastrophically drain. Such a scenario has not yet been documented in scholarly research; therefore its potential effects are unknown.

REFERENCES

ACIA. (2005) Arctic Climate Impact Assessment, Cambridge University Press [online]. 1042 pp. Available from www.acia.uaf.edu.

Anderson, D.E. Goudie, A.S. Parker, A.G. (2007) Global Environments through the Quaternary, Oxford University Press, Oxford.

Bartington Instruments Inc. (2009) For innovation in magnetic measuring systems, from: http://www.bartington.com/.

Belshe, E.F. Schuur, E.A.G. Bolker, B.M. (2013) Tundra ecosystems observed to be CO_2 sources due to differential amplification of the carbon cycle, *Ecology Letters,* Vol. 16: 1307-1315.

Björk, S. Wohlfarth, B. (2001) ^{14}C chronostratigraphic techniques in paleolimnology in: Last, W.M. Smol, J.P. (eds) *Tracking environmental change using lake sediments Volume 1: Basin analysis, coring and chronological techniques*: 205-245.

Bloesh, J. (2004) Sedimentation and lake sediment formation in: O' Sullivan, P.E. *The Lakes Handbook Vol 1: Limnology and Limnetic Ecology* 197-229, United Kingdom.

Brown, S.L. Bierman, P.R. Lini, A. Southon, J. (2000) 10 000 yr record of extreme hydrologic events, *Geology,* Vol. 28: 335–338.

Burn, C.R. Lewkowicz, A.G. (1990) Canadian Landform Examples-17 Retrogressive Thaw Slumps, *The Canadian Geographer*, Vol. 34(3): 273-276.

Burn, C.R. (1997) Cryostratigraphy, paleogeography, and climate change during the early Holocene warm interval, western Arctic coast, Canada, *Canadian Journal of Earth Sciences,* Vol. 34 (7): 912-925.

Canadian Parks and Wilderness Society (2014), Peel Watershed Atlas Retrieved from: http://www.cpawsyukon.org/resources/peel-atlas/A03-watersheds.pdf.

Chapin, F.S. III. Sturm, M. Sereeze, M.C. McFadden J.P. Key, J.R. Lloyd, A.H. McGuire, A.D. Rupp, T.S. Lynch, A.H. Schimel, J.P. Beringer J. Chapman, W.L. Epstein, H.E. Euskirchen, E.S. Hinzman, L.D. Jia, G. Ping, C-L. Thompson, C.D.C. Walker, D.A. Welker, J.M. (2005) Role of land-surface changes in Arctic summer warming, *Science,* Vol. 310: 657-660.

Cockburn, J.M.H. Lamoureux, S.F. (2008) Inflow and lake controls on short-term mass accumulation and sedimentary particle size in a High Arctic lake: implications for interpreting varved lacustrine sedimentary records, *Journal of Paleolimnology,* Vol. 40 (3): 923-942.

Dearing, J.A. (1999) Magnetic susceptibility, in: Walden, J.Oldfield, F. Smith, J. (eds.) *Environmental Magnetism: a practical guide*, Technical Guide No. 6, Quaternary Research Association, London, UK: 35-62.

Deasley, K. Korosi, J.B. Thienpont, J.R. Kokelj, S.V. Pisaric, M.F.J. and Smol, J.P. (2012) Investigating the response of Cladocera to a major salt- water intrusion event in an Arctic lake from the outer Mackenzie Delta (NT, Canada), *Journal of Paleolimnology*, Vol. 48: 287–296.

Dixon, J. Dietrich, J. R. MacNeil, D.H. (1992) *Upper Cretaceous to Pleistocene sequence stratigraphy of the Beaufort-Mackenzie and Banks Island areas, Northwest Canada,* Bulletin 407 Geological Survey of Canada: Ottawa.

Dugan, H.A. Lamoureux, S.F. Lewis, T. Lafrenière, M.J. (2012) The impact of permafrost disturbances and sediment loading on the limnological characteristics of two high arctic lakes, *Permafrost and Periglacial Processes,* Vol. 23 (2): 119-126.

Dyke, A.S. Giroux, D. Roberston, L. (2004) *Paleovegetation maps of Northern North America, 18,000 to 1,000 BP.* Geological Survey of Canada, Open File 4682.

French, H. M. (2007) *The Periglacial Environment* (3rd ed.) Wiley & Sons, West Sussex, England.

French, H.M. Egginton, P. (1973) Thermokarst development, Banks Island, Western Canadian Arctic, in *North American Contribution, Permafrost Second International Conference, Yakutsk,* 13-28 July, 203-212, Washington, DC: National Academy of Sciences.

Gilbert, R. Lamoureux, S. (2004) Processes affecting deposition of sediment in a small, morphologically complex lake, *Journal of Paleolimnology,* Vol.31(1): 37-48.

Gilbert, R. Crookshanks, S. Hodder, K.R. Spagnol, J. Stull, R.B. (2006) The record of an extreme flood in the sediments of montane Lillooet Lake, British Columbia: implications for paleoenvironmental assessment, *Journal of Paleolimnology,* Vol. 35**:** 737-745.

Glew, J.R. Smol, J.P. Last, W.M. (2001) Sediment core collection and extrusion in: *Tracking environmental change using lake sediments: Developments in paleoenvironmental research,* Vol. 1: 73-105.

Government of the Yukon Department of Economic Development (2000) *Petroleum resource assessment of the Peel Plateau, Yukon Territory, Canada* – National Energy Board for Energy Resources Branch ISBN 1-55018-857-7.

Heiri, O. Lotter, A.F. Lemcke, G. (2001) Loss on ignition as a method for estimating organic and carbonate content in sediments: reproducibility and comparability of results, *Journal of Paleolimnology,* Vol. 25: 101-110.

Hirons, K.R. Thompson, R. (1986) Palaeoenvironmental application of magnetic measurements from inter-drumlin hollow lake sediments near Dungannon, Co. Tyrone, Northern Ireland, *Boreas,* Vol. 15(2): 117-135.

Jafarov, E.E. Marchenko, S.S. Romanovsky, V.E. (2012) Numerical modeling of permafrost dynamics in Alaska using a high spatial resolution dataset, *The Cryosphere,* Vol. 6: 613-624.

Jensen, A.E. Lohse, K.A. Crosby, B.T. Mora, C.I. (2014) Variations in soil carbon dioxide efflux across a thaw slump chronosequence in northwestern Alaska, *Environmental Research Letters,* Vol. 9: 025001.

Johannessen, O.M. Bengtsson, L. Miles, M.W. Kuzmina, S.I. Semenov, V.A. Alekseev G.V. Nagurnyi, A.P. Zakharov, V.F. Bobylev, L.P. Pettersson, L.H. Hasselmann, K. Cattle, H.P. (2004) Arctic climate change: observed and modeled temperature and sea-ice variability, *Tellus A,* Vol. 56(5): 559-560.

Jorgenson, M.T. Osterkamp, T.E. (2005) Response of boreal ecosystems to varying modes of permafrost degradation, *Canadian Journal of Forest Research,* Vol. 35(9): 2100-2111.

Kokelj, S.V. Burn, C.R. (2003) Ground Ice soluble cations in near-surface permafrost, Inuvik, Northwest Territories, Canada, *Permafrost and Periglacial Processes,* Vol. 14: 275-289.

Kokelj, S.V. Burn, C.R. (2005) Geochemistry of the active layer and near-surface permafrost, Mackenzie Delta region, Northwest Territories, Canada, *Canadian Journal of Earth Sciences,* Vol. 42: 37-48.

Kokelj, S.V. Jenkins, R.E. Milburn, D. Burn, C.R. Snow, N. (2005) The influence of thermokarst disturbance on the water quality of small upland lakes, Mackenzie Delta region, Northwest Territories, Canada, *Permafrost and Periglacial Processes,* Vol. 16: 343-353.

Kokelj, S.V. Zajdlik, B. Thompson, M.S. (2009) The impacts of thawing permafrost on the chemistry of lakes across the subarctic boreal-tundra transition, Mackenzie Delta region, Canada, *Permafrost and Periglacial Processes,* Vol. 20: 185-199.

Kokelj, S.V. Lantz, T.C. Kanigan, J. Smith, S.L. Coutts, R. (2009) Origin and Polycyclic Behaviour of Tundra Thaw Slumps, Mackenzie Delta Region,

Northwest Territories, Canada, *Permafrost and Periglacial Processes,* Vol. 20**:** 173-184.

Kokelj, S.V. Lantz, T.C. Solomon, S. Pisaric, M.F.J. Keith, D. Morse, P. Thienpont, J.R. Smol, J.P. Esagok, D. (2012) Using multiple sources of knowledge to investigate northern environmental change: regional ecological impacts of a storm surge in the outer Mackenzie Delta, N.W.T. *Arctic,* Vol. 65(3): 257-272.

Kokelj, S.V. Lacelle, D. Lantz, T.C. Malone, L. Tunnicliffe, J. Clark, I.D. Chin, K. (2013) Thawing of massive ground ice in mega slumps drives increases in stream sediment and solute flux across a range of watershed scales, *Journal of Geophysical Research*, Vol.118: 681–692.

Kokelj, S.V. Jorgenson, M.T. (2013) Advances in thermokarst research, *Permafrost and Periglacial Processes,* Vol. 24: 108-119.

Lacelle, D. Bjornson, J. Lauriol, B. (2010) Climatic and geomorphic factors affecting contemporary (1950-2004) activity of retrogressive thaw slumps on the Aklavik Plateau, Richardson Mountains, NWT, Canada, *Permafrost and Periglacial Processes,* Vol.21**:** 1-15.

Lamoureux, S.F. Gilbert, R. (2004) Physical and chemical properties and proxies of high latitude lake sediments in: Pienitz, R. Douglas, M.S.V. Smol, J.P. (eds) *Long-term Environmental Change in Arctic and Antarctic Lakes Volume 8:* 53-87.

Lamoureux, S.F. (2000) Five centuries of interannual sediment yield and rainfall-induced erosion in the Canadian high arctic recorded in lacustrine varves, *Water Resources Research,* Vol 36(1): 309-318.

Lamoureux, S. F. England, J.H. (2000) Late Wisconsinan glaciation of the central sector of the Canadian High Arctic, *Quaternary Research,* Vol. 54(2): 182-188.

Lamoureux S.F. England, J.H. Sharp, M.J. Bush A.B.G. (2001) A varve record of increased “Little Ice Age” rainfall associated with volcanic activity, Arctic Archipelago, Canada, *Holocene,* Vol. 11**:** 243-249.

Lamoureux, S.F. Lafrenière, M.J. (2009) Fluvial impact of extensive active layer detachments, Cape Bounty, Melville Island, Canada, *Arctic, Antarctic, and Alpine Research,* Vol. 41. No.1: 59-68.

Lamoureux S.F. Lafrenière, M.J. Favaro, E.A. (2014) Erosion dynamics following localized permafrost slope disturbances, *Geophysical Research Letters*, Vol. 41. (15): 5499-5505.

Lantz, T. C. Kokelj, S.V. (2008) Increasing rates of retrogressive thaw slump activity in the Mackenzie Delta region, N.W.T. Canada, *Geophysical Research Letters,* Vol. 35, L06502.

Last, W. M. Smol, J.P (2001) Tracking Environmental Change Using Lake Sediments: *Vol 2 Physical and Geochemical Methods,* Kluwer Academic Publishers.

Lawrence, D.M. Slater, A.G. Tomas, R.A. Holland, M.M. Deser, C. (2008) Accelerated Arctic land warming and permafrost degradation during rapid sea ice loss, *Geophysical Research Letters,* Vol. 35 L11506.

Lewkowicz, A. G. (1986) Rate of short-term ablation of exposed ground ice, Banks Island, Northwest Territories, Canada, *Journal of Glaciology,* Vol. 32(112): 511–519.

Lewkowicz, A.G. (1987) Nature and importance of thermokarst processes, Sand Hills Moraine, Banks Island, Canada, *Geografiska Annaler,* Vol. 69a: 321-327.

Mackay, J.R. (1966) Segregated epigenetic ice and slumps in permafrost Mackenzie Delta area, N.W.T. *Geographical Bulletin,* Vol. 8: 59-80.

Malone, L. Lacelle, D. Kokelj, S.V. Clark, I.D. (2013) Impacts of hillslope thaw slumps on the geochemistry of permafrost catchments (Stony Creek watershed, NWT, Canada) Chemical Geology Vol. 356: 38-49.

Moskowitz, B.M. (1995) Fundamental physical constants and conversion factors, in: Global Earth Physics – A Handbook of Physical Constants, AGU Reference Shelf 1. American Geophysical Union, Washington DC, USA: 346-355.

Muir, D.C.G. Rose, N. L. (2004) Lake sediments as records of Arctic and Antarctic pollution, in: Pienitz, R., Douglas, M.S.V., Smol, J.P. (eds) *Long-term Environmental Change in Arctic and Antarctic Lakes Vol 8:* Published: Dordrecht, The Netherlands, 209-240.

Murton J, B. (2009) Stratigraphy and paleoenvironments of Richards Island and the eastern Beaufort Continental Shelf during the last glacial-interglacial cycle, *Permafrost and Periglacial Processes,* Vol. 20: 107-125.

Nowaczyk, N.R. (2001) Logging of magnetic susceptibility, in: Last, W.M. Smol, J.P. (eds) *Tracking Environmental Change Using Lake Sediments Volume 1: Basin Analysis, Coring and Chronological Techniques*, Kluwer Academic Publishers, Dordrecht, The Netherlands: 155-170.

Northwest Territories Geological Survey (2014) *Shale basin evolution in the Central NWT,* Government of Northwest Territories from: http://www.nwtgeoscience.ca/project/summary/shale-basin-evolution-central-nwt.

Osterkamp, T.E. Jorgenson, J.C. (2005) Warming of permafrost in the Arctic National Wildlife Refuge, Alaska, *Permafrost and Periglacial Processes,* Vol. 17: 65-69.

Pisaric, M.F.J. Thienpont, J.R. Kokelj, S.V. Nesbitt, H. Lantz, T.C. Solomon, S. Smol, J.P. (2011), Impacts of a recent storm surge on an Arctic delta ecosystem examined in the context of the last millennium, *Proceedings of the National Academy of Sciences*, Vol. 108: 8960–8965.

Porinchu, D.F. MacDonald, G.M. (2003) The use and application of freshwater midges (Chironomidae: Insecta: Diptera) in geographical research, *Progress in Physical Geography,* Vol. 27: 378-422.

Porter, T.J. Pisaric, M.F.J. Field, R.D. Kokelj, S.V. Edwards, T.W.P. DeMontigny, P. Healy, R. LeGrande, A. (2014) Spring-summer temperatures since AD 1780 reconstructed from stable oxygen isotope ratios in white spruce tree-rings from the Mackenzie Delta, northwestern Canada, *Climate Dynamics*, Vol. 42: 771-785.

Pyle, L.J. Jones, A.L. Gal, L.P. (2006) Geoscience Knowledge Synthesis: *Peel Plateau and Plain, a prospective hydrocarbon province in the Northern Mackenzie Corridor*, Geological Survey of Canada, Open File 5234, Northwest Territories Open File 2006-01.

Ritchie, J.C., Hare, F.K. (1971) Late-quaternary vegetation and climate near the arctic tree line of northwestern North America, *Quaternary Research,* Vol 1(3): 331-342

Ritchie J.C. Cwynar L.C. Spear, R.W. (1983) Evidence from northwest Canada for an early milankovitch thermal maximum, *Nature,* Vol. 305: 126–128.

Ritchie, J.C. (1984) Past and present vegetation of the far northwest of Canada, *Boreas,* Vol. 15(2): 116.

Romanovsky, V. E. Smith, S.L. Christiansen, H.H. (2010) Permafrost Thermal State in the Polar Northern Hemisphere during the International Polar Year 2007-2009: a synthesis*, Permafrost and Periglacial Processes*, Vol. 21:106-116.

Romanovsky, V.E. Smith, S.L. Christiansen, H.H. Shiklomanov, N.I. Streletskiy, D.A. Drozdov, D.S. Oberman, N.G. Kholodov, A.L. Marchenko S.S. (2013) Permafrost, in: Jeffries, M. O. Richter-Menge, J.A. Overland, J.E. (eds) *Arctic Report Card 2013*, http://www.arctic.noaa.gov/reportcard.

Rowan D.J. Kalff J. Rasmussen, J.B. (1992) Profundal sediment organic content and physical character do not reflect lake trophic status, but rather reflect inorganic sedimentation and exposure, *Canadian Journal of Fisheries and Aquatic Sciences,* Vol. 49: 1431–1438.

Schuur, E.A.G. Bockheim, J. Canadell, J.G. Euskirchen, E. Field, C.B. Goryachkin, S.V. Hagemann, S. Kuhry, P. Lafleur, P.M. Lee, H. Mahzhitova, G. Nelson, F.E. Rinke, A. Romanovsky, V.E. Shiklomanov, N. Tarnocai, C. Venevsky, S. Vogel, J.G. Zimov, S.A. (2008) Vulnerability of permafrost carbon to climate change: implications for the global carbon cycle, *BioScience,* Vol. 58: 701–14.

Schuur E.A.G. Vogel, J.G. Crummer, K.G. Lee, H. Sickman, J.O. Osterkamp, T.E. (2009) The effect of permafrost thaw on old carbon release and net carbon exchange from tundra, *Nature,* Vol. 459: 556–559.

Schuur, E. Abbott, B. (2011) High risk of permafrost thaw, *Nature,* Vol. 480: 32–33

Serreze, M.C. Walsh, J.E. Chapin, F.S. III. Osterkamp, T. Dyurgerov, M. Romanovsky, V. Oechel, W.C. Morison, J. Zhang, T. Barry, R.G. (2000) Observational evidence of recent change in the northern high-latitude environment, *Climatic Change,* Vol. 46(1–2): 159-207.

Shuman, B. (2003) Controls on loss-on-ignition variation in cores from two shallow lakes in the northeastern United States, *Journal of Paleolimnology,* Vol. 30: 371-385.

Smith, C.A.S. Meikle, J.C. Roots, C.F. (2004) Ecoregions of the Yukon Territory: Biophysical properties of Yukon landscapes, Agriculture and Agri-Food Canada, PARC Technical Bulletin No.04-01, Summerland, British Columbia, 313.

Smith, S.L. Burgess, M.M. (2000) *Ground temperature database for northern Canada*, Geological Survey of Canada, Open File Report 3954.

Smith, S. L. Romanovsky, V.E. Lewkowicz, A.G. Burn, C.R. Allard, M. Clow, G.D. Yoshikawa, K. Throop, J. (2010) Thermal State of Permafrost in North America—A Contribution to the International Polar Year, *Permafrost and Periglacial Processes*, Vol. 21: 117-135.

Smith, S. L.Throop, J. Lewkowicz, A.G. (2012) Recent changes in climate and permafrost temperatures at forested and polar desert sites in northern Canada, *Canadian Journal of Earth Science*, Vol. 49: 914-924.

Spear, R.W. (1993) The palynological record of Late-Quaternary arctic tree-line in northwest Canada, *Review of Palaeobotany and Palynology,* Vol. 79: 99-111.

Stanek, W. Alaxander, K. Simmons, C.S. (1981) Reconnaissance of vegetation and soils along the Dempster Highway, Yukon Territory: 1. Vegetation types. Environment Canada, Canadian Forestry Service, BC-X-217, Victoria, British

Columbia

Stantec (2012) Status and Trends of the Water Quality, Suspended Sediment Quality, and Hydrology of the Peel River Watershed. Report prepared for: Aboriginal Affairs and Northern Development Canada

Steinhilber, F. Beer, J. Fröhlich, C. (2009) Total solar irradiance during the Holocene, *Geophysical Research Letters,* 36

Stuiver, M. Reimer, P.J (1993) Extended ^{14}C Data Base and Revised CALIB 3.0 ^{14}C Age Calibration Program, *Radiocarbon*, Vol. 35: 215-230.

Thienpont, J.R. Johnson, D.H. Nesbitt, H. Kokelj, S.V. Pisaric, M.F.J. Smol, J.P. (2012) Arctic coastal freshwater ecosystem responses to a major saltwater intrusion: A landscape-scale palaeolimnological analysis, *Holocene*, Vol. 22: 1447–1456.

Thienpont J.R. Kokelj S.V. Korosi, J.B. Cheng, E.S. Desjardins, C. Kempe, L.E. Blais, J.M. Pisaric, M.FJ. Smol, J.P. (2013) Exploratory hydrocarbon drilling impacts to Arctic lake ecosystems, *Public Library of Science ONE,* Vol. 8(11).

Thompson, R. Battarbee, R.W. O'Sullivan, P.E. Oldfield, F. (1975) Magnetic susceptibility of lake sediments, *Limnology and Oceanography,* Vol.20(5): 687-698.

Tomkins, J. D. Antoniades, D. Lamoureux, S.F. Vincent, W.F. (2008) A simple and effective method for preserving the sediment-water interface of sediment cores during transport, *Journal of Paleolimnology,* Vol. 40: 577-582.

United States Environmental Protection Agency (2012) *Water monitoring and assessment*, from: http://water.epa.gov/type/rsl/monitoring/vms59.cfm

Vermaire, J.C. Pisaric, M.F.J. Thienpont, J.R. Courtney Mustaphi, C.J. Kokelj, S.V. Smol, J.P. (2013) Arctic climate warming and sea ice declines lead to increased storm surge activity, *Geophysical Research Letters,* Vol. 40: 1-5.

Yukon Ecoregions Working Group (2004) Peel River Plateau, in: *Ecoregions of the Yukon Territory: Biophysical properties of Yukon landscapes*, Smith, C.A.S. Meikle, J.C. Roots, C.F. (eds), Agriculture and Agri-Food Canada, PARC Technical Bulletin No. 04-01, Summerland, British Columbia, p.63-72

Zhang, T. Barry, R.G. Knowles, K. Heginbottom, J.A. Brown, J. (1999) Statistics and characteristics of permafrost and ground-ice distribution in the Northern Hemisphere, *Polar Geography*, Vol. 23(2): 132–154.

Zhang, T. Barry, R.G. Knowles, K. Heginbottom, J.A. Brown, J. (2008) Statistics

and characteristics of permafrost and ground-ice distribution in the Northern Hemisphere, *Polar Geography,* Vol. 21 (1-2): 47-68.

Zolitschka, B.J. Mingram, S. Van Der Gaast, J.H. Jansen, F. Naumann, R. (2001) Sediment logging techniques, in: Last, W.M. Smol, J.P. (eds) *Tracking Environmental Change Using Lake Sediments Volume 1: Basin Analysis, Coring and Chronological Techniques,* Kluwer Academic Publishers, Dordrecht, The Netherlands: 137-154.

APPENDICES

Appendix I: Results of ^{210}Pb dating from core FM1-KB2.

Top (cm)	Bottom (cm)	Pb-210 (Bq/g)	Precisn (%) 1 STD
0.0	0.5	0.032	12.5
0.5	1.0	0.052	7.6
1.0	2.0		
2.0	2.5	0.046	8.9
2.5	3.0		
3.0	3.5	0.042	7.7
3.5	4.0		
4.0	4.5	0.038	8.8
4.5	5.0		
6.0	6.5	0.036	11.5
6.5	8.0		
8.0	8.5	0.042	7.3
8.5	10.0		
10.0	10.5	0.034	7.8
10.5	12.0		
12.0	12.5	0.041	10.3
12.5	14.0		
14.0	14.5	0.036	8.0
14.5	15.0		
15.0	15.5	0.043	6.4
15.5	16.0		
16.0	16.5	0.042	8.6
16.5	17.0	0.047	7.1
17.0	17.5	0.055	7.2
17.5	18.0	0.042	10.5

Results of ^{210}Pb dating of core FM1-KB2 from MyCore Scientific Inc.

Appendix II: Aerial photographs.
i)

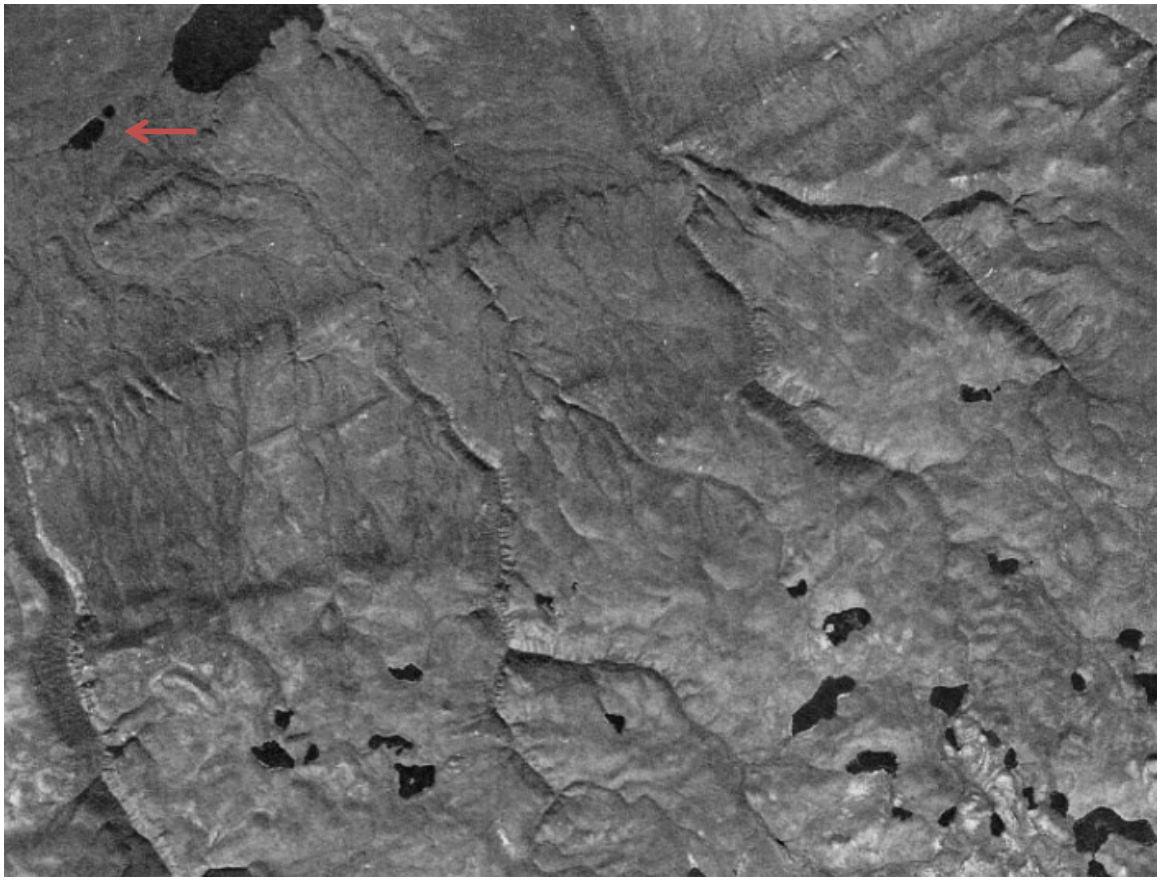

Aerial photograph of the study site taken in 1953. Note the dark colour of the lake (pointed out by the red arrow) and the absence of the thaw slump (site circled in red).

Appendix II: Aerial photographs.

ii)

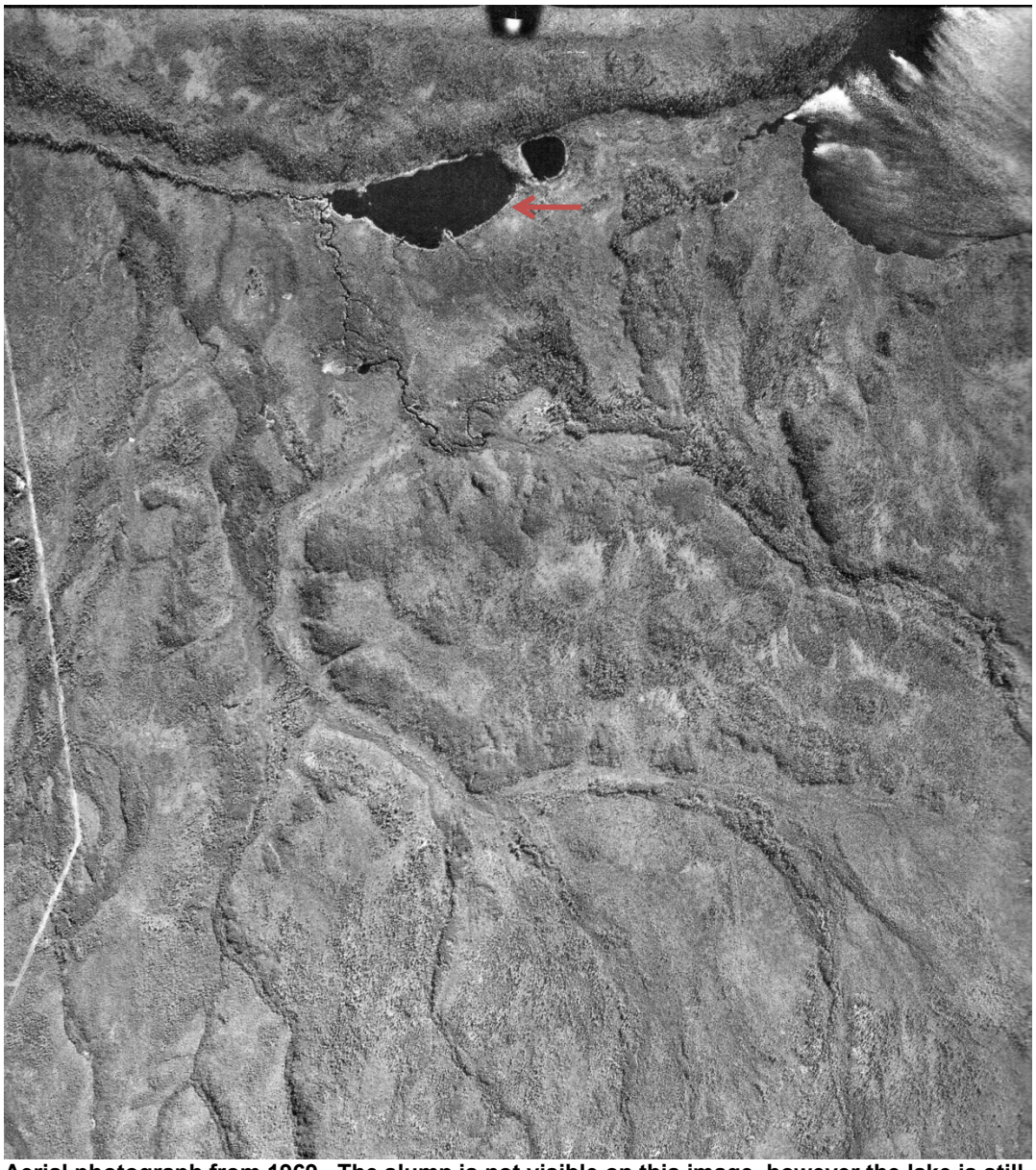

Aerial photograph from 1969. The slump is not visible on this image, however the lake is still Observed to be dark in colour (pointed out with the red arrow).

Appendix II: Aerial photographs.

iii)

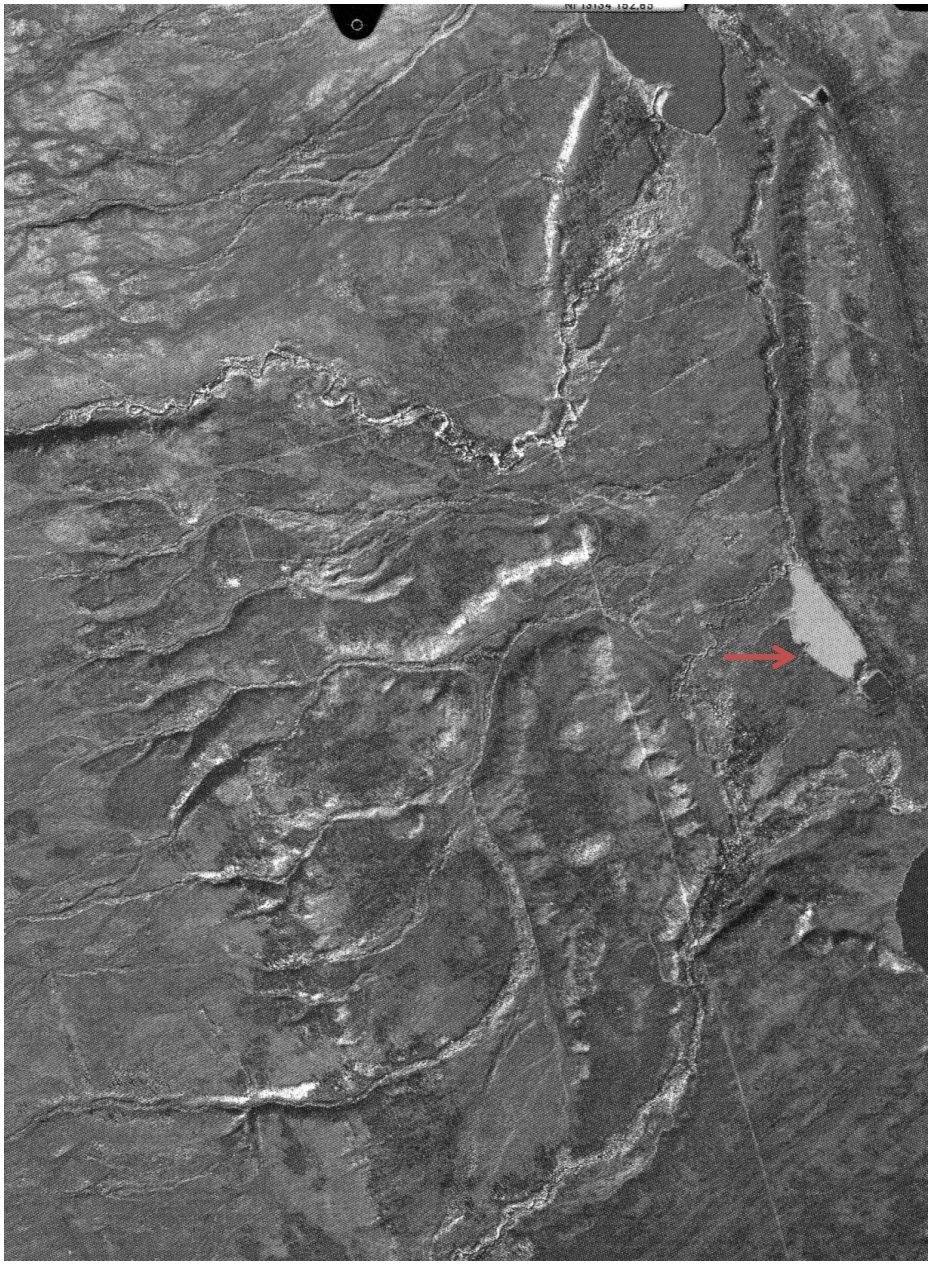

Aerial photograph from 1990. The thaw slump is not within sight on the image either; however shade of the Lake (pointed out by the red arrow) is much lighter in contrast than before, indicating a change in sediment influx

Appendix III: Water quality data for Husky Lake.

Water quality data for samples collected from Husky Lake and adjacent streams flowing into Husky Lake. Each sampling site was sampled three times and data collected includes: Temperature (°C), dissolved oxygen (ppm), % dissolved oxygen, conductivity (µS/cm), turbidity (NTU) and pH. The data shows that water quality is fairly consistent except for elevated values for conductivity and turbidity in the vicinity of the disturbed site (HU2).

Sample ID	Date	Coordinates	Description	Status	Temp (°C)	Dissolved Oxygen (ppm)	% Dissolved Oxygen	Conductivity (µS/cm)	Turbidity (NTU)	pH
HU1-ST1	06/08/2012	67° 31' 57.7554" N 135° 11' 48.1554"W	undisturbed stream North Husky Lake	undisturbed	4.6	13.03	n/a	1577	4.56	6.89
HU1-ST2	06/13/2012	67° 31' 57.7554" N 135° 11' 48.1554"W	undisturbed stream North Husky Lake	undisturbed	3.2	13.8	103.3	561	21.8	6.76
HU1-ST3	06/14/2012	67° 31' 57.7554" N 135° 11' 48.1554"W	undisturbed stream North Husky Lake	undisturbed	4.2	13.3	101.4	528	14.4	6.65
HU1-VAN1	06/08/2012	67° 32' 14.5674"N 135° 11' 7.1154" W	surface sample, North Husky basin	undisturbed	7.7	9.21	n/a	1078	20.9	7
HU1-VAN1	06/13/2012	67° 32' 14.5674"N 135° 11' 7.1154" W	surface sample, North Husky basin	undisturbed	8.5	10.29	87.7	1087	20.8	7.04
HU1-VAN1	06/14/2012	67° 32' 14.5674"N 135° 11' 7.1154" W	surface sample, North Husky basin	undisturbed	9	10.46	90.3	1097	19.9	7.03
HU1-VAN2	06/08/2012	67° 32' 24.0714"N 135° 10' 42.132" W	surface sample, North Husky Lake	undisturbed	6.6	9.41	80.1	1081	18.6	6.1
HU1-VAN2	06/13/2012	67° 32' 24.0714"N 135° 10' 42.132" W	surface sample, North Husky Lake	undisturbed	8	10.33	87.1	1103	20.8	7.22
HU1-VAN2	06/14/2012	67° 32' 24.0714"N 135° 10' 42.132" W	surface sample, North Husky Lake	undisturbed	9.3	10.52	91.5	1102	19.1	7.11
HU1-VAN2	06/08/2012	67° 32' 24.0714"N 135° 10' 42.132" W	sample taken at 11m depth (1m from lake bottom)	undisturbed	n/a	n/a	n/a	n/a	n/a	6.97
HU1-VAN2	06/13/2012	67° 32' 24.0714"N 135° 10' 42.132" W	sample taken at 11m depth (1m from lake bottom)	undisturbed	n/a	n/a	n/a	n/a	n/a	6.97
HU1-VAN2	06/14/2012	67° 32' 24.0714"N 135° 10' 42.132" W	sample taken at 11m depth (1m from lake bottom)	undisturbed	n/a	n/a	n/a	n/a	n/a	6.97
HU2-ST1	06/08/2012	67° 31' 31.6554" N 135° 9' 23.0754" W	slump impacted stream Middle Husky Lake	disturbed	8.2	12.11	102.9	1735	451	7.6
HU2-ST2	06/12/2012	67° 31' 31.6554" N 135° 9' 23.0754" W	slump impacted stream Middle Husky Lake	disturbed	4.6	13.26	102.8	2006	n/a	7.84
HU2-ST3	06/14/2012	67° 31' 31.6554" N 135° 9' 23.0754" W	slump impacted stream Middle Husky Lake	Disturbed	6.2	12.55	101.7	1285	320	7.62
HU2-VAN1	06/08/2012	67° 31' 39.0714"N 135° 8' 55.572" W	surface sample, middle husky basin(near delta)	Disturbed	7.8	10.2	86.1	1065	20.4	6.95
HU2-VAN1	06/12/2012	67° 31' 39.0714"N 135° 8' 55.572" W	surface sample, middle husky basin(near delta)	Disturbed	7.8	10.93	94.5	1121	20.6	7.26
HU2-VAN1	06/14/2012	67° 31' 39.0714"N 135° 8' 55.572" W	surface sample, middle husky basin(near delta)	Disturbed	10.8	10.99	99.1	1098	21.4	7.34

Appendix III: Water Quality data for Husky Lake, continued

Table illustrates the water quality data from samples collected from Husky Lake. Each sampling site was sampled three times and data collected includes: Temperature (°C), dissolved oxygen (ppm), % dissolved oxygen, conductivity (µS/cm), turbidity (NTU) and ph. The data shows that water quality is fairly consistent except for elevated values for the conductivity and turbidity of the disturbed site (HU2).

Sample ID	Date	Coordinates	Description	Status	Temp (°C)	Dissolved Oxygen (ppm)	% Dissolved Oxygen	Conductivity (µs/cm)	Turbidity (NTU)	pH
HU2-VAN2	06/08/2012	67° 31' 42.3114"N 135° 8' 51.8274" W	surface sample, middle husky lake (near delta)	Disturbed	7.6	10.9	84.9	1073	13.6	6.92
HU2-VAN2	06/12/2012	67° 31' 42.3114"N 135° 8' 51.8274" W	surface sample, middle husky lake (near delta)	Disturbed	7.7	11	92	1100	14.9	7.36
HU2-VAN2	06/14/2012	67° 31' 42.3114"N 135° 8' 51.8274" W	surface sample, middle husky lake (near delta)	Disturbed	10.5	10.92	97.6	1096	19.9	7.36
HU3-ST1	06/09/2012	67° 30' 27.8634"N 135° 7' 43.4994" W	undisturbed stream, South Husky Lake	undisturbed	5.8	12.28	98.1	605	13.6	6.3
HU3-ST2	06/12/2012	67° 30' 27.8634"N 135° 7' 43.4994" W	undisturbed stream, South Husky Lake	undisturbed	3.9	13.21	100.1	631	23	6.66
HU3-ST3	06/14/2012	67° 30' 27.8634"N 135° 7' 43.4994" W	undisturbed stream, South Husky Lake	undisturbed	6.8	12.25	100.3	640	51.2	6.4
HU3-VAN1	06/08/2012	67° 30' 30.852"N 135° 7' 29.2074" W	surface sample, South Husky basin	undisturbed	8.1	9.92	84.6	1072	12.7	7.02
HU3-VAN1	06/12/2012	67° 30' 30.852"N 135° 7' 29.2074" W	surface sample, South Husky basin	undisturbed	7.4	11.15	92.8	1039	9.31	7.16
HU3-VAN1	06/14/2012	67° 30' 30.852"N 135° 7' 29.2074" W	surface sample, South Husky basin	undisturbed	9.8	11.05	97.5	1043	14.7	7.06
HU3-VAN2	06/09/2012	67° 30' 38.7" N 135° 6' 49.788" W	surface sample, South Husky Lake	undisturbed	6.6	10.37	84.6	997	9.81	6.96
HU3-VAN2	06/12/2012	67° 30' 38.7" N 135° 6' 49.788" W	surface sample, South Husky Lake	undisturbed	7	11.05	90.7	1041	9.08	7.18
HU3-VAN2	06/14/2012	67° 30' 38.7" N 135° 6' 49.788" W	surface sample, South Husky Lake	undisturbed	9.5	10.9	95.5	1082	18.1	7.14
HU3-VAN2	06/09/2012	67° 30' 38.7" N 135° 6' 49.788" W	sample taken 1m from bottom (14m depth)	undisturbed	n/a	n/a	n/a	n/a	n/a	n/a
HU3-VAN2	06/12/2012	67° 30' 38.7" N 135° 6' 49.788" W	sample taken 1m from bottom (14m depth)	undisturbed	n/a	n/a	n/a	n/a	n/a	n/a
HU3-VAN2	06/14/2012	67° 30' 38.7" N 135° 6' 49.788" W	sample taken 1m from bottom (14m depth)	undisturbed	n/a	n/a	n/a	n/a	n/a	n/a

Appendix IV: Loss-on-ignition properties of sediment captured by sediment traps deployed in Husky Lake.

The number of samples column displays how many samples the values are based on (note that those with only one sample are not average values). The number of samples used was based on the volume of collected sediment within the traps. A higher number of samples were analyzed in traps in which a larger volume of sediment was collected in order to more efficiently represent the sample as a whole.

TRAP ID	# OF SAMPLES	% WATER	% ORGANIC	% CARBONATE	% SILICICLASTIC
HU1-SED1	1	71.8386	18.8927	1.7135	79.3936
HU1-SED2	1	13.8093	11.5912	1.5912	86.8174
HU1-SED3	1	62.6397	13.3933	1.7141	84.8925
HU1-SED4	1	55.9439	10.3278	2.4262	87.2459
HU2-SED1	5	34.5680	6.9504	1.6309	91.4185
HU2-SED2	5	35.5057	6.8444	1.6364	91.5191
HU2-SED3	7	39.3559	9.6033	1.1025	89.2941
HU3-SED1	5	51.1532	13.3803	1.4756	85.1440
HU3-SED2	5	45.6269	12.7672	1.7000	85.5326
HU3-SED3	1	59.8193	13.6543	2.0341	84.3114
HU3-SED4	3	73.8527	13.5659	2.4959	83.9381
NH	5	73.9849	23.8317	3.1043	73.0639

Appendix V: Sediment trap volume and particle size data.

As with the LOI analysis, the number of samples used was based on the quantity of collected sediment. For each sample, wet and dry sediment weights were measured, sediment volume and bulk density were calculated and the mean grainsize was measured. Values of sediment weight, volume, bulk density and mean grainsize are generally higher in the traps of the disturbed site (HU2) than the undisturbed (HU1 & HU3).

SEDIMENT TRAP ID	NUMBER OF SAMPLES	WET SEDIMENT WEIGHT (g)	DRY SEDIMENT WEIGHT (g)	sediment volume (cm3)	bulk density (g/cm3)	date deployed	date retrieved	average arithmetic mean grainsize (μm)
HU1-SED1	1	5.1085	1.439	5.73	0.25113438	June 9th 2012	August 24 2012	10.39
HU1-SED2	1	9.8528	8.492	11.45	0.74165939	June 9th 2012	August 24 2012	20.9668
HU1-SED3	1	16.817	6.283	16.03	0.39195259	June 9th 2012	August 24 2012	21.666
HU1-SED4	1	26.4971	11.674	26.34	0.44320425	June 9th 2012	August 24 2012	4.486
HU2-SED1	5	77.3945	50.641	83.02	0.60998555	June 9th 2012	August 24 2012	16.91633
HU2-SED2	5	105.2561	67.884	80.16	0.84685629	June 9th 2012	August 24 2012	23.78
HU2-SED3	5	683.035	414.220	336.23	1.23195432	June 9th 2012	August 24 2012	43.2
HU3-SED1	5	63.4049	30.971	48.67	0.63765699	June 9th 2012	August 24 2012	16.4
HU3-SED2	5	missing*	n/a	57.26	n/a	June 9th 2012	August 24 2012	16.13
HU3-SED3	1	14.4958	5.823	14.89	0.39106783	June 9th 2012	August 24 2012	8.96
HU3-SED4	3	26.1936	6.849	20.61	0.33231441	June 9th 2012	August 24 2012	4.804
NH	5	118.512	30.831	74.43	0.414228134	June 9th 2012	August 24 2012	11.7

Appendix VI: Sedimentological analyses of core HU1-MG.
A) Magnetic susceptibility (SI units); B) LOI: oercent organic, carbonate and siliciclastic matter; C) Arithmetic mean grain size of sediment; D) Percent sand, silt and clay of sediment.

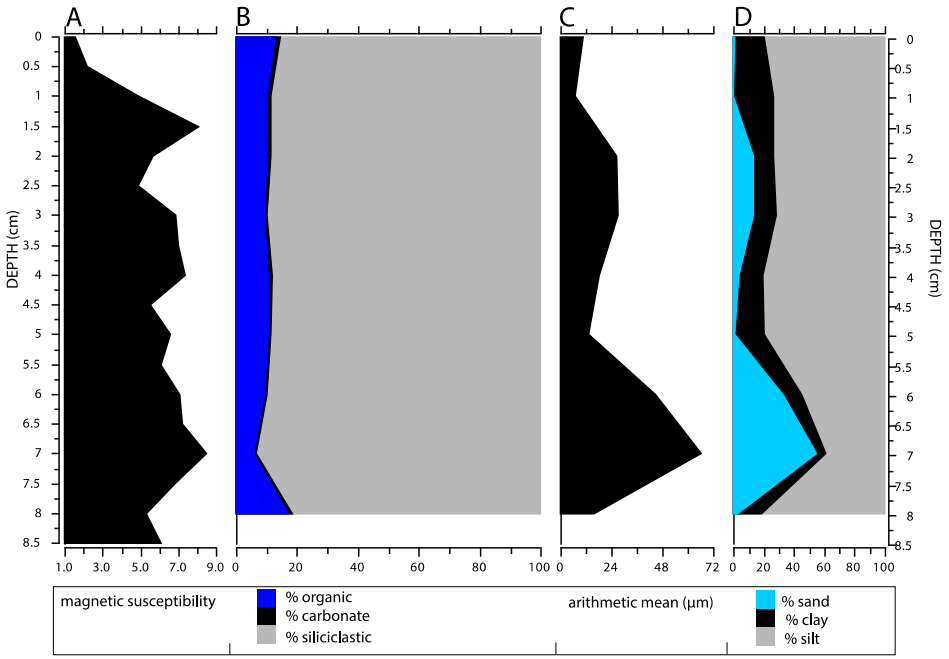

Summary: HU1-MG was collected from the centre of the HU1 basin. The magnetic susceptibility of the sediments is low throughout the core, varying between 1.6 and 8.5 x 10^{-6} SI units. Two peaks in magnetic susceptibility occur at 1.5 cm depth (8.1 x 10^{-6} SI units) and 7 cm depth (8.5 x 10^{-6} SI units). The peak in magnetic susceptibility of core HU1-MG occurs at the same depth interval as the lowest value of percent organic matter. Organic matter has a minimum of 5.5% at 7 cm depth and a maximum of 17.1% at 8 cm depth. The average organic matter content is 10.6% throughout the core. The percent carbonate is stable throughout the core, varying between 0.88% to 1.19%. The remainder of the sediment within the core consisted of siliciclastic material (ranging from 81.5% to 93.4%).The particle size distributions demonstrate that silt (3.9- 62.5 µm) dominates every measured depth of the core except for at 7 cm depth where sand (62.5- 2000 µm) is most pronounced with 55% of the sediment being comprised of sand-sized particles. This peak in sandy material occurs at the same depth as the previously mentioned peak in magnetic susceptibility and decline in organic matter.

Appendix VII: Sedimentological analyses of core HU2-MG.
A) Magnetic susceptibility (SI units); B) LOI: Percent Organic, Carbonate and Siliclastic Matter; C) Arithmetic mean grainsize of sediment; D) Percent sand, silt and clay of sediment.

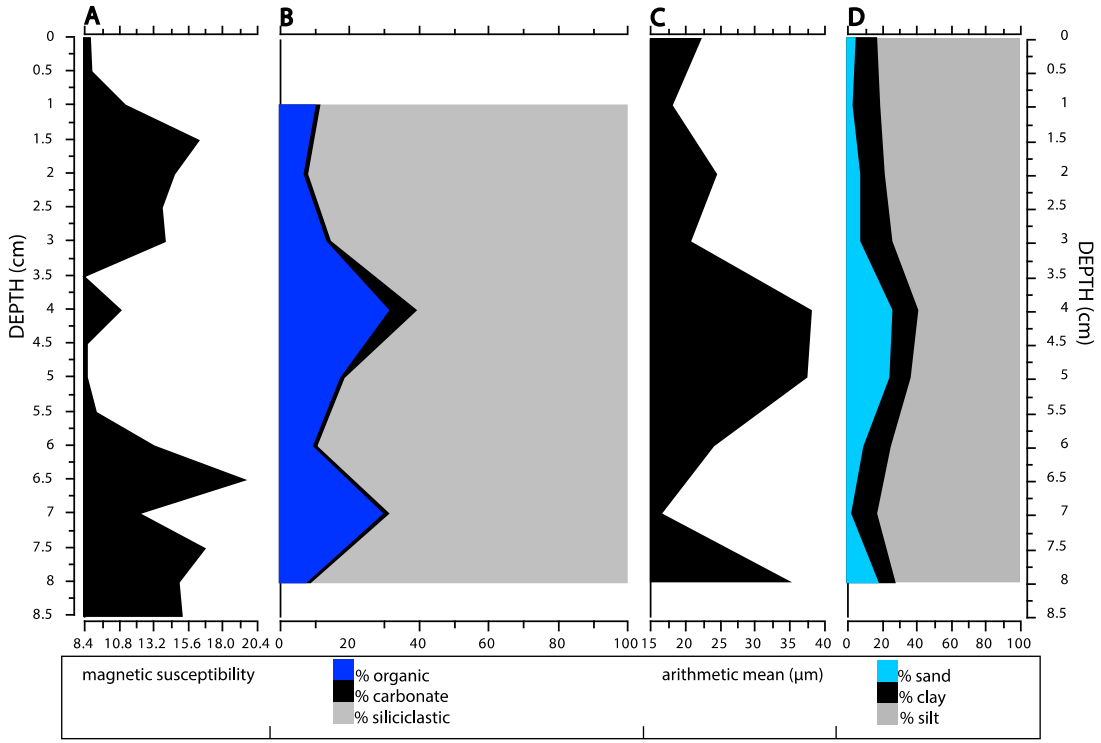

Summary: HU2-MG was collected from the centre of the HU2 basin. The magnetic susceptibility of core HU2-MG is generally higher than that of HU1-MG, ranging from 8.4 x 10^{-6} SI units at 3.5 cm depth and 19.6 x 10^{-6} SI units at 6.5 cm depth.There are also smaller peaks at 1.5, 3, 4 and 7.5 cm depth as the magnetic susceptibility appears to fluctuate between higher and lower values at roughly every one and a half centimetre interval down core.The percent organic matter throughout the core ranges between 6.8% at 2 cm depth and 31.2% at 4 cm depth. There is another smaller peak in organic matter to ~30% at 7 cm depth. The percentage of siliciclastic material is very high for this core, correlating inversely with percent organic matter and percent carbonate, with its lowest value (60.8%) at 4cm depth and its highest value (91.9%) at 2 cm depth. The arithmetic mean particle size ranges between 16.8 µm (7 cm depth) and 38.2 µm (4 cm depth) and averages 26.5 µm throughout the core.HU2-MG is predominantly silt, averaging 74.6% throughout the core.

Appendix VIII: Sedimentological analyses of core HU3-MG.
A) Magnetic susceptibility (SI units); B) LOI: Percent Organic, Carbonate and Siliclastic Matter; C) Arithmetic mean grainsize of sediment; D) Percent sand, silt and clay of sediment

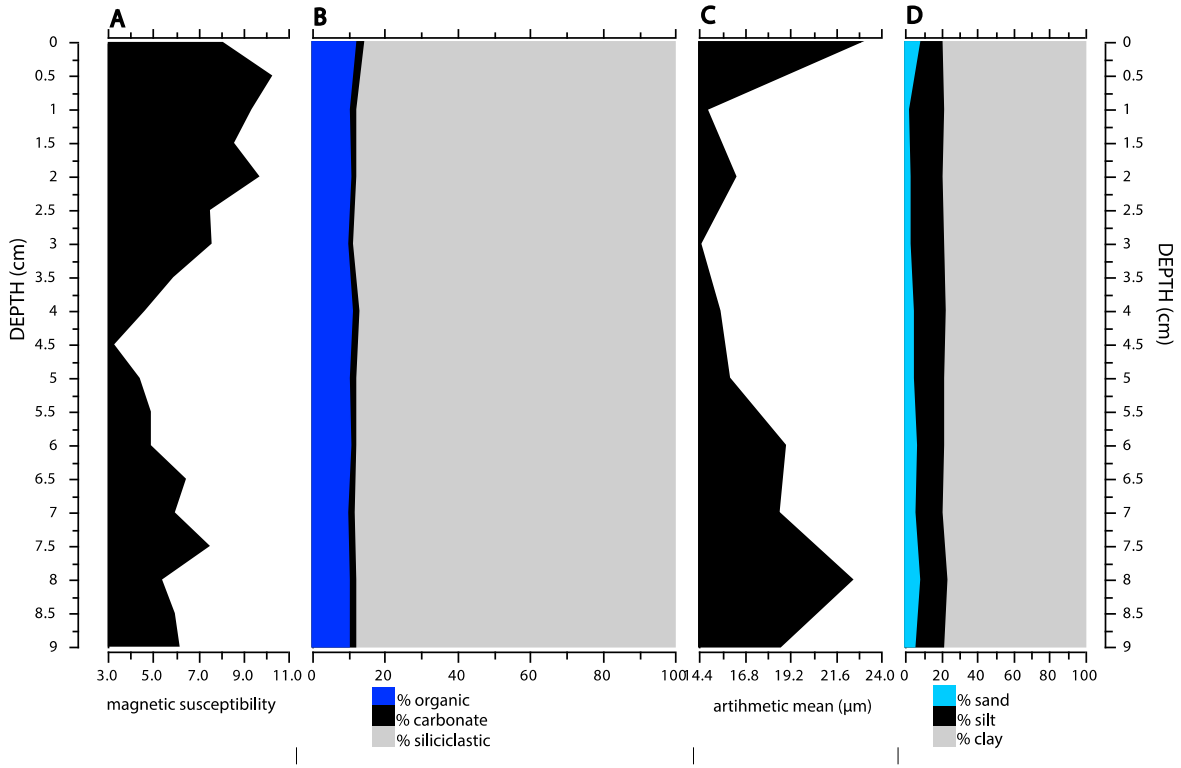

Summary: HU3-MG was collected from the centre of the HU3 basin. The magnetic susceptibility of core HU3-MG ranges from 3.3 x 10^{-6} SI units at 4.5 cm depth and 10.3 x 10^{-6} SI units at 0.5 cm depth. The values are generally lower than that of HU2-MG and fluctuate in pulses from low to high values at approximately every one and a half centimetre down-core. The percent organic matter has a maximum of 11.2% at 4 cm depth and a minimum of 9.5% at 3cm.The percent content of siliciclastic materials is high and dominates the compostion of the sediment core. The mean grainsize is lower than that in the other cores, ranging between 14.48 µm at 3cm and 22.9 µm at the sediment-water interface. Subsequently, the sand content is also very low with a maximum of 8% at 7 cm and the sediment-water interface and a minimum of 2% at 1cm depth. Clay content reaches its peak at 1cm with 19% clay and is lowest (12%) at the sediment-water interface. The sediment is primarily characterized as silt.

Appendix IX: Core FM1-KB2.

Core FM1-KB2: Laminations can be seen in the top portion of the collected core.